الجمهورية الجزائرية الديمقراطية الشعبية
République Algérienne Démocratique et Populaire
Ministère de l'Enseignement Supérieur et de la Recherche Scientifique

Université Mohamed Khider Biskra
Faculté des Sciences et de la Technologie
Département de Génie Mécanique
Filière : Métallurgie
Option : Métallurgie physique

Réf:.....

Mémoire de Fin d'Etude

En vue de l'obtention du diplôme de :

MASTER

Thème

Optimisation du procédé de compactage et frittage des poudres non-métalliques

Présenté par :
Wafa MELIK

Proposé et dirigé par :
Pr. Zakaria BOUMERZOUG

Promotion : Juin 2017

الجمهورية الجزائرية الديمقراطية الشعبية
People's Democratic Republic of Algeria
Ministry of Higher Education and Scientific Research

University Mohamed Khider Biskra
Faculty of Science and Technology
Department of Mechanical Engineering
Filed: Metallurgy
Option: Physical metallurgy

Ref:.....

End of Study dissertation

In order to obtain the diploma of:

MASTER

Theme

Optimization of the compaction and sintering process of non-metallic powders

Submitted by:

Wafa MELIK

Supervisor:

Pr. Zakaria BOUMERZOUG

Promotion: June 2017

Dedications

To my mother and father for their patience and sacrifice

To my sisters and dear brother (Mohamed) for their love

To all my friends for their support

Acknowledgements

First and foremost, I would like to thank my supervisor ***Pr. Zakaria BOUMRZOUG*** for providing me with an opportunity to work with him. He has always guided me through my work and at the same times given me enough freedom to learn and produce original ideas. Thank you, sir, for being as patient with me as you were.

.

I extend my gratitude to the members of the panel of examiners namely, ***Dr. Karima OUNNES***, and ***Dr.Hamza BENTRAH*** for having accepted to read and examine my dissertation, and I would like to thank my teacher ***Ms..Moussa ATHMANI*** for his advices.

I would like also to thank all, for helping me to understand and prepare this dissertation:

Mr. ***Youcef NANI***, electrotechnical engineer in AMOURI brothers, Biskra factory.

Mr. ***Tarik OTMANE***, the head of the laboratory of soil analysis CRSTRA, Biskra.

Mrs. ***Fatna LAKHNACH***, the head of the laboratory of civil engineer, University of Biskra.

Mrs. ***Hayet BEN MACHICH,*** the head of the laboratory of chemistry in department of the sciences of the mater, University of Biskra.

Mr. ***Ibrahim GUESMI***, the head of the laboratory of DRX, University of Biskra.

I would like to thank all my ***teachers of the department of mechanical engineer***ing and the ***promotion 2017 of physical metallurgy***.

Wafa MELIK

List of figures

List of figures

List of figures

List of figures

List of tables

List of abbreviation

XRD: X-ray diffraction

V: Exterior volume

D: Weight of dried specimen

W: Weight of soaked specimen suspended in air.

S: Weight of dried specimen suspended in water

Mf: Modulus of fineness

M1: Mixture of clay and Biskra sand

M2: Mixture of clay and Sahara sand

AP: Apparent porosity

WA: Water absorption

BD: Bulk density

Contents

Contents

Contents

Contents

General introduction

Powder metallurgy (PM) is a manufacturing method that has gained interest over the last decades as an economic and fast method to produce different parts as for instance structural components. It has become a great industrial potential for companies to gain market advantages over other companies using conventional manufacturing methods.

Today, this production process is commonly used in the manufacturing industry such as those in the ceramic forming. Cold compaction is an important part of this process. The granulated material is consolidated by the application of pressure. The powder is formed into a desired shape with rigid tools and a die, and then sintered at high temperatures. Sintering is a thermal treatment that bonds particles together into a solid, coherent structure.

In our research, we have studied the effect of compaction and sintering process of non-metallic powders which are ceramic powders (clay and sand) to produce the brick product. During firing of brick, a series of transformation occurs which determine the final properties of the brick product. The main factors involved in manufacturing bricks are the type of raw materials, fabrication method, firing temperature, and firing profile.

The aim of this research is the optimization of compacting and sintering process of brick. Two types of bricks have been studied: The first one is a bricks produced by SARL Eloutaya. And the second type is prepared in our laboratory with specific conditions. For this reason we used some techniques like: infrared spectroscopy, microscopic observation, X-ray diffraction, and different tests (Water absorption, apparent porosity, bulk density).

This dissertation contains four chapters:

Chapter I: Compaction and sintering of non-metallic powders. It is about powder metallurgy of non-metallic powders, describes the preparation of powders (milling and mixing), compaction and sintering process.

Chapter II: Research studies on non-metallic powders. It presents some previous scientific examples about compacting and sintering of brick product.

Chapter III: Materials and experimental techniques. This chapter presents the different steps of preparing the brick product in SARL Eloutaya.Poterie and describes the experimental techniques used in laboratory for synthesis and characterizing the prepared samples.

Chapter IV: Results and discussions. This chapter presents the results of our work and the different discussions of these results.

Chapter I:

Compaction and sintering of non-metallic powders

I .1 Introduction

Powder Metallurgy (PM) deals with products and processes which use raw material in the form of powders that are compacted into the required shape and size, using suitable moulds. These compacted powders are called ”Green Compacts”. The properties of the component produced by PM processes are influenced by powder characteristics such as composition, morphology, particle size, distribution, and method of compaction. The first step in PM process is preparation of green compacts [1], and then sintering the green compact at an elevated temperature in a furnace under a protective atmosphere. During sintering the compact becomes consolidated and strengthened [2].

I .2 Preparation of non-metallic powder

I.2.1. Crushing process

I.2.1.1 Definition

Crushing, grinding and milling operations are part of many mineral processes. Crushing can consist of primary, secondary and tertiary processes, which can be followed by wet or dry grinding and milling. These operations are commonly used for reducing the particle size of ores for further processing downstream. They are also performed in processes where the final product is a powder, before mixing and moulding operations [3] **(Fig. I.1)**.

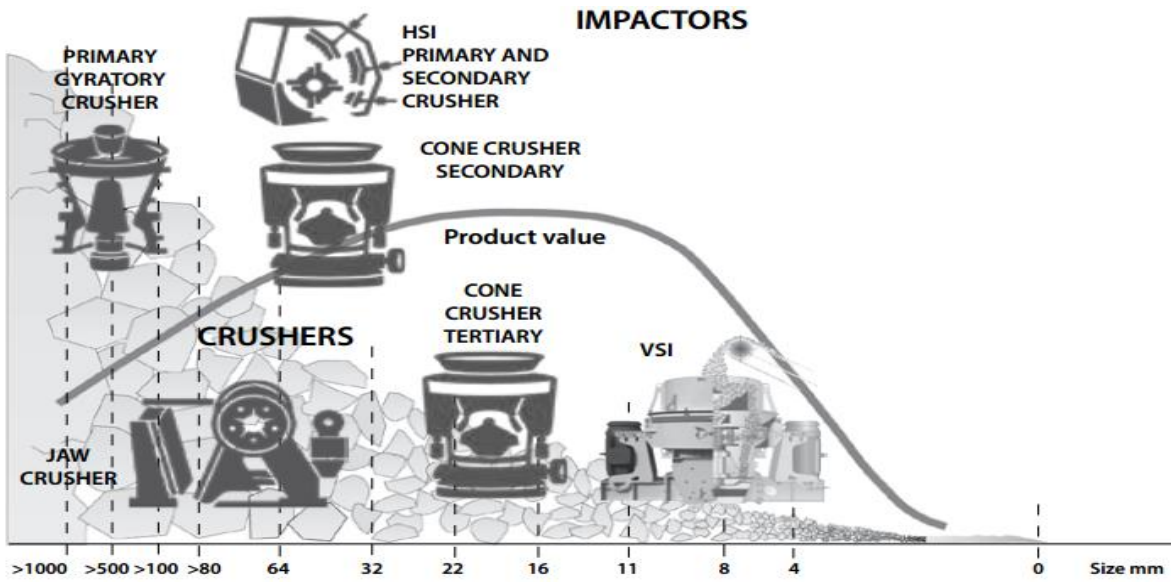

Fig.I.1: Crushing operation in minerals processing [4].

I .2.2 Milling process

I.2.2.1 Definition

The simplest device is ball mill where milling is performed by mechanical impact of hard milling objects carried up by a rotary motion of drum onto the disintegrated powder. The milling objects, ball, rollers or rods inserted into the milling drum, are manufactured from unalloyed and stainless steel, pottery…ect, depending on hardness, milling capability and demanded cleanliness powder. Milling can be carried dry or wet whereas the application of suitable surface active liquid makes the disintegration easier. The work needed for disintegration can be formulated as follows: [5]

$$\Delta A = \Delta S.\gamma \ldots\ldots\ldots\ldots (\text{Equ. I. 1})$$

Where **ΔS** is the enlargement of surface area (m^2) and γ is the surface stress (N/m).

Stress **σ** needed to disintegrate a brittle material when milling depends on a structure of imperfections and susceptibility to the crack propagation:

$$\sigma = (2\,E.r/D)^{1/2} \ldots\ldots\ldots\ldots (\text{Equ. I. 2})$$

Where **E** is Young's modulus; **r** is a radius of a tip of an existing crack or defect; **D** is a particle size.

The particle becomes stronger. The reduction of the limiting particle size may be achieved by wet milling as opposed to dry milling (**Fig.I.2**).

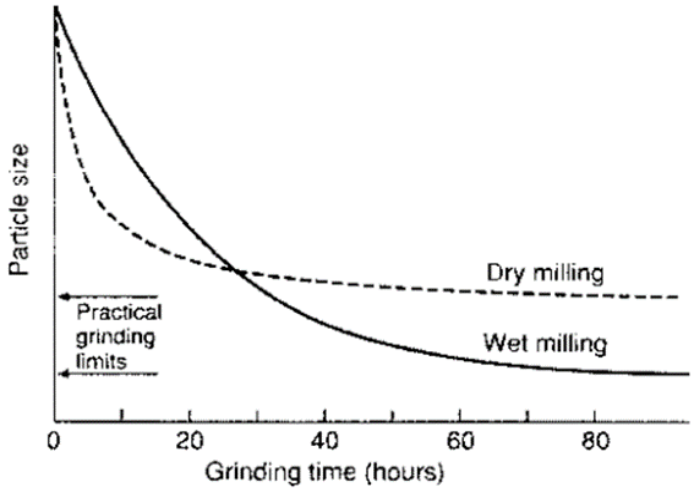

Fig. I.2: Particle size versus grinding time for ball milling [6].

I.2.2.2 Ball mills

The high-compression roller mills and jet mills just described achieve comminution without the use of grinding media. For mills that incorporate grinding media (balls or rods), comminution occurs by compression, impact, and shear (friction) between the moving grinding media and the particles. Rod mills are not suitable for the production of fine powders, whereas ball milling **(Fig.I.3)** can be used to produce particle sizes from 10 m to as low as a fraction of a micrometer. Ball milling is suitable for wet or dry milling [7].

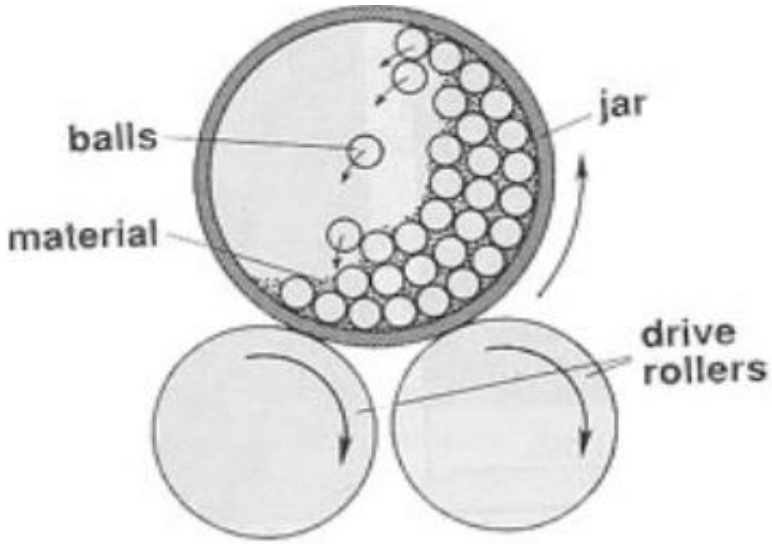

Fig.I.3: Schematic of a ball mill in cataracting motion [8].

I.2.2.3 Milling time

The time of milling is the most important parameter. Normally the time is so chosen as to achieve a steady state between the fracturing and cold welding of the powder particles. The times required vary depending on the type of mill used, the intensity of milling and the temperature of milling.

These times have to be decided for each combination of the above parameters and for the particular powder system. But, it should be realized that the level of contamination increases and some undesirable phases form if the powder is milled for times longer than required [9].

I.2.3 Mixing/blending of non- metallic powders

The mixing and blending of raw materials is quite common when minerals are involved as raw materials in any process. There is a large variety of mixing equipment and there are also a number of different types of mixing. Mixing types are usually defined by the mechanism used for agitation (**Fig.I.4**) and the conditions under which the mixture is treated [3]. The purpose of mixing or blending is to combine the constituents of a ceramic powder to produce a more chemically and physically homogenous material for forming. Pug mills often are used for mixing ceramic materials. Several processing aids may be added to the ceramic mix during the mixing stage.

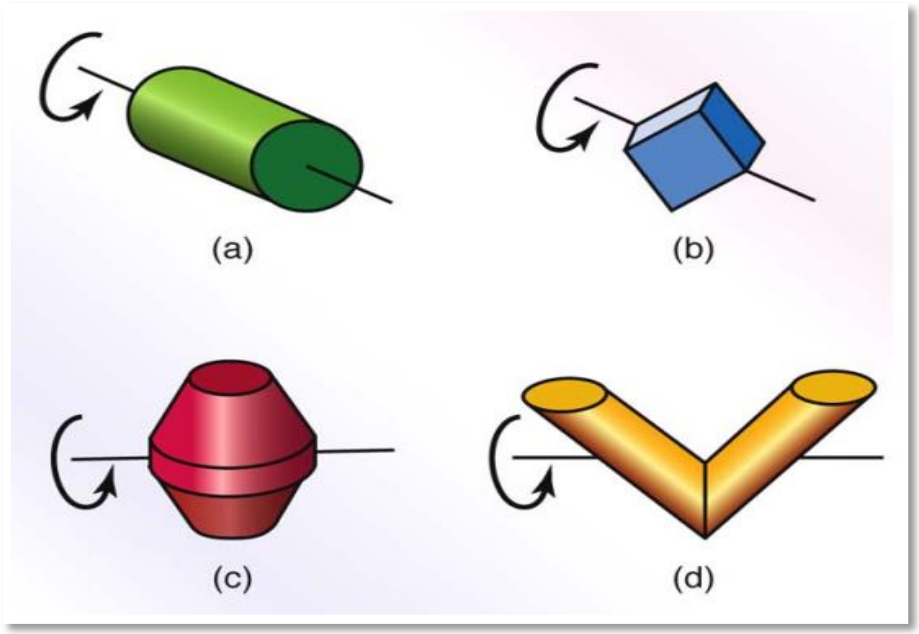

Fig.I.4: Various types of mixing machine: a) and b) rotating drum, c) rotating double cone, d) blade mixer [10].

I .3 Compaction

I .3.1 Definition

Compaction is the process in which the blended powders are pressed into shapes in dies. So basically, we apply some pressure (can be single or double acting press) we put the metal or ceramic powder into the die cavity. Then we apply some pressure, so when the pressure is applied, the powder takes the form of the die cavity [11].

Compaction of powder is done in a form with a desirable shape, the shape of the final detail. Initially the form is filled with the mixed powder.

I.3.2 Compacting Press

Fig.I.5 shows examples of hydraulic automatic powder Compacting presses for producing parts into the desired shapes: using metal oxidized powder of various kinds, such as Iron, copper, ferrite, ceramic, tungsten, carbide [12].

Fig.I.5: Hydraulic auto powder compacting press; a) cold press ranging from 30 tons to 500 tons, b) Hot press with mold heating systems (400℃), ranging from 30 tons to 2000 tons [12].

I.3.3 Mechanisms of compaction

In the typical powder, pressing process a powder compaction press is employed with tools and dies. Normally, a die cavity that is closed on one end (vertical die, bottom end closed by a punch tool) is filled with powder. The powder is then compacted into a shape and then ejected from the die cavity **(Fig.I.6)**.When pressing these shapes, very good dimensional and weight control are maintained. In a number of these applications the parts may require very little additional work for their intended use; making for very cost efficient manufacturing.

The pressing process consists of the following stages [13]:

• Die filling

At this stage, a controlled amount of the powder is fed into the die cavity.

•Compaction

Upper punch moves down and presses the powder with a predetermined pressure.

• **"Green" compact part ejection and removal** ("green" compact – unsintered powder compact).

The pressing cycle repeats, depending on the press type, powder filling properties and the part size and geometry...

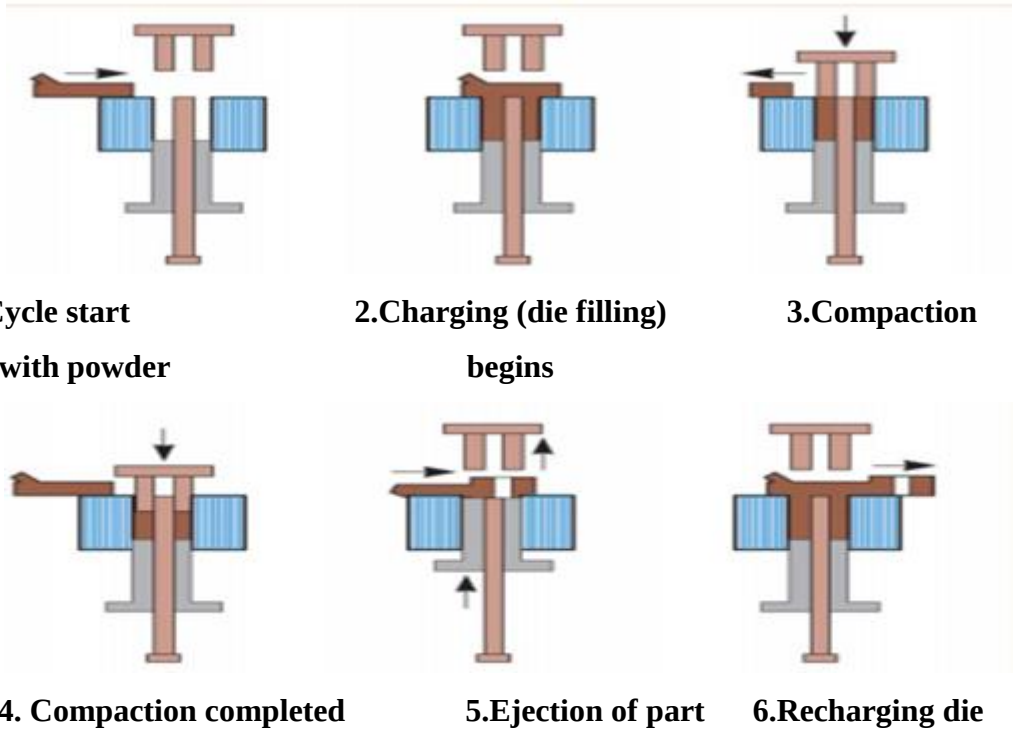

Fig.I.6: The scheme of the die pressing method [13].

I .3.4 Stages of compaction

The compaction process can be roughly divided into three stages [14]; **Fig.I.7**presents a schematic of the steps involved in uni-axial pressing.

In stage 1, the particles get re-arranged with substantial increase in green density.

In stage 2, which begins at higher pressure, individual particles are deformed.

In stage 3, cold welding occurs between particles providing dimensional stability and green strength required for easy handling and further processing.

Green compacts can be prepared with or without binders depending on the composition of the elemental powders and subsequent sintering process. Higher green

strength results in more robust handling of green parts prior to the sintering operation and reduced levels of green scrap [14].

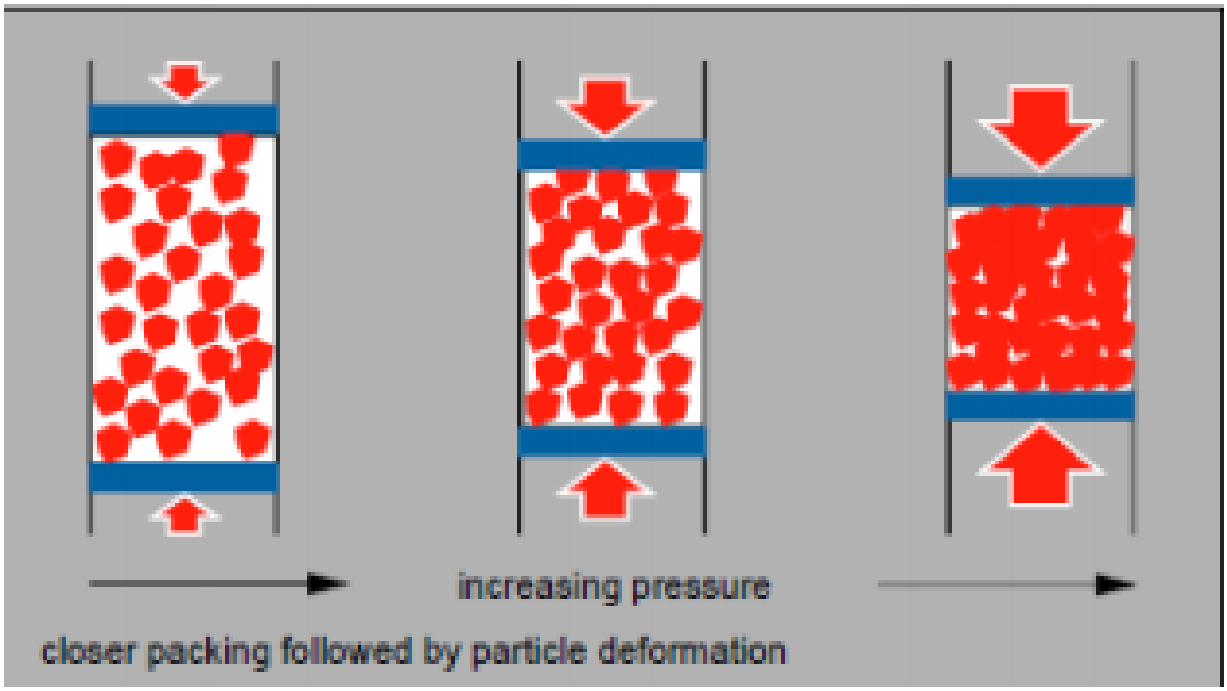

Fig.I.7: Steps in preparation of green compact [14].

I.3.5 Relation between compaction pressure and density

The primary characteristic of powder is the relative density achieved at a given compaction pressure, expressed in the form of a pressure–density plot, as illustrated in **Fig.8** The mean density starting from the filling density initially increases rapidly, then saturates at high pressure. The compaction pressure P used in these plots is the macroscopic "technical" compaction pressure, usually derived from die pressing experiments in which P is simply the load F acting on the punches, divided by the cross-sectional area A of the compact:

$$P = \frac{F}{A} \dots\dots\dots\dots (\text{Equ. I. 3})$$

The state of stress and the stress distribution in the compact are not taken into consideration. The compaction behavior of monolithic (metallic) powders and ceramic granulates, both of which can plastically deform, are described in the following subsections, together with discussions of the state of stress, advanced modeling, and the practice of uniaxial compaction.[15] .These steps are illustrated in **Fig.I.8.**

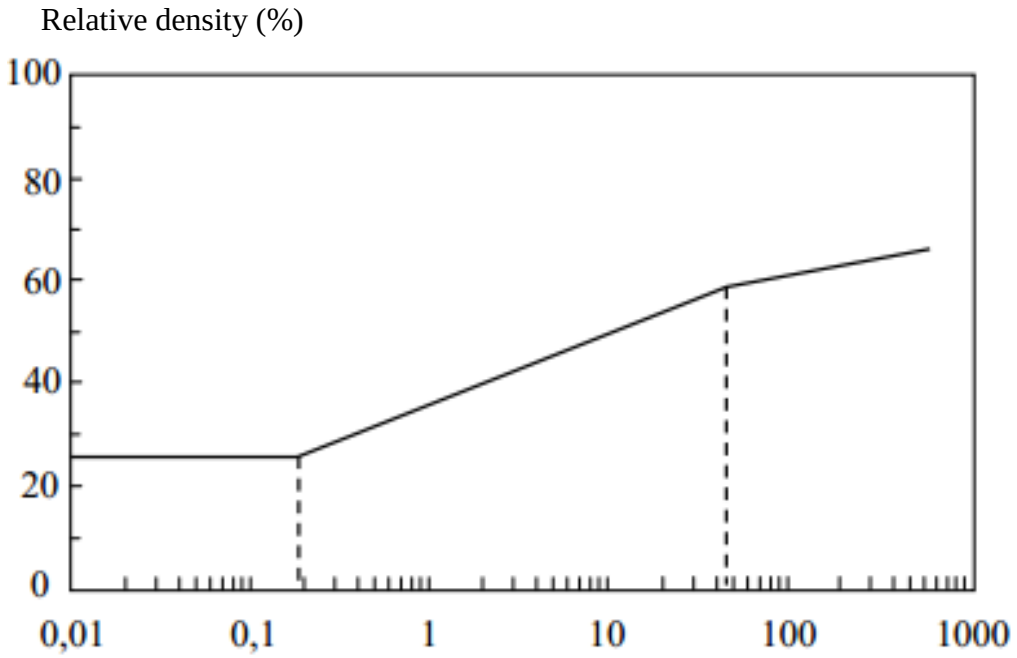

Fig.I.8: Evolution of the density as a function of the shaping pressure [16].

I.3.6 Types of compaction

There are many types of compaction process, the most used are:

I.3.6.1 Cold compaction

Cold compaction is the first step in giving shape to powders in PM processes in room temperature. There are different methods of cold compaction, such as uni-axial pressing, cold isostatic pressing, bi-axial and tri-axial pressing, explosive compaction and hydrostatic pressing [1]. However, uni-axial pressing is the simplest and most widely used process for preparation of green compacts [17].

I.3.6.2 Hot isostatic pressing

Hot Isostatic Pressing is a forming and densification process using heated gas (most commonly argon or nitrogen) under very high pressure. Unlike mechanical force which compresses a work piece from one or two sides **(Fig.I.9)**, isostatic pressure is applied uniformly on all sides of an object, eliminating internal porosity without changing its net shape. The process can be used to treat preformed metal, ceramic or composite parts

(Fig.I.10), and for compaction of containerized powder shapes. Maximum standard operating pressures can be specified from 10 to 207 MPa Temperatures can range up to 2000°C [18,19].

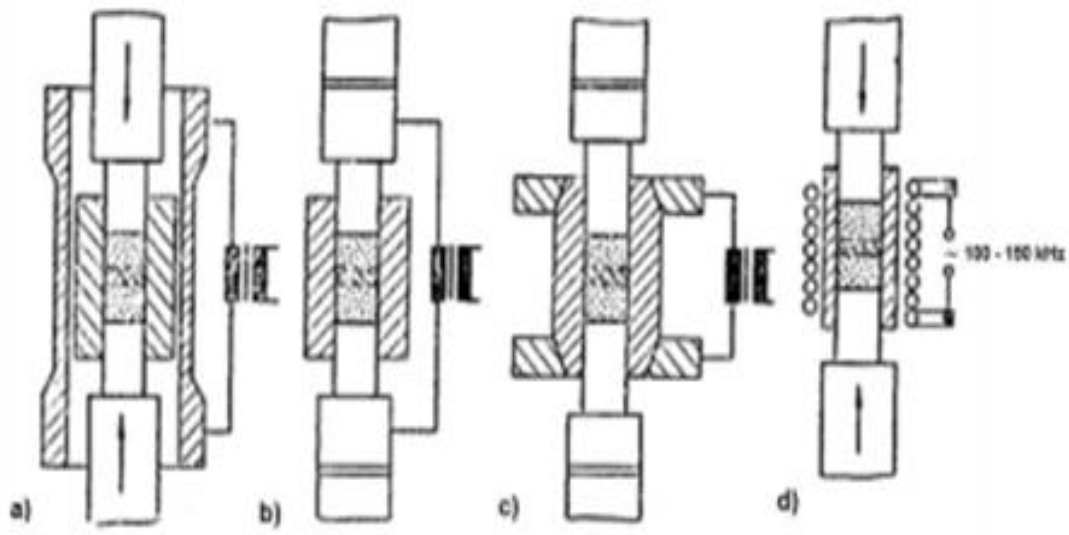

Fig.I.9: Schematic depiction of the hot pressing equipment; a) indirect through a heating tube or a heating spiral, b) direct heating by passing current through punches, c) direct heating of die, d)induction heating of die or a compact[19].

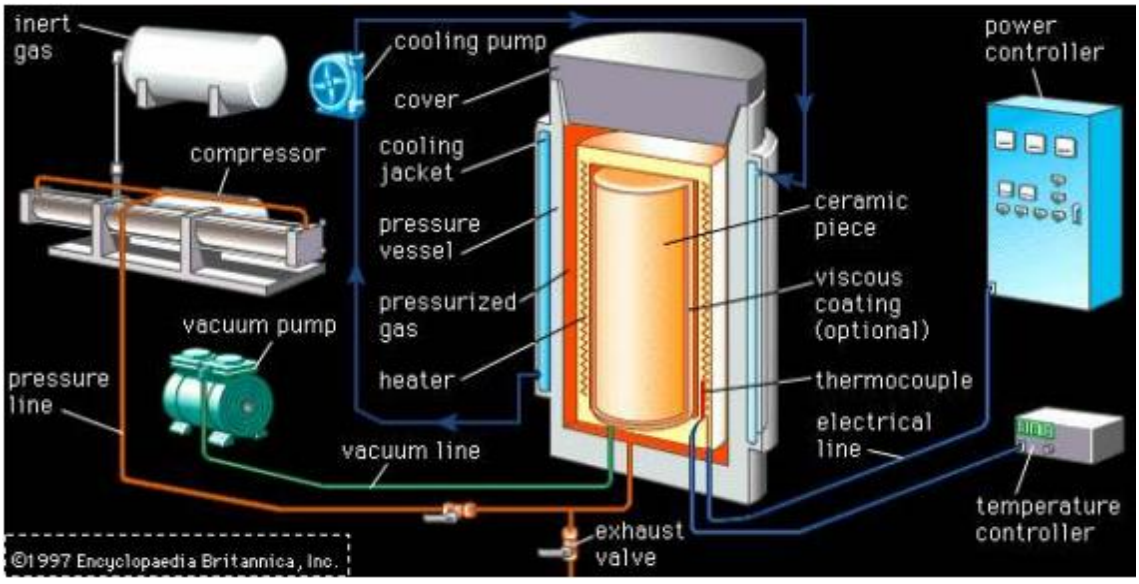

Fig.I.10: Hot isostatic press unit, used for ceramic material [18].

1.3.7 Drying

Drying is a process in which the water content in the ceramic is removed. As the ceramic dries it also experiences shrinkage. The drying rate is controlled by temperature and humidity.

The purpose of drying is usually to drive off excess moisture. After drying the ceramic piece is fired at high temperatures .The firing temperature depends on the composition and the desired property of the finished piece.

I.4 Sintering

I.4.1 Definition

Sintering (Firing) of ceramic materials is a manufacturing process in which a fine powder that has been formed into a shape is subsequently fired at high temperatures below the melting point. The compact, when fired, densifies and becomes non-porous. More formally, it is a thermal treatment that bonds particles together into a solid, coherent structure, by means of mass transport mechanisms occurring largely at the atomic level [20],(**Fig.I.11)**.

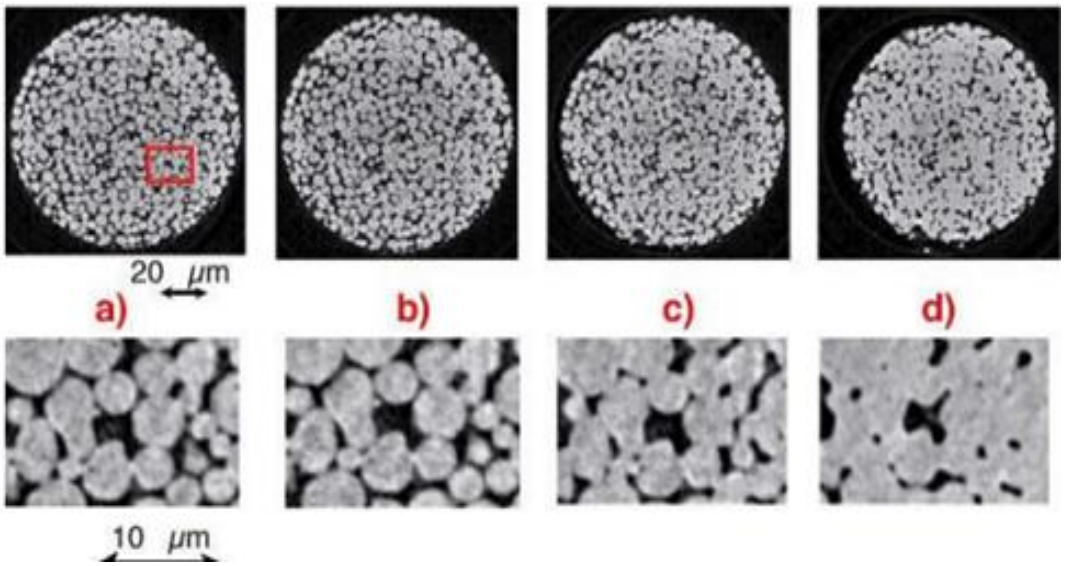

Fig.I.11: Schematic representation of sintering [13].

I.4.2 Sintering furnace

There is a very wide variety of furnaces, which can be classified into two main categories: Discontinuous furnaces and continuous furnaces. Most commonly used are continuous furnaces a continuous furnace **(Fig.I.12)** of recent design for the sintering of mechanical parts made of powder usually consists of three different utility zones:

1. The preheating zone where the powder products start heating.
2. The heating zone where the powder products are sintered at high temperature.
3. The cooling zone where the sintered parts are cooled before being vented.

Fig.I.12: PM Continuous sintering furnace, courtesy of Elino furnaces GmbH [21].

I.4.3 Sintering parameters

Sintering is a manufacturing process consisting of heating powder without melting it. Under the effect of heat, the grains are welded. Sintering is a very complex phenomenon because it is based on many factors [22].

1. Factors depending on conditions of the operation: temperature, time; compression.
2. Factors depending on the nature of the atmosphere in which sintering is performed: vacuum atmosphere reducing, oxidizing…
3. Factors dependent on the powder: morphology, particle size, purity.

I.4.3.1 Temperature

The temperatures are chosen in principle within a limited range between two thirds (2/3) and the three quarter (3/4) of Tm where Tm is the melting temperature of the core compact with relatively short durations to avoid excessive grain growth. Sintering of powder which contains several components may be performed at temperature to avoid a melting of these compounds [23].

I.4.3.2 Sintering duration

The sintering duration decrease by the increase of the sintering temperature [24].

I.4.3.3 Compression

The density and hardness of the finished product are a function of the compression pressure. Therefore, it should not be forget that there is an optimum pressure for each mixture and that to overcome this pressure do not significantly improve the quality of the finished product [22].

I.4.3.4 Grain size

The nature and grain size affect the mechanical properties of the parts obtained by sintering, such as deformation, the hardness and physical properties such as density, porosity.

I.4.3.5 Sintering atmosphere

The atmosphere should be neutral or reducing and completely dry, to avoid oxidation propagate into the bulk of the reducing atmosphere promotes compressed by removing the film oxide which covers the powder grains [22].

I .4.4 Sintering changes in the green compact

The process of sintering provokes certain physical as well as chemical changes in the material [12]. The chemical changes can be illustrated as:

- ✓ Change in composition or decomposition.
- ✓ New phase formation or decomposition followed by phase change.
- ✓ New phase formation due to chemical changes

The physical changes that take place are:

- ✓ Change of grain size.
- ✓ Change of pore shape and pore size.

All these changes bring about the complete change in microstructure, which bring about the complete change in the properties of the material. Change in grain size is brought about by recrystallization where as densification or solid state sintering is responsible for change of pore shape and size [12].

I.4.5 Mechanisms of sintering

Sintering of crystalline materials can occur by several mechanisms (atomic transport path and their associated sources and sinks): vapor transport (evaporation/condensation),

surface diffusion, lattice (volume) diffusion, grain boundary diffusion, and dislocation motion. **Fig.I.13** shows a schematic representation of matter transport path for two sintering particles. A distinction is commonly made between densifying and non-densifying mechanisms. Vapor transport, surface diffusion, and lattice diffusion from the particle surfaces to the neck lead to neck growth and coarsening of the particles without densification. Grain boundary diffusion and lattice diffusion from the grain boundary to neck are the most important densifying mechanisms in polycrystalline ceramics. Diffusion from grain boundaries to the pores permits neck growth as well as shrinkage (densification).plastic flow by dislocation motion can cause neck growth and densification through deformation (creep) of the particles in response to the sintering stress .Plastic flow is more common in the sintering of metal powders. For glass powders, which cannot have grain boundaries, densification and neck growth occur by viscous flow, involving deformation of the particles [25].

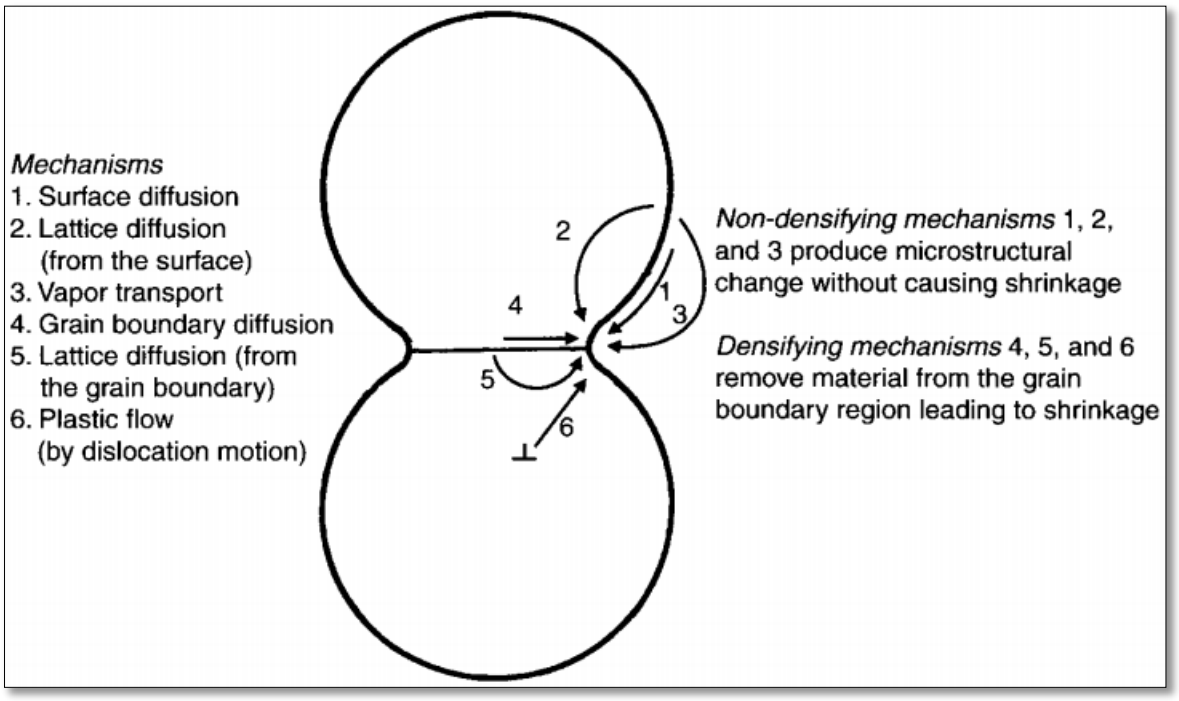

Fig.I.13: Schematic representation of sintering mechanisms for a system of two particles [25].

I.4.6 Stages of sintering

The sintering process has historically been divided into four stages. These are described in **Tab.I.1** and **Fig.I.14**.

Tab.I.1: The classic stage of sintering [21].

Stage	Process	Surface area loss	Densification	Coarsening
Adhesion	Contact formation	Minimal, unless compacted at high pressures	None	None
Initial	Neck growth	Significant, up to 50%loss	Small at first	Minimal
Intermediate	Pore rounding and elongation	Near total loss of open porosity	Significant	Increase in grain size and pore size
Final	Pore closure , final densification	Negligible further loss	Slow and relatively minimal	Extensive grain and pore growth

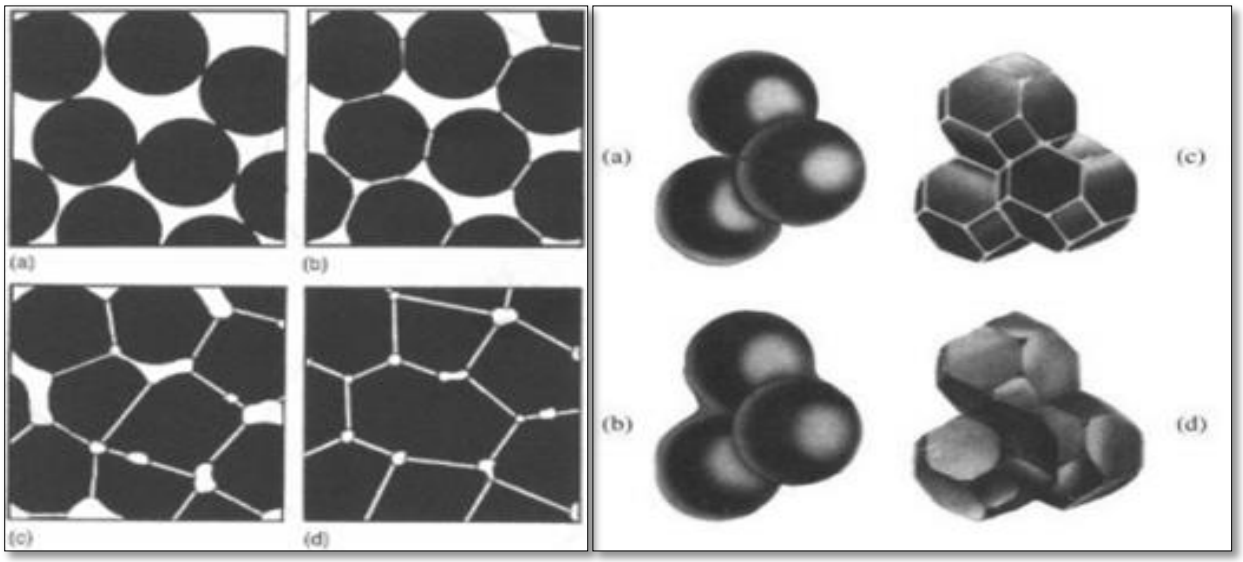

Fig. I.14: Schematic microstructures of the various stages of sintering ; a) stage 0, contact formation; b)initial stage, neck growth; c) intermediate stage, pore rounding and elongation; d) final stage, pore closure, final densification [26].

I.4.6.1 Stage zero (Adhesion) and initial stage

Before sintering, in the first stage called initial stage grains were contacted each other, grain boundary areas grew and grains started to merge. In this stage, grains were smaller than merged grains formed because of sintering; however, pores were larger before sintering process [27].

I.4.6.2 Intermediate stage

In the intermediate stage**,** necks were formed between adjacent grains. There were small numbers of large grains instead of large number of small grains. Pores were smaller than pores before sintering. However, grain merging was not completed. Grain growing was continued in this stage. The surface area of the powder in this stage is smaller than surface area before sintering [27].

I.4.6.3 Final stage

In the final stage merging was completed. Grains were larger than calcined ceramic's grains. Small pores were formed, Porosity does not change and small pores remain even after long sintering times Surface area was decreased. It is smaller than the surface area in the other two stages [27, 28].

I.4.7 Types of sintering

There are three types of sintering with different densification mechanisms:

I.4.7.1 Solid phase sintering

The powder is heated at high temperature but none of the constituents melts. The bonds between the particles are mainly by displacement of atoms. This process is done by diffusion of matter in the solid state. The driving force of this spontaneous process, activated by temperature, is the reduction of the large surface energy present in the material at the beginning of sintering. This reduction is effected by different material transfer mechanisms, depending on the system in question. Active sintering occurs when the sintering atmosphere interacts with the material [29].

I.4.7.2 Liquid phase sintering

In this sintering process, one of the (minority) constituents of the powder mixture passes into the liquid phase. As in solid-phase sintering, interfacial energy reduction is the driving force. The property of wetting of the solid phase by the liquid phase is important for carrying out the sintering. The densification during the liquid phase sintering takes place in

three steps**:** rearrangement, dissolution-reprecipitation and grain growth as can be seen in **Fig.I.15** during heating to reach the melting temperature of one of the components, solid phase densification can occur. It can be consistent for some systems. Once the phase of lowest point of melting becomes liquid, the grain rearrangement step is activated. Then there is an adjustment of the shape of the grains which leads to an important pore removal. Finally, during the last stage a microstructural growth is observed, during which the average grain and pore size increases continuously [21].

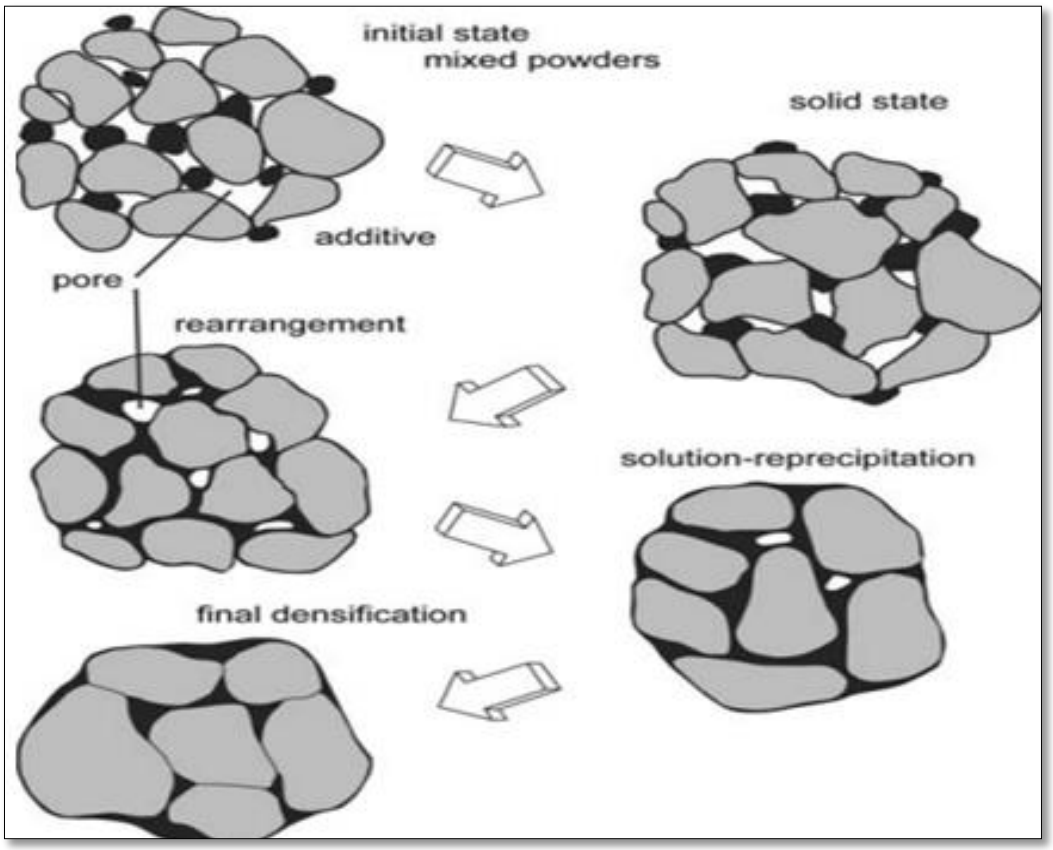

Fig.I.15: Steps of sintering process at liquid state of the powder [21].

I.5 Conclusion

From this chapter the powder metallurgy (PM) is the art as well as science of producing powders and using them to make useful objects. Products in powder metallurgy are often made with a mix of different powders or may sometimes even contain constituents in order to improve the bonding qualities of the particles and properties of the final product**.**

Chapter II:

Research studies on non-metallic powders

Chapter II Research studies on non-metallic powders

II.1 Introduction

The different previous studies about compacting and sintering of non- metallic powders will be presented in this chapter.

This chapter presents brief of these scientifics examples about compacting and sintering of brick product, and presents also some results (the effect of compaction and sintering processes on the final properties of the brick product).

II.2 The first examples of a research study

Agarwal et al [13], have studied the sintering behavior of red mud compacts for different parameters such as composition, temperature, time of soaking during sintering and studies their effect on compressive strength, phase transformation.

II.2.1 Materials and techniques

• They used red mud sample from NALCO (Damanjori) and compacted with the help of press at a load of 4 tones.

• In their work, the parameters, which changed during sintering, are as follows:

1) Temperature: 430, 650, 970 and 1100 °C.

2) Soaking time: 30 mins, 1hr and 2hr for each temperature.

• Then testing of the sintered product is done by various tests, which are:

1) Micro-hardness test, by using micro-hardness tester to determine the hardness of each sample.

2) Compression Test in Instron 1195 to determine the load bearing capacity of the sintered product, which can be used for building bricks.

3) X-Ray Diffraction Test by X-Ray diffractometer. It is used to determine and study the phases present.

II.2.2 Collection and compaction of the samples

They collected the red mud which is in coarse shape which having brick red colour. Then the sample is dried at 110°C for complete removal of moisture which's done by placing the sample in the furnace for 1hr. After removal of moisture, the sample is crushed in a ball mill to obtain grain with fine size. Then appropriate amount of sample is taken in a die such that the ratio of diameter and thickness remains between 2-2.5. Then compact is done in compact machine and the process is repeated for making a number of samples **(Fig II.1)**.

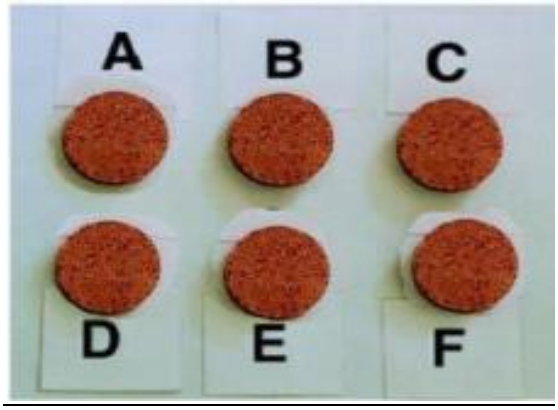

Fig II.1: Macrographic view of red mud compacts [13].

II.2.3 Results

The main results of authors are:

II.2.3.1 Density Change

Initially it is observed that density decreases when the sample is sintered at 400°, but after wards there is a constant rise in density up to 1100° after which density again decreases **(Fig II.2).** According to the authors, initial decrease may be due to loss of volatiles present in the red mud sample.

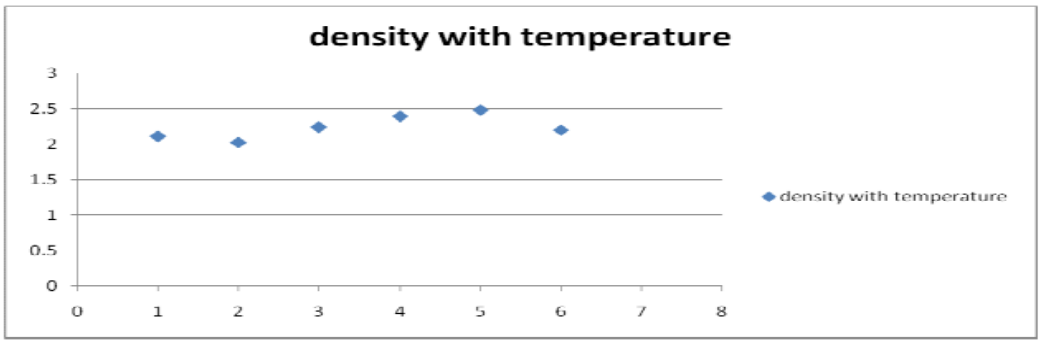

Fig.II.2: Density v/s temperature curve [13].

II.2.3.2 Mechanical properties

The hardness of samples at deferent sintering temperature is presented in **Tab. II.1**.

Tab. II.1: Hardness of samples at deferent sintering temperature [13].

	VHN		
Time	**Sample sintered at 430°c**	**Sample sintered at 650°c**	**Sample sintered at 970°c**
30 mins	9.6	19.5	35.5
60 mins	11.32	21.39	41.47
120 mins	14.10	32.0	46.05

The mechanical properties; hardness and compressive strength increase in the value with increase in sintering temperature. The increase is not uniform. In particular a slower rate of increase is noted above 1000°C. The temperature range chosen here is the most interesting range, since the mechanical properties in this range compare well with those of commercial ceramics. Just beyond 1050°C a solid solution is formed between hematite and rutile (TiO2). Also soda feldspar and silica form a binary eutectic at 1062°C. These transformations are probably responsible for the "discontinuity" in most of the curves.

After their work, they summarize, the following important conclusions deduced from the data and observations presented in this work:

1) The particle size and the mineralogy of bauxite waste allow developing ceramics of high strength and toughness.

(2) The toughness of this red mud ceramic is comparable or superior, depending on sintering temperature, to values obtained for other porous ceramics.

II.3 The second example of a research study

Jie-Guang et al [30], have investigated the" Effect of the sintering technology on the properties of fired brick from quartz sands".

They focused on the effect of sintering temperature on the final proprieties of fired brick from sands.

II.3.1 Materials and techniques

They used river sands as the main raw materials to prepare bricks. The component analysis of the river sands are shown in **Tab.II.2**. Sintering additives (5 wt% CaO) were mixed with the river sands by a ball milling method, and then the composite raw materials were molded by different methods, drying, sintering under a normal atmosphere with a muffle furnace and tested.

The phase analysis was perfomed by X-ray powder diffraction (XRD) (Model: D/Max-RB, Japan). The compressive strengths of fired brick were tested by a universal mechanical tester (Model: AGS-5KNJ, Japan), and the microstructural analysis of the fired bricks was performed by scanning electron microscopy (SEM) (Model: JSM- 5610 LV, Japan).

Tab.II.2: The component analysis of the river sand [30].

Chemical composition	**SiO_2**	**Al_2O_3**	**CaO**	**MgO**	**Other**	**Ignition loss**
Content (wt %)	84.21	6.69	1.47	1.01	2.04	4.58

II.2.3 Finding

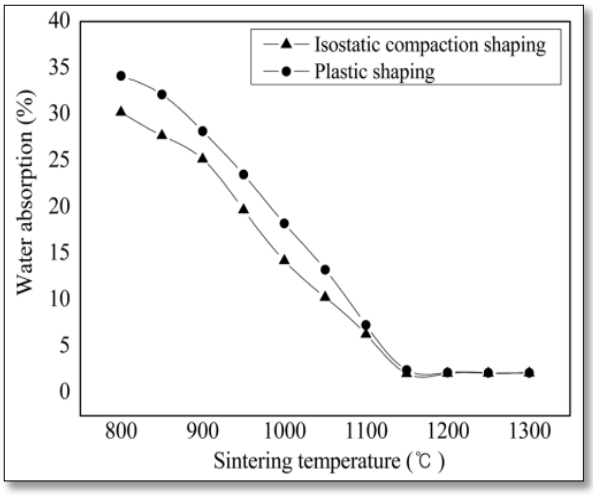

Fig.II.3: Effect of sintering temperature on water absorption of fired bricks[30].

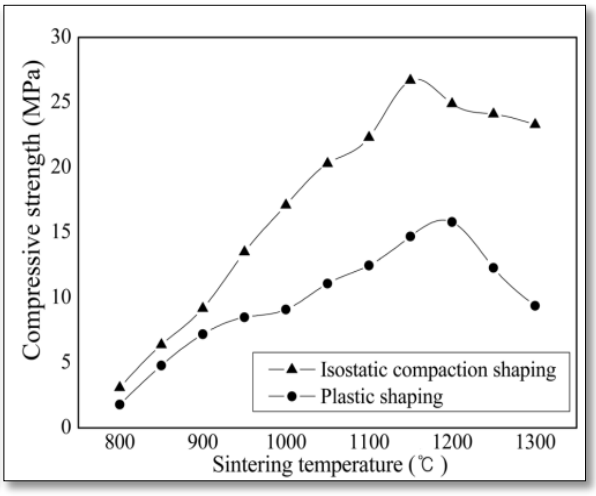

Fig.II.4: Effect of the sintering temperature on the compressive strength of fired bricks[30].

The effect of the sintering temperature on the water absorption of bricks is shown in **Fig.II.3**, the water absorption of bricks is first decreased and then increased with an increase in the sintering temperature. The effect of the sintering temperature on the compressive strength of bricks is shown in **Fig.II.4**, the compressive strength of bricks is first increased

and then decreased with an increase in the sintering temperature, the compressive strength of a brick reaches 28 MPa at 1150 ^{o}C using the 20 MPa isostatic compaction shaping method.

Fig.II.5 shows the phase analysis of raw materials, fired bricks at different temperatures; the quartz sands include quartz, potassium feldspar, and white mica. The voids formed in the brick are then filled by the liquid glass phase to decrease the porosity, which increases the density **(Fig.II.6)** and compressive strength.

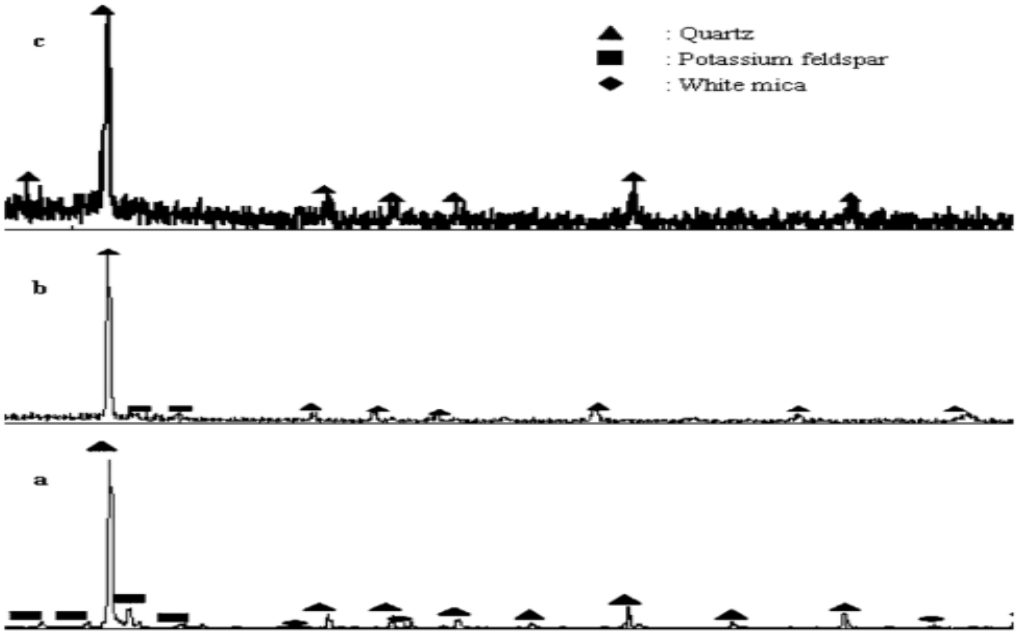

Fig.II.5: Phase analysis of raw materials and fired bricks; a) raw materials, b) sintering at 1100 °C and c)intering at 1150 ^{o}C),[30].

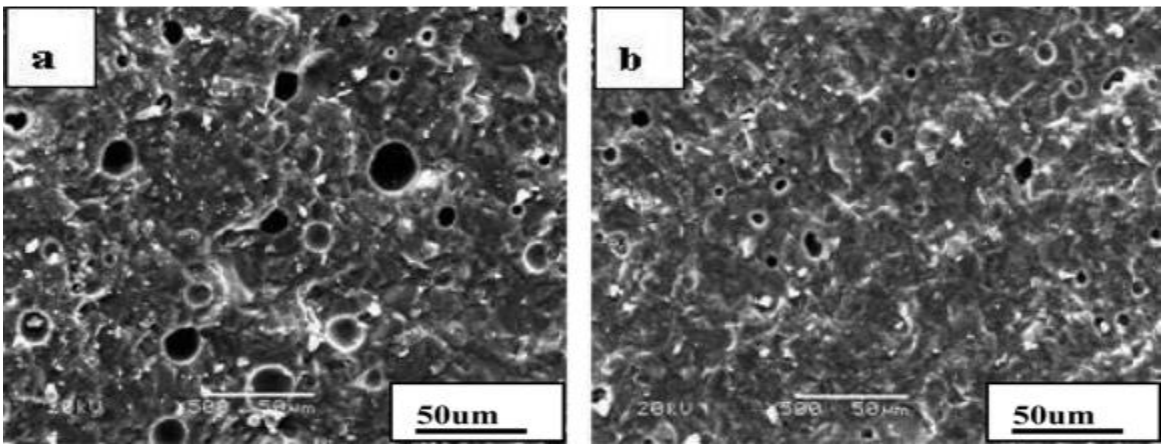

Fig.II.6: Effect of the sintering temperature on the microstructure of fired bricks made by the 20 MPa isostatic compaction shaping method (a-1100 ^{o}C and b-1150 ^{o}C)[30].

II.4 The third examples of a research study

Johari et al [31], have interested to study the "Effect of the change of firing temperature on microstructure and physical properties of clay bricks from beruas (malaysia)".

II.4.1 Materials and techniques

They used clay from Beruas, (Malaysia) and they apply different techniques of characterization:

1) Identification of phase changes before and after firing clay was investigated by the XRD technique using a Bruker D8 advance machine.
2) An X-Ray spectrometer machine, Rigaku RIX 3000, was used to determine the chemical composition of the clays.
3) A muffle furnace, model Carbolite 1400. For firing the deferent samples from 800°C to 1250°C, with 1 hour soaking time, respectively.
4) The particle morphology of the materials was performed by scanning electron microscopy (SEM).field emission scanning electron microscope (FESEM) with high resolution imaging was used to characterize the samples.
5) The fired-clay brick samples were subjected to compressive strength, water absorption and porosity tests. It was performed according to BSEN 772-1 (2000), BSEN 772-7 (1998) and ASTM C20 respectively.

II.4.2 Properties of clay

The physical colour of clay supplied was grey. After the sintering process, the colour of fired-clay brick turned into dark red at the temperature of 1200°C and indicated that there is a Fe_2O_3 content. It is shown from the XRF analysis as tabulated in **Tab.II.3**. The clay contained less than 3 wt% fluxing components (K_2O, Na_2O and CaO).

Tab.II.3: XRF analysis of clay from Beruas, Malaysia (wt %) [31].

Component	SiO_2	Al_2O_3	Fe_2O_3	K_2O	MgO	Na_2O	CaO	P_2O_5	LOI
Wt%	67	26	2.9	2.1	1.2	0.069	0.00	0.036	8.75

II.4.3 Results

II.4.3.1 Phase identification

Fig.II.7 presents the XRD patterns of clays. The clay is contains two major minerals, kaolinite $Al_2(Si_2O_5)(OH)_4$ and quartz SiO_2 Other minerals such as microline $KAlSi_3O_8$ and

muscovite $K(MgAl)_{2.04}(Si_{3.34}Al_{0.66})O_{10}(OH)_2$ were detected. **Fig.II.8** presents XRD of fired-clay bricks at different temperatures.

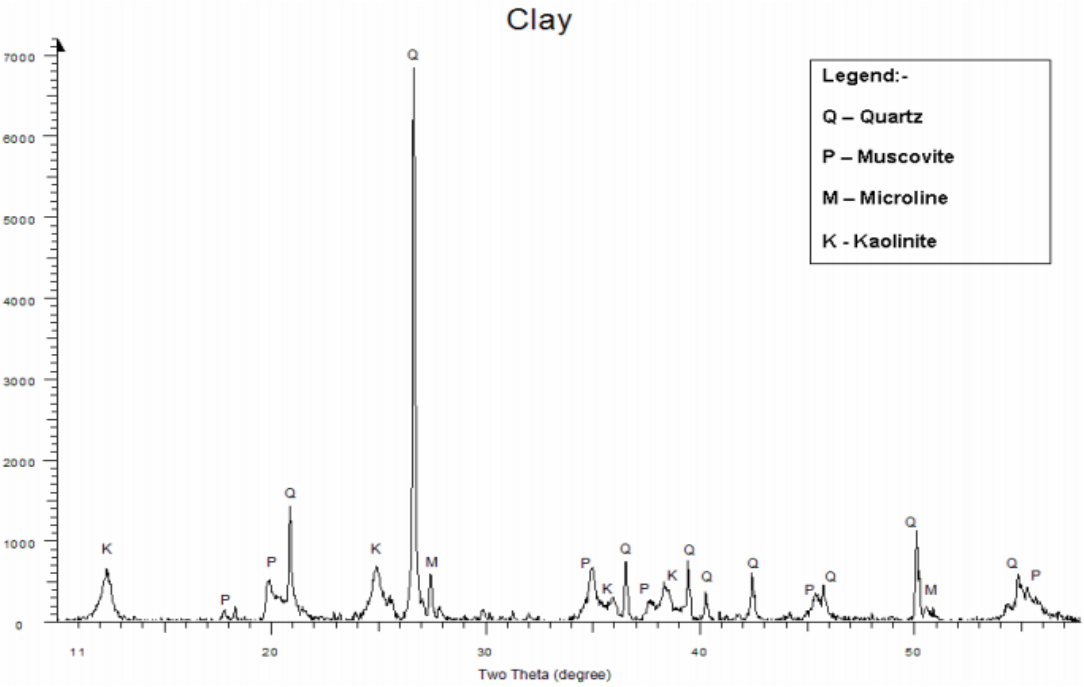

Fig.II.7: XRD of clay taken from Beruas, (Malaysia) [31].

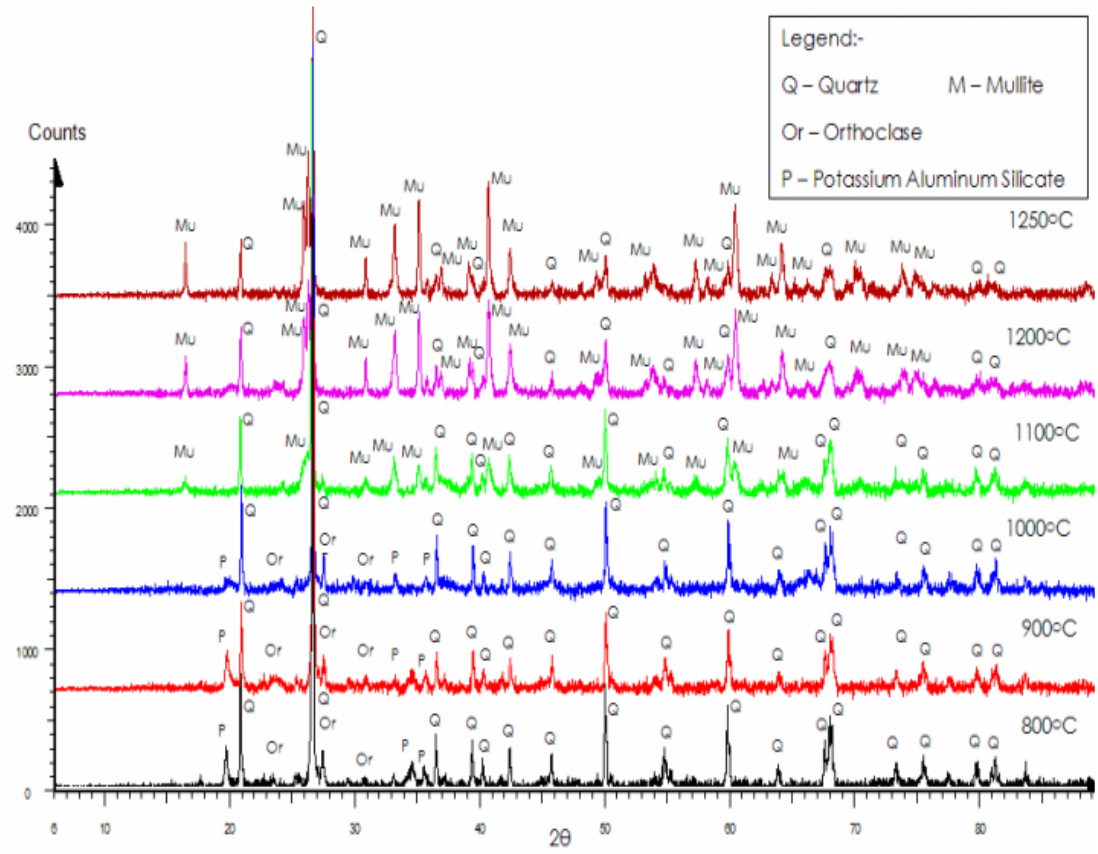

Fig.II.8: XRD of the clay fired at different temperatures [31].

II.4.3.2 Microstructure of clay brick

Fig.II.9 shows the microstructure of the fracture surface of the clay bricks sintered from 800°C to 1250°C for 1 hour. The microstructure changes with the sintering temperature. At 800°C and 900°C, the brick has not yet experienced full solid-state sintering process since the individual clay particles are still existent. Because the brick structure formed at lower temperatures (840-960 °C) remained essentially the same until temperatures of over 1080°C are reached.

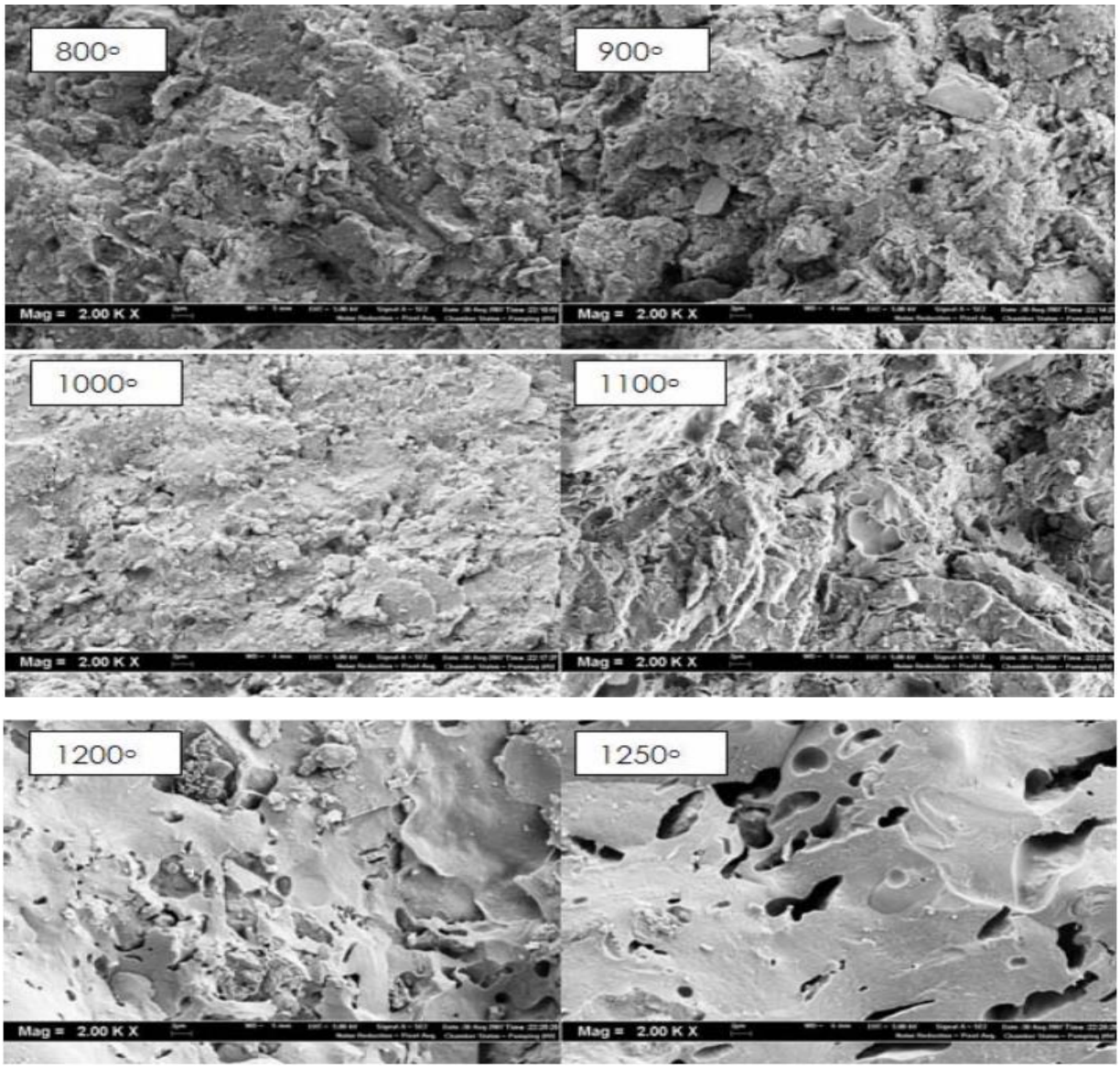

Fig.II.9: SEM micrographs for the clay fired at different temperatures [31].

II.4.3.3 Porosity and water absorption

The porosity of brick shows an increment of 1.4% and 0.1% from 800 °C to 900 °C and 900 °C to 1000°C, respectively (**Fig.II.10**). The increasing in porosity was the result of diffusion at relatively low temperature without significant shrinkage. The shrinkage value for temperature 800°C, 900°C and 1000°C is 0.31%, 0.50% and 1.04%, respectively. The bricks that were sintered until 1000°C are considered as having a porous structure since their water absorption rates are higher than 25%, as shown in **Fig.II.11**.

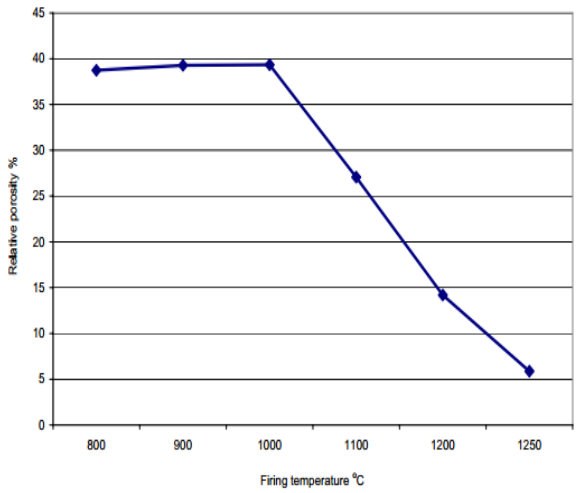

Fig.II.10: Effect of firing temperature of the clay on the porosity[31].

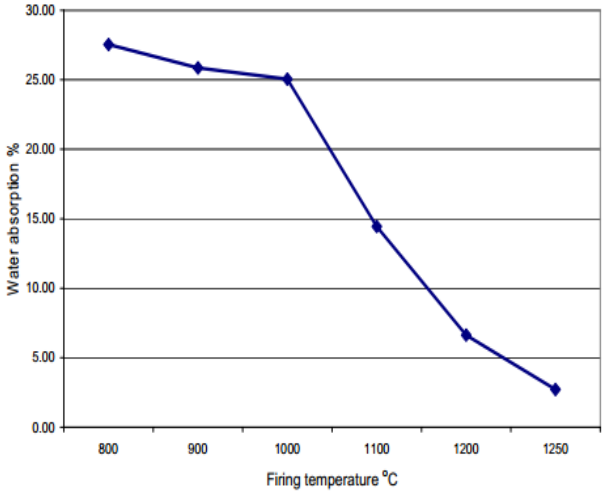

Fig.II.11: Effect of firing temperature of the clay on the water absorption[31].

Between 1000°C to 1100°C, the solid state sintering becomes very significant since the clay body had been fully sintered. Very few pores can be seen in the microstructure. Brick porosity value reduces significantly from 39.33% to 27.06% and it was 31% reduction. The shrinkage value increases 74% causing the reduction in volume for brick sintered from temperature 1000°C to 1100°C. A progressive gain in strength can be observed on brick sintered at 1100°C where the compressive strength increased from 25.4N/mm^2 to 71.8 N/mm^2.

During liquid phase process, the reduction of pores becomes more significant as the compacted structure starts to increase its performances, such as strength and water permeability.

The fired-clay brick sintered at 1100°C begins to diffuse and shrink as the liquid phase starts to form and fill up the pores, creating smaller pores. The brick shrunk 37% when sintered from 1100°C to 1200°C causing the porosity to reduce 47.5%. The effect of firing

also causes the water absorption value to reduce 42% lower than the value for brick sintered at 1000^{o}C.

The sintering process reached the optimum temperature at 1200°C, where by its microstructure contains minimum pores with porosity value 14.2 % and produces the highest strength, 89.5 MPa.

II.5 The fourth examples of a research study

Amkpa et al [32] have investigated the "influence of sintering temperatures on physico-mechanical properties and microstructure of refractory fireclay bricks".

They prepared their samples after milling the clay into fine powder particles, and passed the specimen powder into pallets using Caver hydraulic pressing machine. A force of 4 tonnes was applied with a holding time of 60 seconds. The samples were then transferred into furnace and subjected to thermal treatment by sintering process at varied sintering temperatures of 900^{0}C, 1000 ^{0}C, 1100 ^{0}C and 1200 ^{0}C for 8 hours as soaking time with heating rate of 2.5 °C/min.

II.5.1 Materials and techniques

The main techniques of characterization are*:*

The X-ray diffraction (XRD) patterns were achieved using a BRUKER D8 ADVANCE machine. The chemical composition was determined using the Oxford X-Supreme 8000 (XRF) technique. The Scanning Electron Microscopy (SEM), JEOL JSM-6380LA and energy dispersive X-ray spectroscopy (EDX) were used to determine the elements dominate in the fireclay brick specimens and to observe the surface morphology of the deferent fireclay bricks.

II.5.2 Results

II.5.2.1 Microstructures

The SEM micrographs were taken on X1500 magnification. Both clay samples showed a remarkable improvement on densification. As sintering temperatures increases, there was progressive improvement on the surface morphology of Kpata and Qua'an Panfireclay bricks as presented in **Fig.II.12** and **Fig.II.13**. Percentage porosity reduced as sintering temperatures were increased.

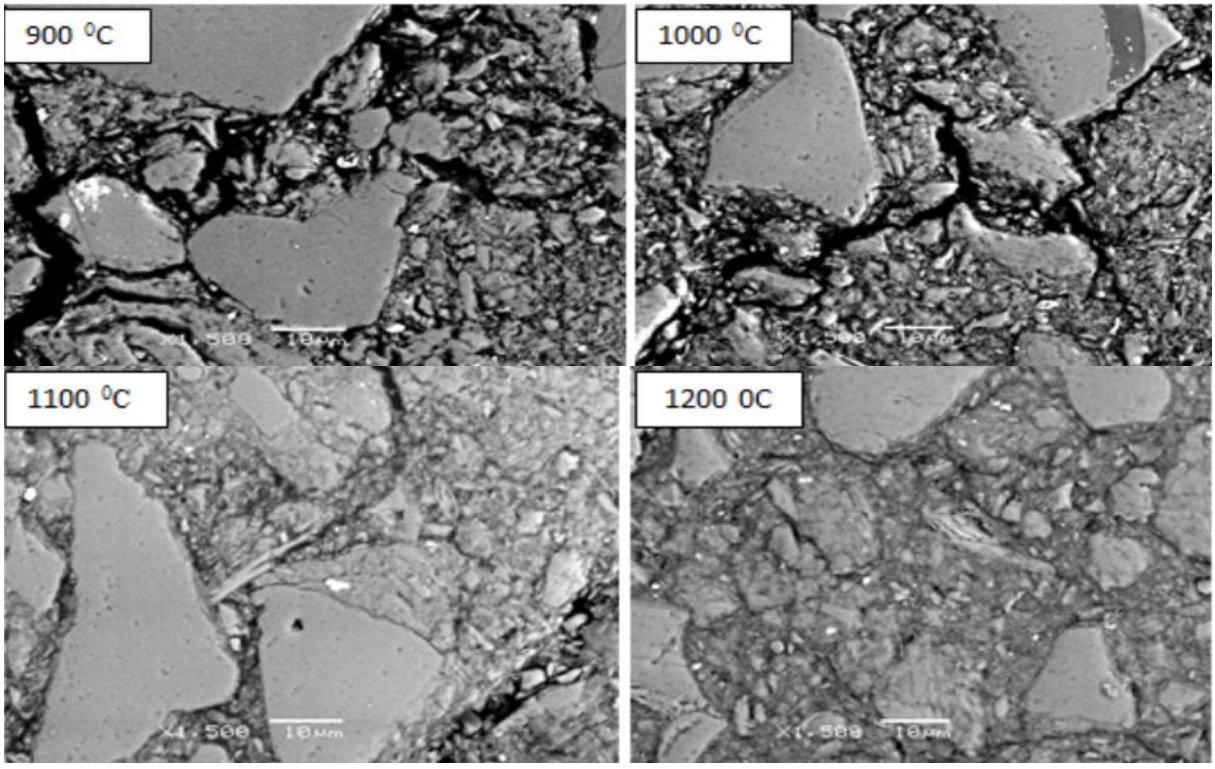

Fig.II.12: SEM micrographs (X1500) of Kpata fireclay brick and surface morphology at varied sintering temperatures [4].

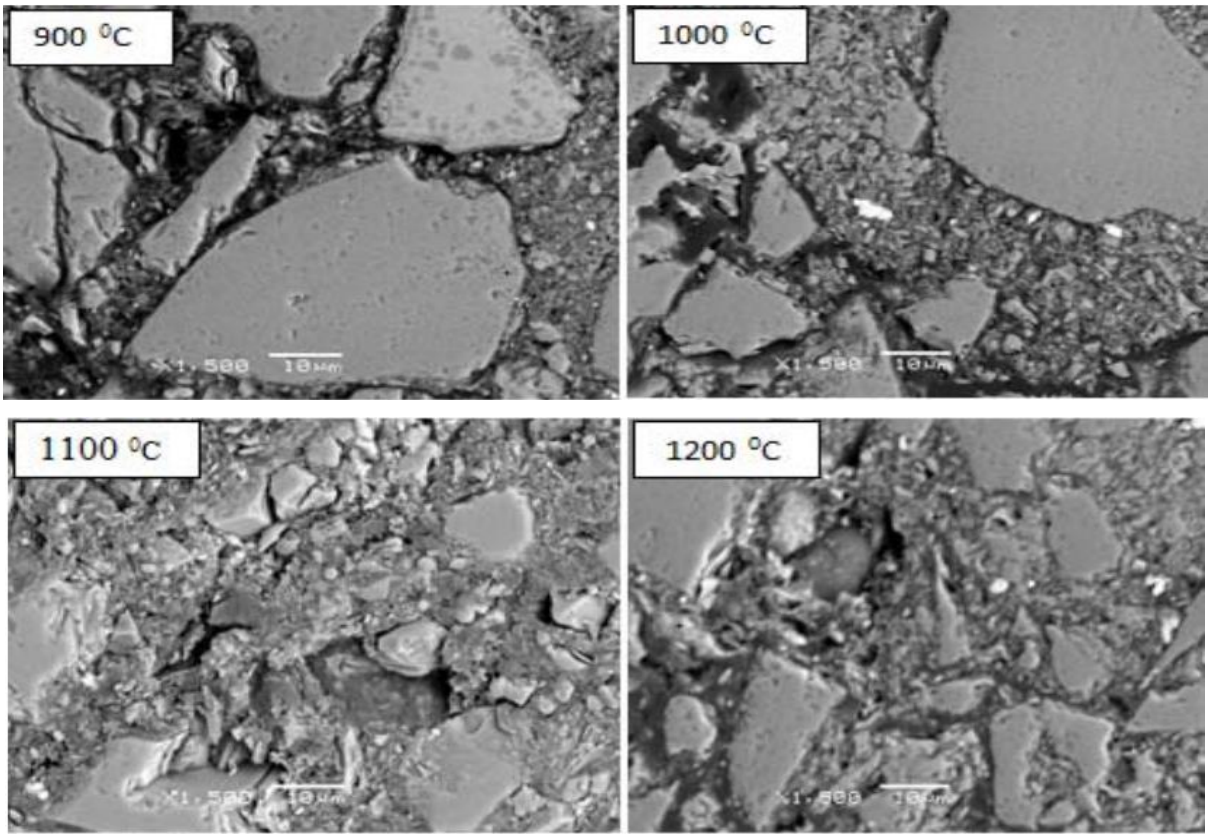

Fig.II.13: SEM micrographs (X1500) of Qua'an Pan fire clay brick and surface morphology at varied sintering temperatures [32].

II.5.2.2 Porosity

In the evaluation of physical and mechanical chattels, the evaluated results of percentage porosity strength in **Fig.II.14** of Kpata fireclay brick and of Qua'an Pan fireclay brick respectively, exhibited that Kpata fireclay brick had maximum porosity of 43.76 % at 900 ^{0}C sintering temperature, with then minimum porosity of 25.41 % attained at the best sintering temperature of 1200 ^{0}C. The Al_2O_3 was responsible for the strength in the clay material.

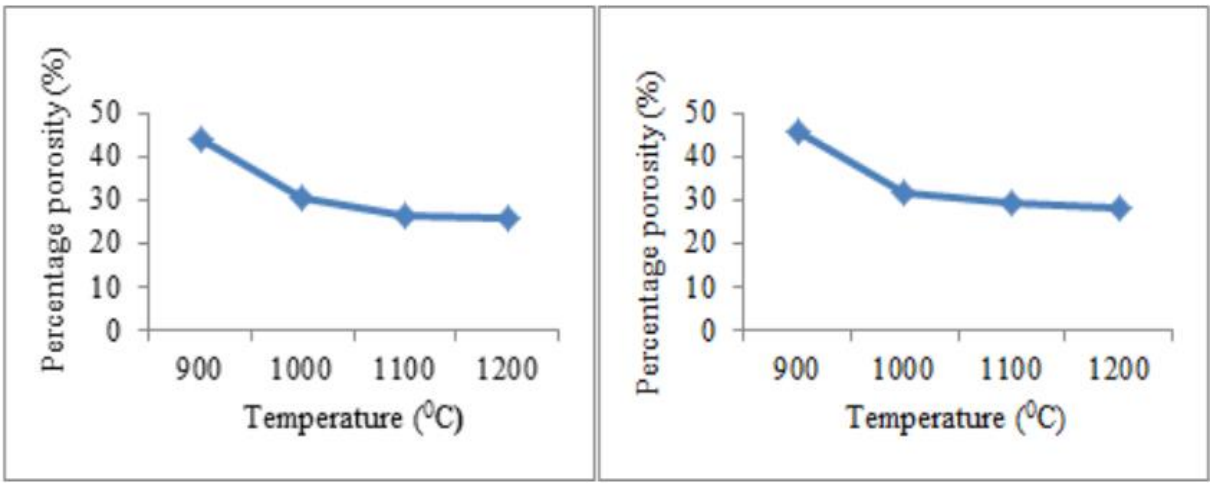

Fig.II.14: Percentage porosity against varied sintering temperatures of Kpata and Qua'anPan fireclay bricks [32].

II.6 Conclusion

From these previous studies, we can conclude that the firing has a positive influence on the microstructure of brick promoting a dense structure with low permeability.

Their results indicate that the physical and mechanical properties (compressive strength, porosity and water absorption value) of bricks can be controlled to a significant extent by varying the firing temperature.

In our studies, we will investigate the effect of change of sintering temperature, type of sand and the loads of compaction on the final properties of brick.

Chapter III:

Materials and experimental techniques

III.1 Introduction

This chapter presents the different steps of preparing the brick product in"SARL Eloutaya.Poterie and describes our experimental techniques used in laboratory for synthesis and characterizing the prepared samples.

The analysis and techniques of characterization used in this work are: particle size analysis, X-ray diffraction (XRD), Infrared spectroscopy, optical microscopy, water absorption and bulk density.

III.2 The brick product preparation in "SARL Eloutaya. Poterie"

III.2.1 The different steps of preparation

The different steps and conditions of preparing the brick product, in"SARL Eloutaya. Poterie" are summarized below:

Step 1: Extraction of clay and sand from Braniss and Eloutaya respectively and storing them in the factory **(Fig.III.1)**.

Fig.III.1: The raw materials: sand and clay.

Step 2: Wet milling process of clay **(Fig.III.2)** in three stages to reduce the particles size less than 2 mm.

Fig.III.2: Wet milling process

Step 3: Mixing 30% of sand with 70 % of clay.

Step 4: Molding the green compact (green brick) with adding amount of water at pressure equal to 36 bar, followed by cutting process to obtain brick (**Fig.III.3)**.

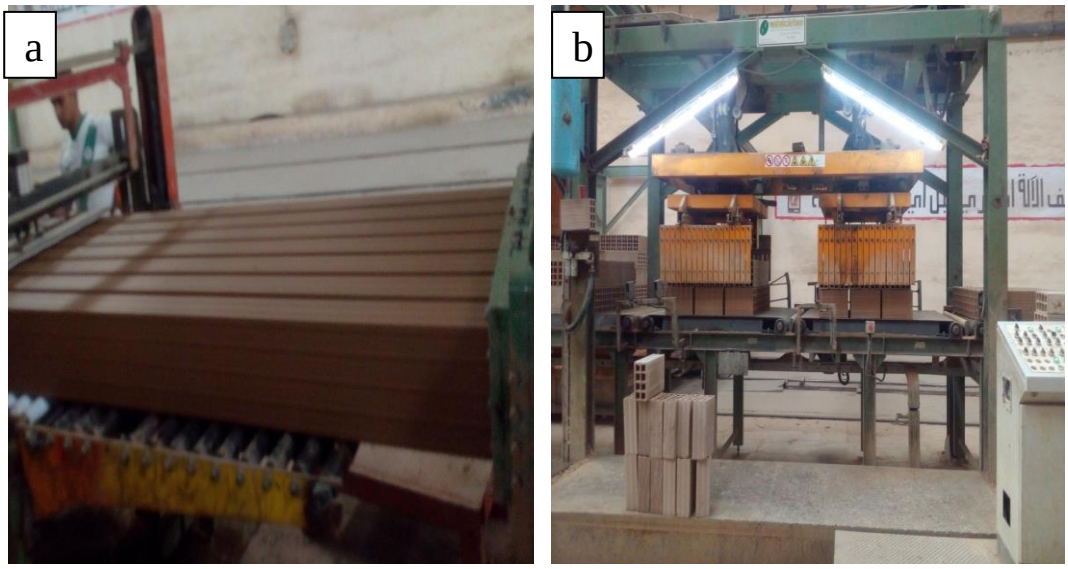

Fig.III.3: The molding and cutting processes: a) molding, b) cutting.

Step 5: Drying the green brick in kiln at 80°C for 24h.

Step 6: Sintering (firing) the green brick in continuous furnace at 850°C **(Fig.III.4).** The output of brick product is presented in **Fig.III.5.**

Fig.III.4: Continuous furnace of the factory.

Fig.III.5: The output of bricks product from the furnace.

Step 7: Finish products. **Fig.III.6** shows the final product (bricks).

Fig.III.6: The finish product(bricks product).

III.2.2 Characterization of samples from SARL Eloutaya. Poterie

The three samples of powders (clay and sand), dried brick and fired brick are presented in **Fig.III.7** these samples belong to SARL Eloutaya. Portrie.

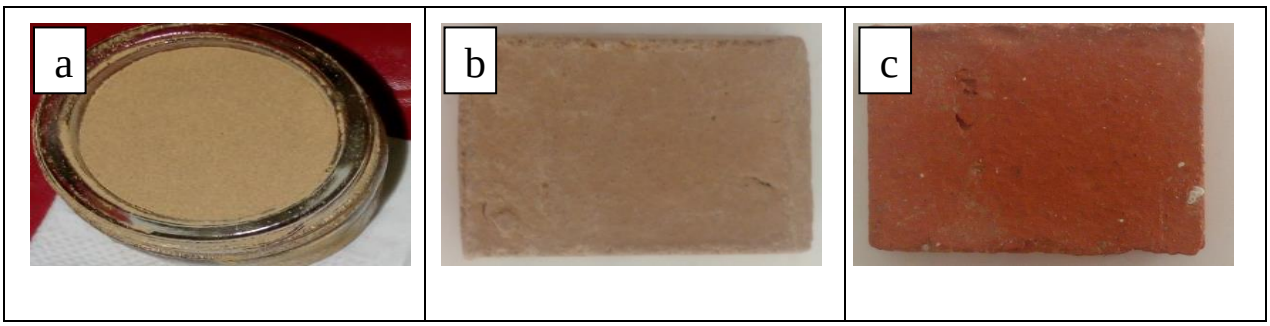

Fig.III.7: Samples from SARL Eloutaya. Poterie; a) mixture of powders before molding, b) dried sample at 80°C, c) sintered sample at 850°C

Identification of samples phases was proceeding out by the XRD technique, the microstructure of sample (c) by optical microscopy and the characteristics was tested by water absorption, apparent porosity and bulk density.

III.3 Materials and experiment techniques of synthesis and testing of samples.

III.3.1 Studied material

The studied material in this work is brick which contain 30% of sand and 70 % of clay. The clay and the sand are obtained from"SARL Eloutaya. Poterie".

In this work, Biskra sand was replaced with dunes sand (Ouargla), the different characteristics of this brick product was studied **(Fig.III.8)**.

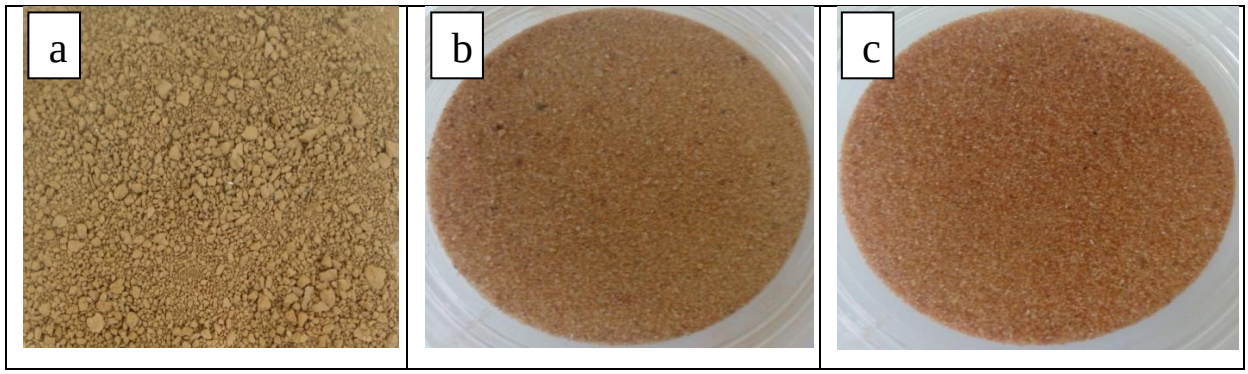

Fig.III.8: The studied materials; **a**) Clay of Branis (Biskra), b) Sand of Eloutaya (Biskra) and c) Sand of Ouargla (Sahara).

III.3.1.1 Chemical analysis

The Chemicals analysis of the raw materials (clay, Biskra sand and Sahara sand) are in the **Tab. III.1.**

Tab. III.1: XRF analysis (chemical composition) of raw materials

Component (%)	SiO_2	Al_2O_3	Fe_2O_3	CaO	MgO	Na_2O	SO_3	Cl^-	LOI	H_2O
Clay	56.54	17.82	5.25	11.25	3.26	0.68	1.44	0.2901	17.48	0.57
Biskra sand	79.85	2.39	0.6	9.33	1.22	0	0.45	0.009	4.24	1.02
Sahara sand	85.75	1.26	0.39	5.86	1.06	0	0.6	0.053	1.27	0.01

III.3.2 Preparation of powders (Collection and milling)

III.3.2.1 Clay preparation

The clay was supplied by brick factory of SARL Eloutaya.Poterie,Biskra. The material collected was wet and in coarse form, and was then exposed to ambient sun for 7 days to be dry. After that was milled manually in laboratory into mortar and was sieved to obtain the desired particle size **(Fig.III.9)**.

Fig.III.9: Milling and sieving operations in laboratory:a) coarse clay, b) milling and sieving, c) fine clay(grain sise less then315um).

III.3.2.2 Sands preparation

III.3.2.1.1Particle size analysis (granulometric analysis) of Biskra sand

III.3.2.1.1 Purpose of granulometric analysis

This test is performed to determine the percentage of different grain sizes contained within sand, and to know if the curves are continuous or discontinuous as it has been indicated in chapter IV.

III.3.2.1.2 Definition

Granulometric analysis is a procedure, which is used to assess the particle size distribution of a granular material. The size distribution is often of critical importance of the brick application. A sieve analysis can be performed on any type of non-organic or organic granular materials including sands, clays, and soil, a wide range of manufactured powders, grain and seeds, down to a minimum size depending on the exact method. Being such a simple technique of particle sizing, it is probably the most common [33].

III.3.2.1.3 Principle of the particle size analysis

1) Write down the weight of each sieve as well as the bottom pan to be used in the analysis.
2) Weight 2000 g of dry sand sample (**Fig.III.10.a**).
3) Make sure that all the sieves are clean, and assemble them in the ascending order of sieve numbers (2.5mm sieve at top and 0.08 mm sieve at bottom). Place the pan below 0.08mm sieve. Carefully pour the sand sample into the top sieve and place the cap over it.
4) Place the sieve stack in the automatic sieve shaker D407 and shake for 10 minutes (**Fig.III.10.b**).
5) Remove the stack from the shaker and carefully weigh and record the weight of each sieve with its retained soil. In addition, remember to weigh and record the weight of the bottom pan with its retained fine sand.

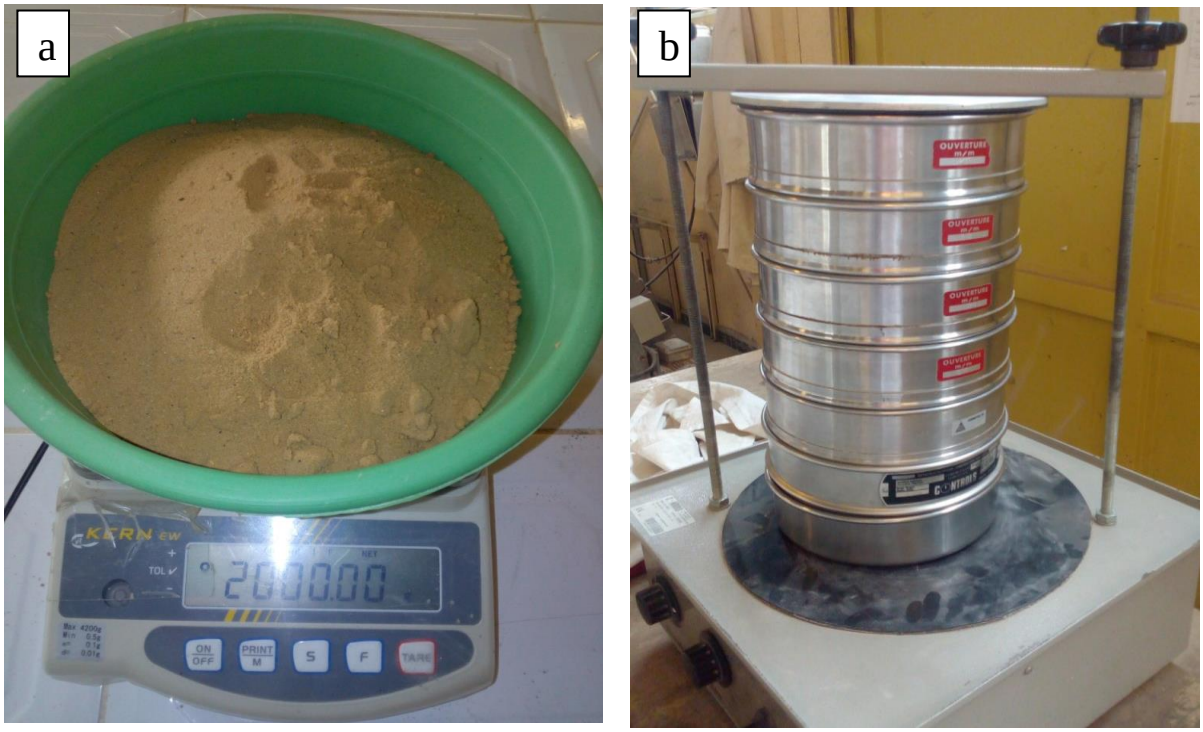

Fig.III.10: Granulometric analysis operations; a) Sand sample in the balance, b) set of sieves at sieve Shaker.

The percent retained is calculated as:

$$\text{Retained}(\%) = \frac{\text{mass retained}}{\text{total mass}} \dots\dots\dots\dots\dots (\text{Equ. III. 1})$$

From this, the

$$\text{Passing}(\%) = 100 - \text{retained}\ (\%) \ldots\ldots\ldots\ldots\ldots \text{(Equ. III. 2)}$$

According to French Standard [NFP 18-540][34]:

The modulus of fineness is equal to 1/100 of the sum of the cumulative refusals (retained) expressed in percentages on the sieves of 0,16 - 0,315 - 0,63 - 1,25 - 2,5 -5 mm.

$$\text{Mf} = \frac{1}{100}\sum \text{retained}(\%)\text{of sieves}\ \{0.16, 0.315, 0.63, 1.25, 2.25, 5\} \ldots\ldots \text{(Equ. III. 3)}$$

When Mf is between:

- < 1.8: sand very fine grain
- 1.8 and 2.2: sand is mostly fine grain
- 2.2 and 2.8: there is preferential sand
- 2.8 and 3.3: the sand is a bit coarse.

Note: We repeat the same steps with Sahara sand.

III.3.2.3 Mixing and blending the powders

In our work two mixtures of powders were prepared. The first contains 70 % of Biskra clay and 30% of Biskra sand and the second contains70 % of Biskra clay and 30% of Ouargla sand. We note that each mixture was mixed for the homogenization of powders.

III.3.3 Infrared spectroscopy technique

III.3.3.1 Definition

Infrared spectroscopy is the study of interaction of infrared light with matter, the method or technique of infrared spectroscopy is conducted with an instrument called an infrared spectrometer (or spectrophotometer) to produce an infrared spectrum. An IR spectrum is essentially a graph of infrared light absorbance (or transmittance) on the vertical axis vs. frequency or wavelength on the horizontal axis. Typical units of frequency used in IR spectra are reciprocal centimeters, with the symbol cm^{-1}. Units of IR wavelength are commonly given in micrometers, symbol μm, which are related to wave numbers in a reciprocal way. A common laboratory instrument that uses this technique is a Fourier transform infrared (FTIR) spectrometer [35].

III.3.3.2 Principle

Infrared region is further divided into three subregions: near-infrared, mid-infrared and far-infrared. The most commonly used is the middle infrared region, since molecules can absorb radiations in this region to induce the vibrational excitation of functional groups. By passing infrared light through a sample and measuring the absorption or transmittance of light at each frequency, an infrared spectrum is obtained, with peaks corresponding to the frequency of absorbed radiation. Since all groups have their characteristic vibrational frequencies, information regarding molecular structure can be gained from the spectrum [36].

The molecular structure of the raw materials (two mixtures) has been identified in the infrared region with Infrared spectroscopy analysis named FTIR 8400S (**Fig.III.11)**, in the wavelength range of 450 cm^{-1} to 4000 cm^{-1}.

Fig.III.11: Machine of infrared spectroscopy analysis (FTIR 8400S).

III.3.4 X-ray diffraction (XRD) technique

III.3.4.1 Definition

Coherent scattering of X-rays from crystalline materials, leads to diffraction. Since its discovery in 1912 by von Laue, x-ray diffraction (XRD) has provided a wealth of information about the structure and chemical composition of crystalline materials. For compositional analysis, the technique is unique in that it is the only analytical method capable of providing

qualitative and quantitative information about the crystalline compounds (phases) present in a solid., the technique can determine the percentage of phases present in a mixture of the compounds, whereas other analytical techniques can only give the percentage of the elements in the mixture [37].

III.3.4.2 Principle

The requirements for X-ray diffraction are the atomic spacing in the solid must be comparable with the wavelength of the X-rays and the scattering centers must be spatially distributed in an ordered way The diffraction of X-rays by crystals was treated by Bragg in 1912. The condition for constructive interference, giving rise to intense diffraction maxima, is known as Bragg's law:

$$2d\sin(\theta) = n\lambda \dots\dots\dots (\text{Equ. III. 4})$$

Where ***d*** is the spacing between the lattice planes of the crystal, **θ** is the angle of incidence (or reflection), **n** is an integer (sometimes referred to as the order of diffraction), and **λ** is the wavelength of the x-rays (0.15406 nm for Cu K radiation). When the reflection angle **θ** does not satisfy. (Equ. III. 4)destructive interference occurs.

Identification of the raw materials and our samples were analyzed by XRD technique using a BRUKER D8 ADVANCE machine **(Fig.III.12).** XRD patterns were scanned in steps of 0.0350º in a range of diffraction angles from 10 º to 90º of 2θº, using Copper (CuKα) as X-ray source with a wavelength (λ) of 1.5406 Å.

Fig.III.12: Bruker D8 advance machine.

III.3.5 Microstructure observation

Polarized light microscope named Hund wilovert S **(Fig.III.13)** equipped with a Canon DC58D **(Fig.III.14)** digital microphotography system was used to observe the microstructure of brick samples, as well as shape and size of pores and particles.

Fig.III.13: Optical microscopy (Hund wilovert S).

III.3.6 Preparation of brick samples

The mixture of powders (clay and sand) were compacted uniaxially in stainless steel cylindrical mould (diameter 13 mm) of compacting press named Specac **(Fig.III.14)**. The compaction loads used are 6 and 4 tonnes. The resulting green compacts were fired at different temperature.

Fig.III.14: Compacting press (Specac).

III.3.7 Sintering process

The resulting green compacts were sintered at different temperatures: 750, 850, 900, 1000, and 1200(°C), in furnace named Nabertherm **(Fig.III.15)**, soaked for 2 hours and allow cooling inside the furnace.

Fig.III.15: Sintering furnace (Nabertherm).

The different prepared samples are presented in **Fig.III.16;** where M1, M2 are the mixture with Biskra sand ,Sahara sand respectively and 6,4 are the loads in tonnes.

M1(6)	M1(4)	M2(6)	M2(4)
			

a) Samples before sintering (green compact).

M1(6)	M1(4)	M2(6)	M2(4)
			

b) Samples sintered at 750°C

M1(6)	M1(4)	M2(6)	M2(4)
			

C) Samples sintered at 1200°C

Fig.III.16: The prepared samples under two loads (6 and 4 tonnes); a) Samples before sintering (green compact),b) Samples sintered at 750°C, and c) Samples sintered at 1200°C.

III.3.8 Testing

According to ASTM C830-00 standard tests [38], the determination of the porosity, bulk density and Water absorption of brick is as follows:

For this, we need to know how we calculate the exterior volume, volume of open pores when the liquid is water.

Determination of exterior volume, V:

The exterior volume of the test specimen is its bulk volume, including all solid material, open pores, and impervious portions. Calculate V in cubic centimeters by subtracting the suspended weight from the saturated weight, both in grams, as follows:

$$V(cm^3) = W - S \dots\dots\dots\dots\dots (Equ.\ III.\ 5)$$

Determination of volume of open pores:

Calculate the volume of open pores in the test specimen in cubic centimeters as follows:

$$\text{Volume of open pores}(cm^3) = W - D \dots\dots\dots\dots (Equ.\ III.\ 6)$$

III.3.8.1 Apparent porosity (AP)

The apparent porosity (AP) expresses as a percentage, it is the relationship of the volume of open pores in the test specimen to its exterior volume. Calculate AP as follows:

$$AP\ (\%) = \left[\frac{W - D}{V}\right] * 100 \dots\dots\dots\dots\dots (Equ.\ III.\ 7)$$

Where: D = Weight of dried specimen, V= the exterior volume of specimen, S = Weight of dried specimen suspended in water, and W = Weight of soaked specimen suspended in air.

The test of samples was sintered at the different temperatures for 2 hours. The dry weight of each fired sample was taken and recorded as D. Each sample was immersed in 100 ml of water for 6 hours at room temperature to soak and weighed while being suspended in air. The weight was recorded as W. Finally, the specimen was weighed when immersed in water. This was recorded as S. The apparent porosity was then calculated from the expression(Equ. III. 7).

III.3.8.2Water Absorption, WA

The water absorption expresses as a percentage, it is the relationship of the weight of water absorbed to the weight of the dry test specimen. Calculate AW as follows:

$$\mathrm{WA}\ (\%) = \left[\frac{\mathrm{W} - \mathrm{D}}{\mathrm{D}}\right] * 100 \ldots\ldots\ldots \ (\mathrm{Equ.\,III.\,8})$$

Where: *D* = Weight of dried specimen, and W = Weight of soaked specimen suspended in air.

The test specimens were sintered at the different temperatures for 2 hours. Their dry weights were measured and recorded. They were immersed in 100 ml of water (Equ. III. 7**)** for 24 hours at room temperature, and then reweighed. The percentage water absorption was calculated as showed the formula (Equ. III. 8).

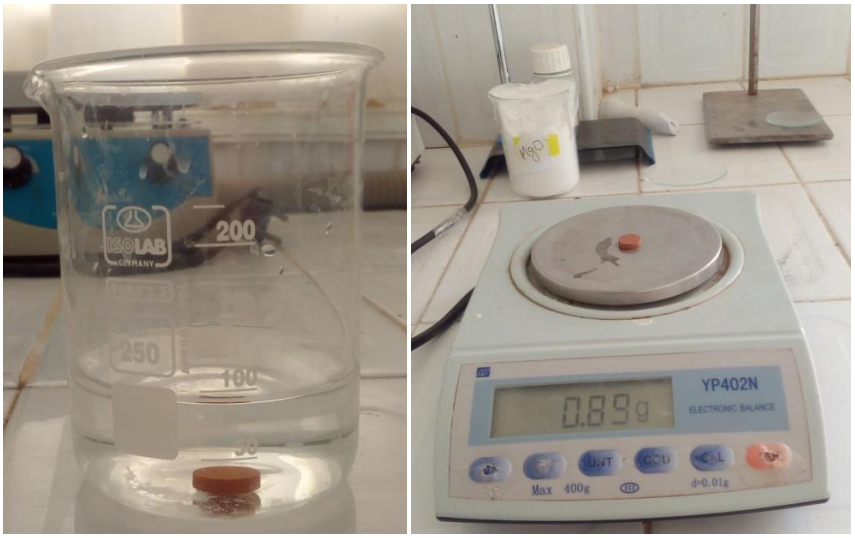

Fig.III.16: Water absorption test (immersion).

III.3.9 Bulk Density, BD

The bulk density (BD) of the test specimen in grams per cubic centimeter is the quotient of its dry weight divided by its exterior volume. Calculate BD as follows:

$$\mathrm{BD}(\mathrm{g/cm^3}) = \frac{\mathrm{D}}{\mathrm{V}} \ldots\ldots\ldots\ldots . \ (\mathrm{Equ.\,III.\,9})$$

Where: D = Weight of dried specimen, and V= the exterior volume of specimen

The test specimens were sintered at the different temperatures for 2 hours. The dry weight of each fired sample was taken and recorded as D. Each sample was immersed in a 100 ml of

water for 6 hours at room temperature to soak and weighed while being suspended in air. The weight was recorded as W. Finally, the specimen was weighed when immersed in water. This was recorded as S. The bulk density was then calculated from the expression(Equ. III. 9).

III.4 Conclusion

In this chapter we have seen the different steps of preparation of the brick product in"SARL Eloutaya.Poterie and the different experimental techniques used in laboratory for synthesis and characterizing the prepared samples. The different results of characterization and testing will showed in chapter IV.

Chapter IV:

Results and discussions

IV.1 Introduction

In this chapter, we present the results of our research and we try to discuss them. The objective is to know the effect of the load and sintering temperature on the brick product.

IV.2 Raw material characterization

IV.2.1 Particle size analysis of sands

The particle size analysis of two sands is presented in the **Tab. IV.1** and **Tab. IV.2**.

Tab. IV.1: The particle size analysis results of Biskra sand.

Diameter(mm)	Retained (g)	Cumulative Retained (g)	Retained (%)	Passing (%)
2.5	1.47	1.47	0.07	99.93
1.25	5.3	6.77	0.33	99.67
0.63	35.29	42.06	3.10	97.9
0.315	1407.19	1449.25	72.46	27.54
0.16	481.65	1930.9	96.54	3.46
0.08	66.66	1997.52	99.87	0.13
Fine powder	1.56	1999.08	99.95	0.05

Tab. IV.2: The particle size analysis results of Sahara sand.

Diameter(mm)	Retained (g)	Cumulative retained (g)	Retained (%)	Passing (%)
2.5	0	0	0	100
1.25	0	0	0	100
0.63	0.01	0.01	0.0005	99.99
0.315	325.07	325.08	16.02	83.98
0.16	1538.89	1863.97	93.19	6.81
0.08	125.89	1989.86	99.49	0.51
Fine powder	10	1999.86	99.99	0.01

The different curves of particle size analysis of two sands are presented in **Fig.IV.1** and **Fig.IV.2**.

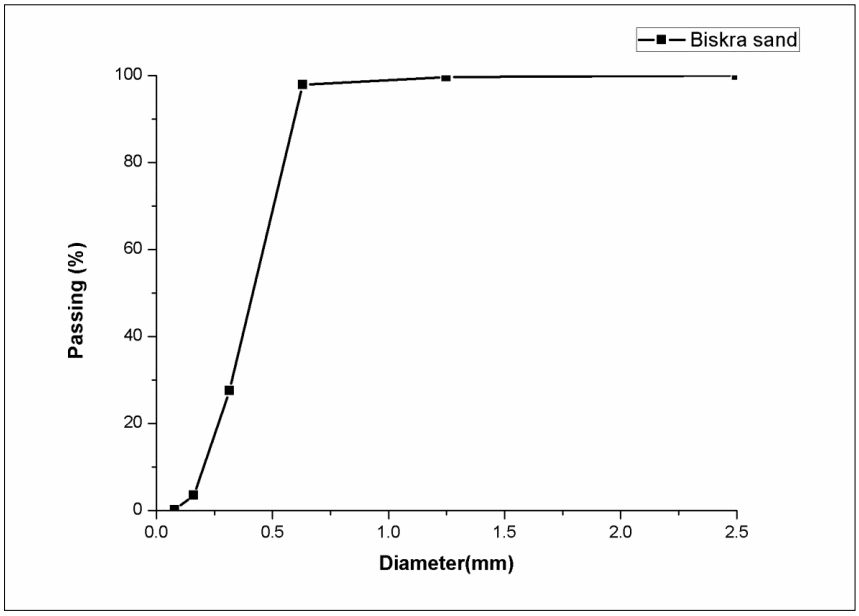

Fig.IV.1: Particle size analysis curve of Biskra sand.

This curve is divided in two parts, the first corresponds to the percent of the majority of particles passed in the sieves, which have a diameter between 2.5-0.63 mm .however, the second part presents the particles have a diameter less than 0.63 mm.

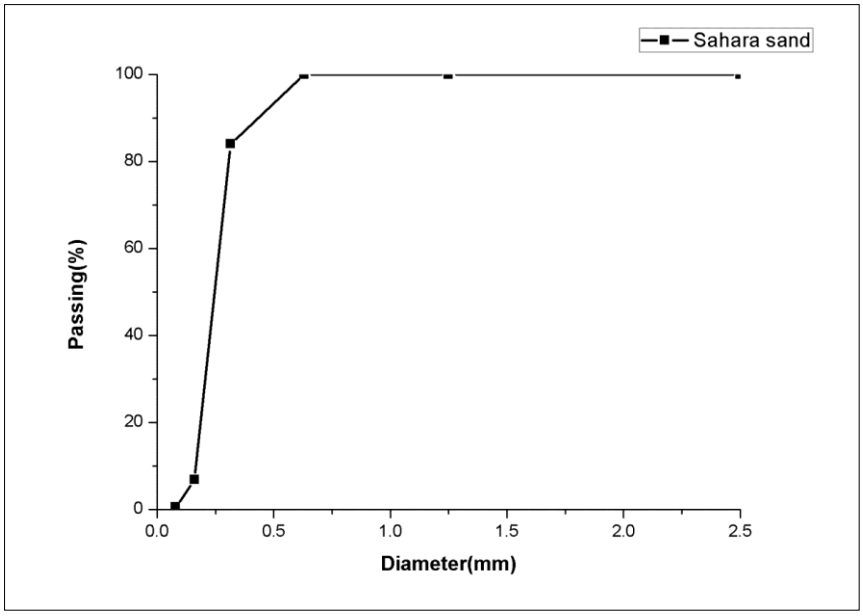

Fig.IV.2: Particle size analysis curve of Sahara sand.

This curve is also divided in two parts; these parts are the same discussed in the curve of Biskra sand.

In order to compare the difference between the two kind of sands, the curves of particles size analysis of Biskra and Sahara sands are presented in **Fig.IV.3**.

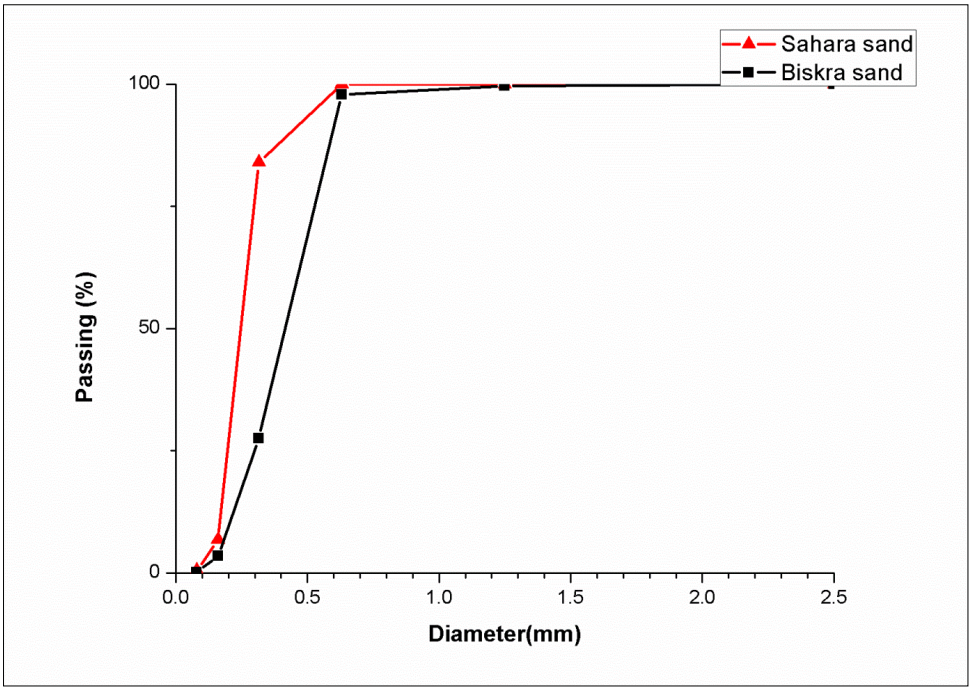

Fig.IV.3: Particle size analysis curves of sands.

- The **Tab. IV.1, Tab. IV.2** and **Fig. IV.3** illustrate that the majority of particles of Biskra and Sahara sands have a size < 0.63mm.
- The curves of the two sands are continuous; we conclude that the distribution of sands particles is homogeneous (uniform).

After calculation of fineness modulus (M_f) of sands, the results are:

M_f of Biskra sand = 1.72

1.72 < 1.8. The sand of Biskra has very fine particle size.

And:

M_f of Sahara sand = 1.08

1.08 < 1.8; So the sand of Sahara also has very fine particle size.

- From this results we say that the Sahara sand can be used in preparation of brick product, because its fineness modulus less than 1.8 (particle size is so fine).

IV.2.2 Phase identification of raw materials

The X-ray diffraction (XRD) results of the two raw materials (two mixtures) are presented in **Fig.IV.4 and Fig.IV.5**. These diffractograms showed that the major phases were detected quartz (SiO_2), Calcite ($CaCO_3$), and montmorillonite ($Na_{0.3}(Al, Mg)_2Si_4O_{10}(OH)_2$ $8H_2O$).

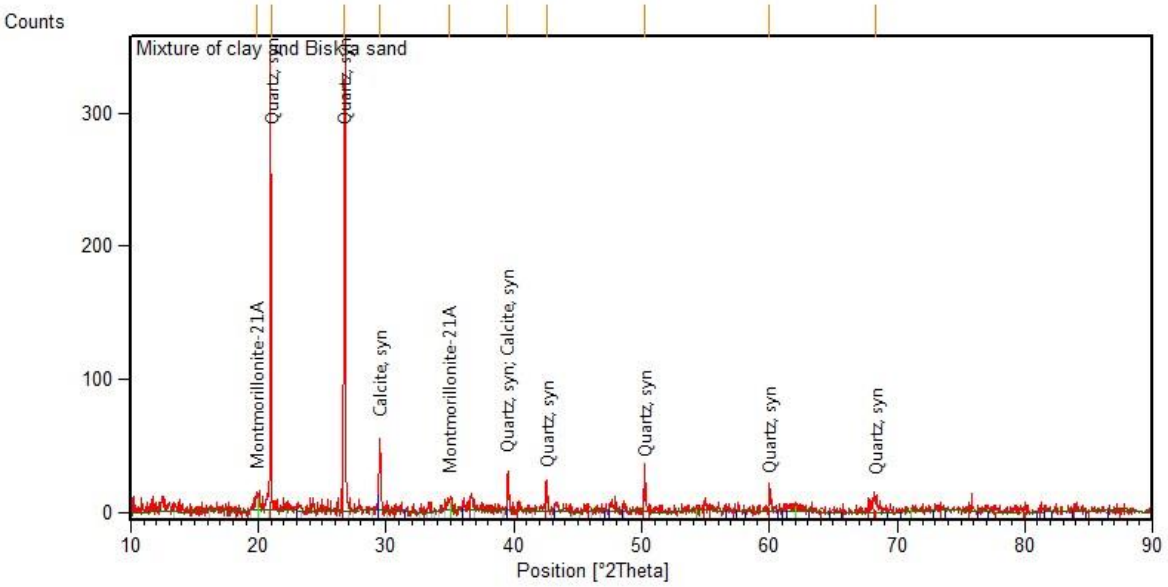

Fig.IV.4: XRD pattern of mixed clay with Biskra sand.

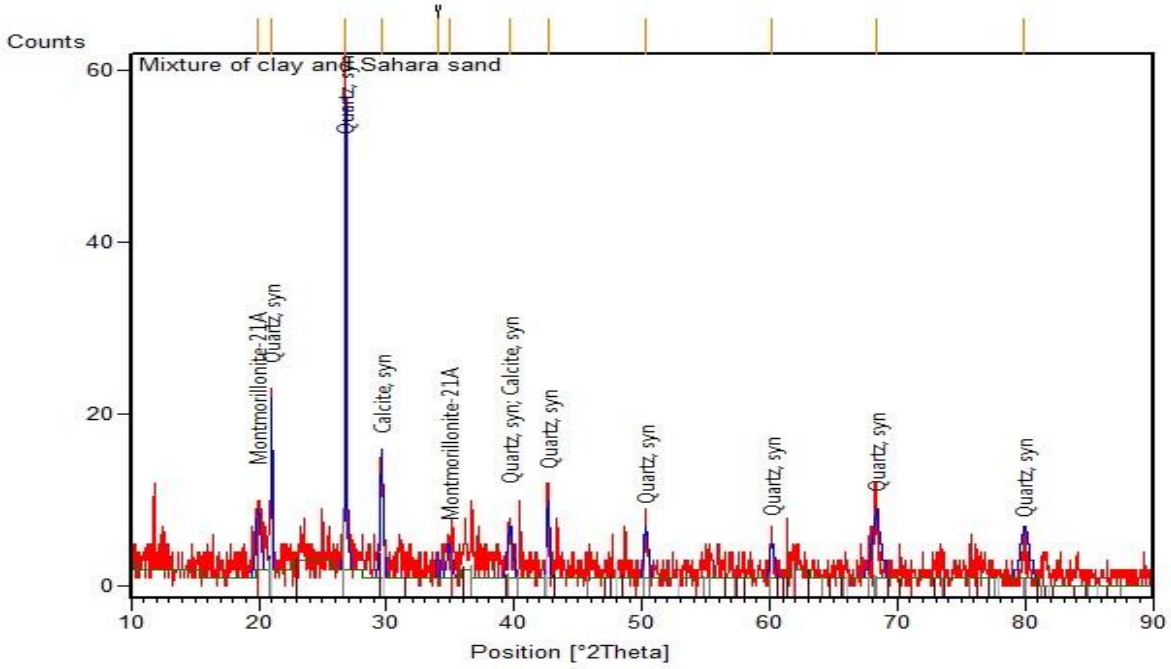

Fig.IV.5: XRD pattern of mixed clay with Sahara sand.

IV.2.3 The molecular structure of raw materials (FTIR)

The molecular structure of raw materials (two mixtures) has been identified by infrared spectroscopy analysis. According to the given IR spectrums in **Fig. IV.6** and **Fig.IV.7.**

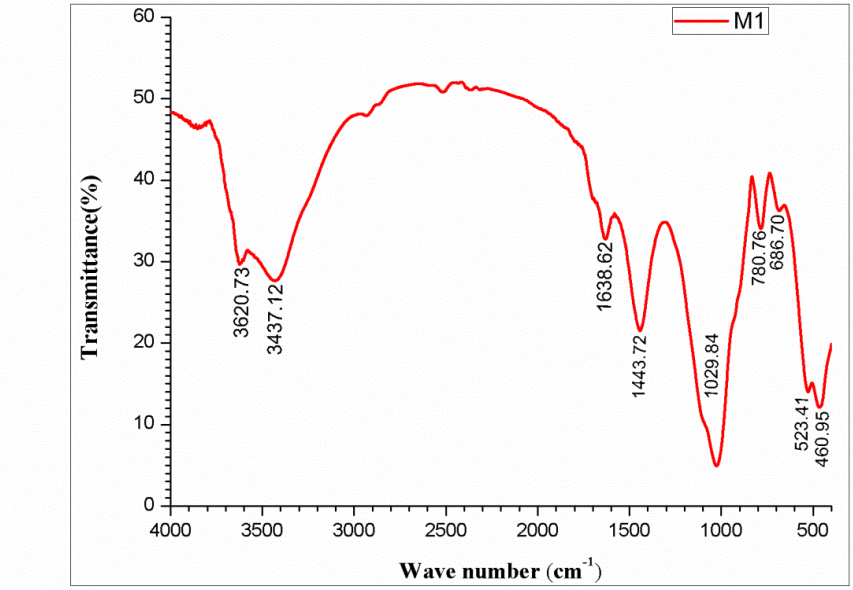

Fig.IV.6: FTIR spectrum of raw material (mixture of clay and Biskra sand).

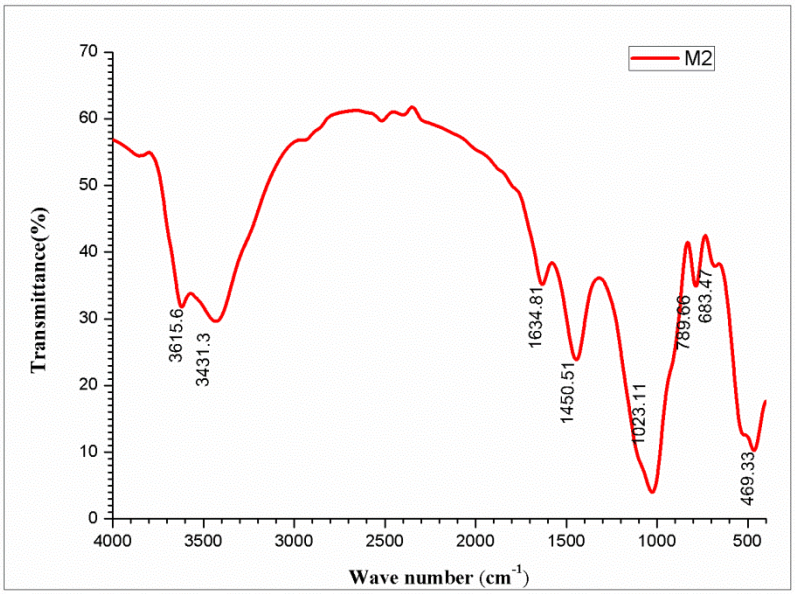

Fig.IV.7: FTIR spectrum of raw material (mixture of clay and Sahara sand).

In order to compare the molecular structure of two raw materials, Their FTIR spectrums are presented in **Fig. IV.8**.

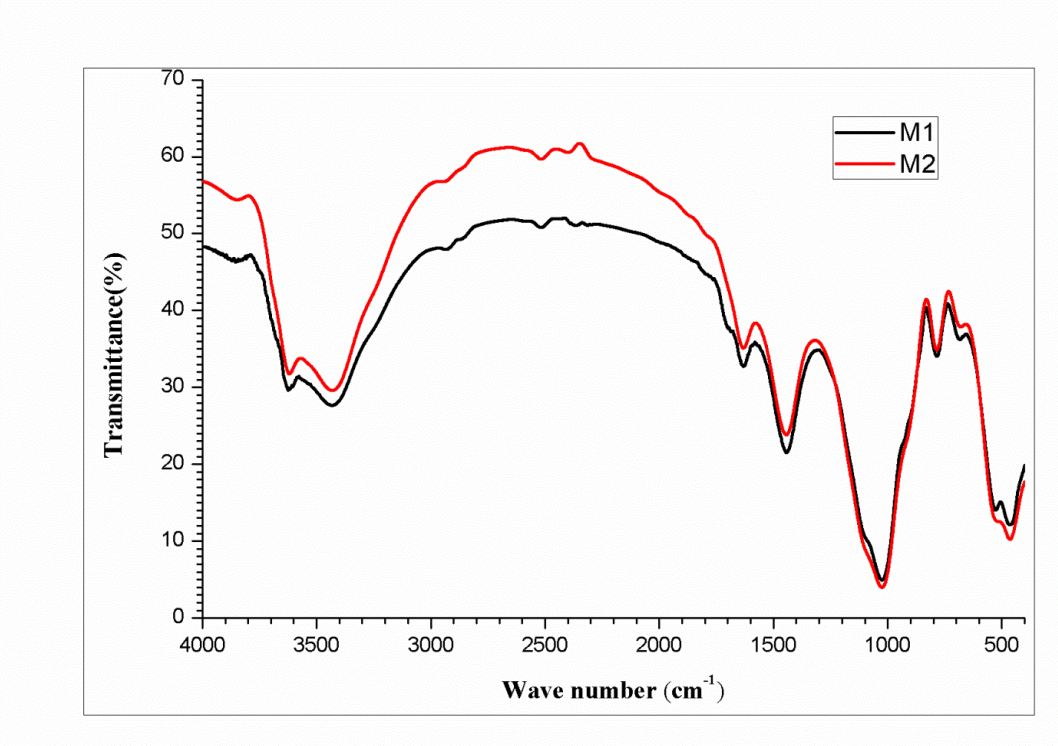

Fig.IV.8: FTIR spectrums of raw materials (Two mixtures).

- **Fig.IV.8** shows that the peaks of FTIR spectrums of two raw materials have a same wave number interval.
  - We conclude that the two mixtures have a same molecular structure.

When we consider a spectroscopy of commercial montmorillonite [39], which are absorbed the energy at particular wave numbers. The band included spectral bands of montmorillonite in our samples (raw materials) only: stretching bands of structural hydroxyl groups (3620.73, 3615.6 cm-^{1}), broad stretching bands of water (3437.12, 3431.3 cm^{-1}), deformation bands of water (1638.6, 1634.81 cm^{-1}), bands of Si-O stretching (1029.84, 1023.11 cm^{-1}), Si-O stretching bands of quartz (780.76, 789.66 cm^{-1}), coupled out-of-plane vibration bands of Al-O and Si-O (686.76, 683.47 cm^{-1}) and deformation bands Al-O-Si (523.41, 460.95cm^{-1} and 469.33 cm^{-1}).

According to the commercial montmorillonite characteristic peak wave number, clays' peak wave numbers were also similar to that. In the result we have concluded that the montmorillonite particles are in our raw material.

D. Dodoo-Arhin [40], found that the bands (1443.72, 1450 cm^{-1}) correspond to the presence of calcium carbonate $CaCO_3$. These peaks were illustrated in **Tab. IV.3** combines the bands of vibrations and deformations from **Fig.IV.8**.

Tab. IV.3: The molecular structure of raw material (absorption bands of raw materials).

Wave number (cm^{-1})		**bands**
M1	**M2**	
460.95, 523.41	469.33	Al-O-Si deformation
686.70	683.47	Coupled Al-O and Si-O out of the plane
780.76	789.66	Si-O stretching of quartz
1029.84	1023.11	Si-O stretching
1443.72	1450.51	$CaCO_3$
1638.6	1634.81	OH deformation of water
3437.12	3431.3	OH stretching of water
3620.73	3615.6	OH stretching of structural free hydroxyl groups

These results are in agreement with those found from XRD. They confirm the presence of quartz, montmorillonite and calcite in our studied materials.

IV.3 Samples characterization (after sintering)

IV.3.1 The weight of samples before and after sintering process

The weight of samples before and after sintering process is presented in **Tab. IV.4**; where M1, M2 are the mixed of clay with Biskra sand ,Sahara sand respectively and we indicate that the applied loads during the compacting step were 6 and 4 tonnes.

Tab. IV.4: The different weights of samples before and after sintering process.

Sintering Temperatures(°C)	Weights of samples (g)							
	Before sintering				After sintering			
	M1(6)	M1(4)	M2(6)	M2(4)	M1(6)	M1(4)	M2(6)	M2(4)
750	098	0.97	0.97	0.97	0.88	0.88	0.86	0.87
850	0.94	0.99	0.97	0.99	0.82	0.87	0.86	0.87
900	0.96	0.97	0.98	0.98	0.85	0.86	0.86	0.87
1000	0.99	0.98	0.97	0.98	0.86	0.87	0.86	0.86

- We can deduce from the **Tab.IV.4** that the weight of different samples decreases after sintering process.

According to Dodoo-Arhin et al [40]**,** before the firing temperature is up to 500ºC, the sample loses ≈8.26% total of its weight. The proportion of physically absorbed water is small. Comparing this result with the results of the XRD analysis, the lost chemically bound water could be mainly attributed to the ehydroxylation of montmorillonite ($Na_{0.3}(Al ,Mg)_2Si_4O_{10}(OH)_28H_2O$) and the decomposition of calcite ($CaCO_3$) into CaO with the release of CO_2 .

Note: At 1200°C the prepared samples were burned.

The samples sintered at 1200°C were burned because the compounds of the clay were passed their milting points; here the type of raw material (clay) is the main reason. Acoording to [41], the kaolinite and muscovite in clay resist high temperatures (1200-1800°C). Ours clay missed this phases. This is not unconnected with the dehydroxylation montmorillonite undergoes when subjected to sintering at high temperatures , However, the dehydroxylation progresses from 800°C upto 1140°C [42], but it is completed in these samples at 1000°C. This is because of the presence of other phases (such calcite) in the samples interacted the dehydroxilation reaction and assisted it to be completed at 1000°C.

IV.3.2 Phase identification of prepared samples

IV.3.2.1 Prepared samples from the mixed of clay and Biskra sand

XRD patterns of sintered samples (prepared from the mixed of clay and Biskra sand) at different temperatures are presented in **Fig.IV.9** and **Fig.IV.10**.

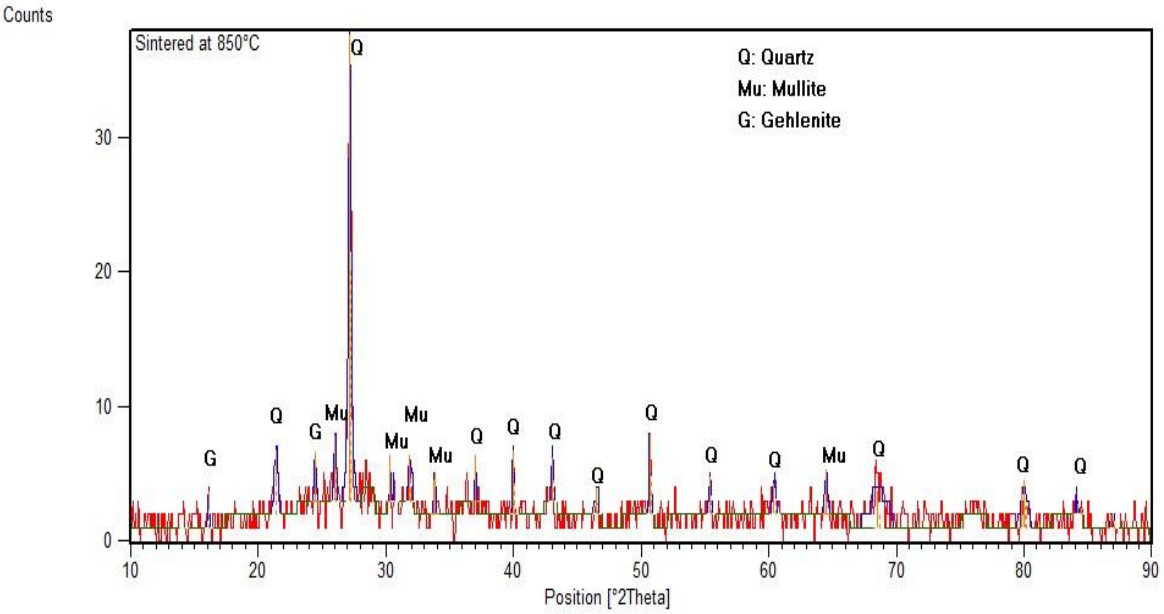

Fig.IV.9: XRD pattern of sample (From mixed of clay with Biskra sand) sintered at 850°C for 2 hours.

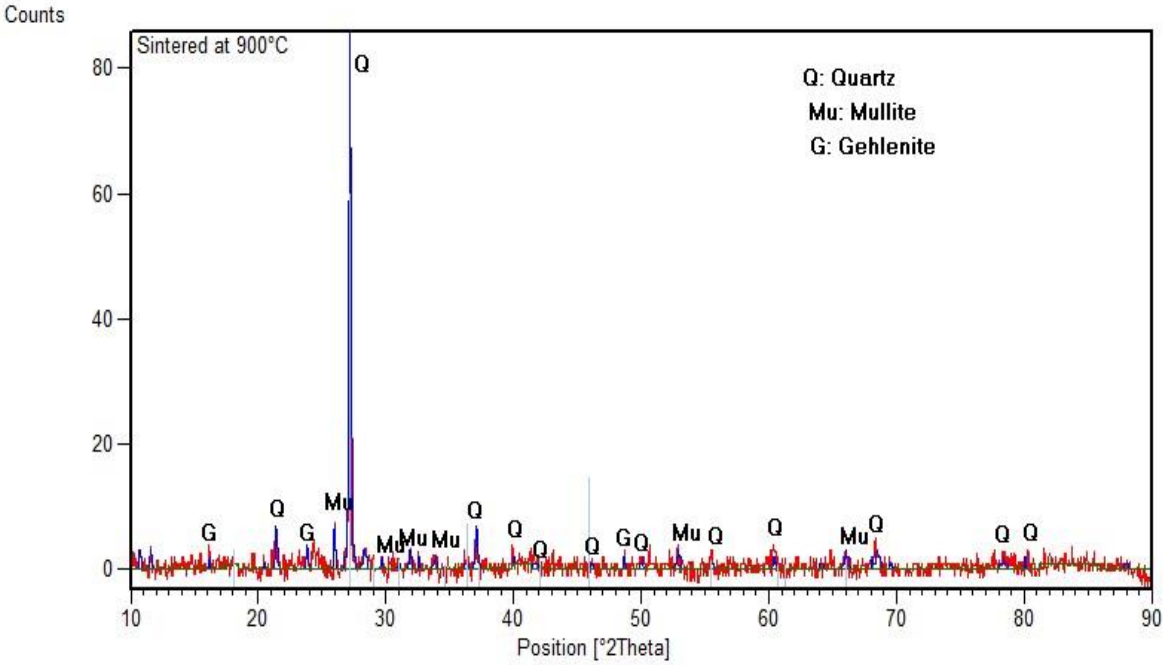

Fig.IV.10: XRD pattern of sample (From mixed of clay with Biskra sand) sintered at 900°C for 2 hours.

In order to compare between the XRD patterns of these samples (prepared from the mixed of clay and Biskra sand), which sintered at different temperatures, we drew them in the same graph (**Fig.IV.11**).

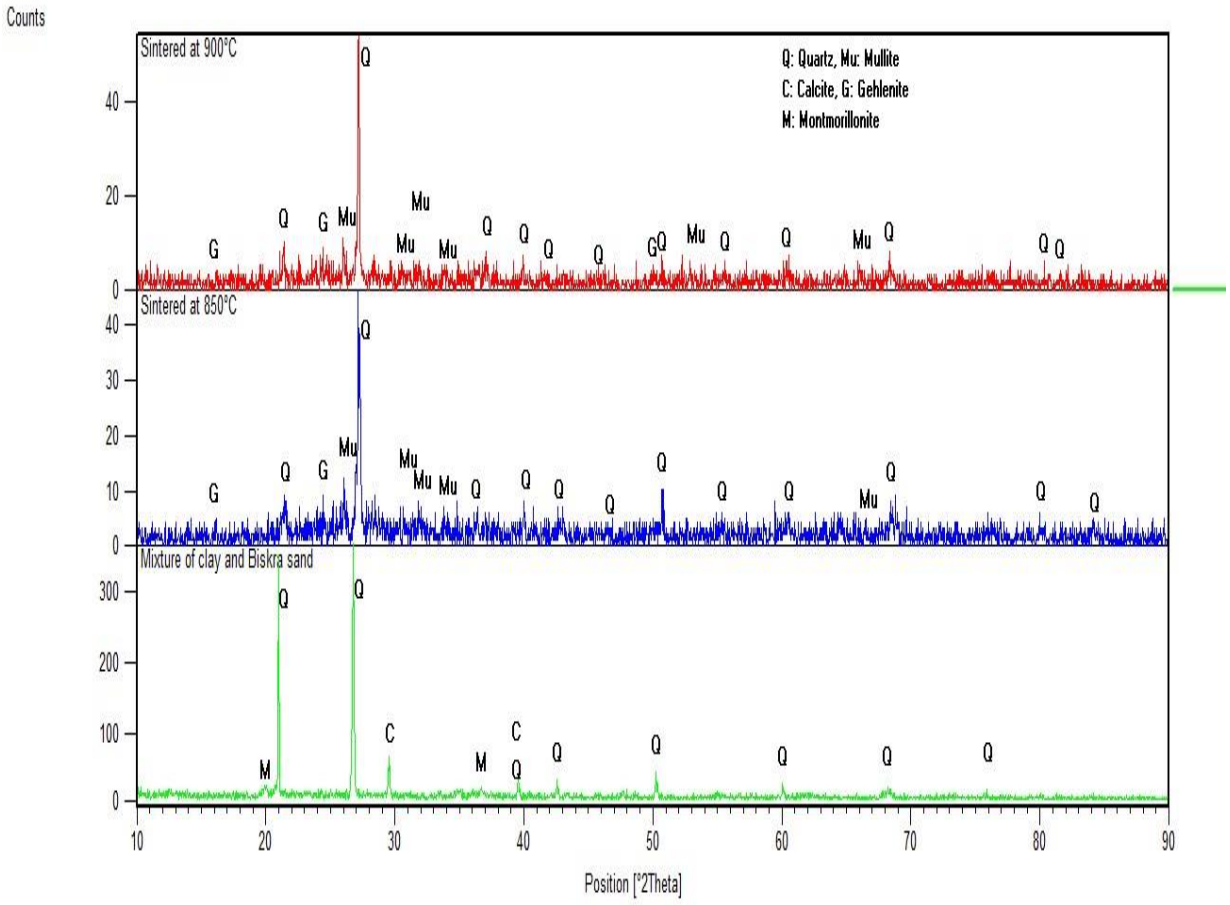

Fig.IV.11: XRD patterns of samples (From mixed of clay and Biskra sand) sintered at different sintering temperatures for 2 hours.

XRD patterns of sintered samples at 850°C and 900°C for 2 hours are presented in **Fig.IV.11**. It can be seen that between the raw material and 900°C the peaks of calcite and montmorillonite disappear. At 850 ◦C the carbonate decomposition (calcite) is complete, and we also see the appearance of the mullite ($3Al_2O_3.2SiO_2$) and gehlenite **(**$Ca_2Al_2SiO_7$). All peaks of quartz remain visible during treatment.

The disappearance of some peaks (peaks of calcite and montmorillonite), when the sintering temperatures between 550–900ºC with a mass change (decrease) of ≈ 21.81% could be attributed to the release of CO_2 [43]. Jie-Guang Song [30], found that the release of CO_2 is

due to the decomposition of Calcite ($CaCO_3$) into CaO. The chemical reactions during this phase transformation are as following:

$$CaCO_3 \rightarrow CaO + CO_2 \ldots\ldots\ldots \text{(IV.1)}$$

$$2CaO + 2Al_2O_3 + SiO_2 \rightarrow 2Ca_2Al_2SiO7 \ldots \text{(IV.2)}$$

The phase of gehlenite ($Ca_2Al_2SiO_7$) starts to develop in the 800–900ºC range. There is no obvious mass change or phase change above 900ºC. This explains the disappearance (absence) of $CaCO_3$ in XRD pattern when the sintering temperature increases.

The raw materials can present different Fe content, which can also explain a variation of the tonality of the color after firing. Fe is generally present in clay minerals, which later in firing are responsible for the formation of mullite. The color tends to be darker even if they contain a lower quantity of transition elements, which is due to the presence of goethite, which can be rapidly decomposed into hematite with temperature, and the low content of newly formed mullite, which could eventually host Fe in the structure [44].

According to A.Oscar et all [45], the quartz decomposes gradually from 800 to 1100 °C, diminishing drastically at 1100 °C, and disappeared at 1200°C. The decomposed and disappearing phases all contribute to the formation of a vitreous phase up to 800 °C. At this step the clay would essentially be an amorphous material with some residual grains of quartz and neoformed mullite and hematite and other high temperature mineral phases such as microcline. Therefore, quartz was a residual phase; On the contrary, mullite, hematite and other silicates were formed during firing. Clays showed phyllosilicate destruction at temperature ranging from 700 to 900 °C, followed by vitrification, which is significant at temperature > 1000°C.

IV.3.2.2 Prepared samples from the mixed of clay and Sahara sand

The XRD patterns of sintered samples (prepared from the mixed of clay and Sahara sand) at different temperatures are presented in **Fig.IV.12** and **Fig.IV.13**.

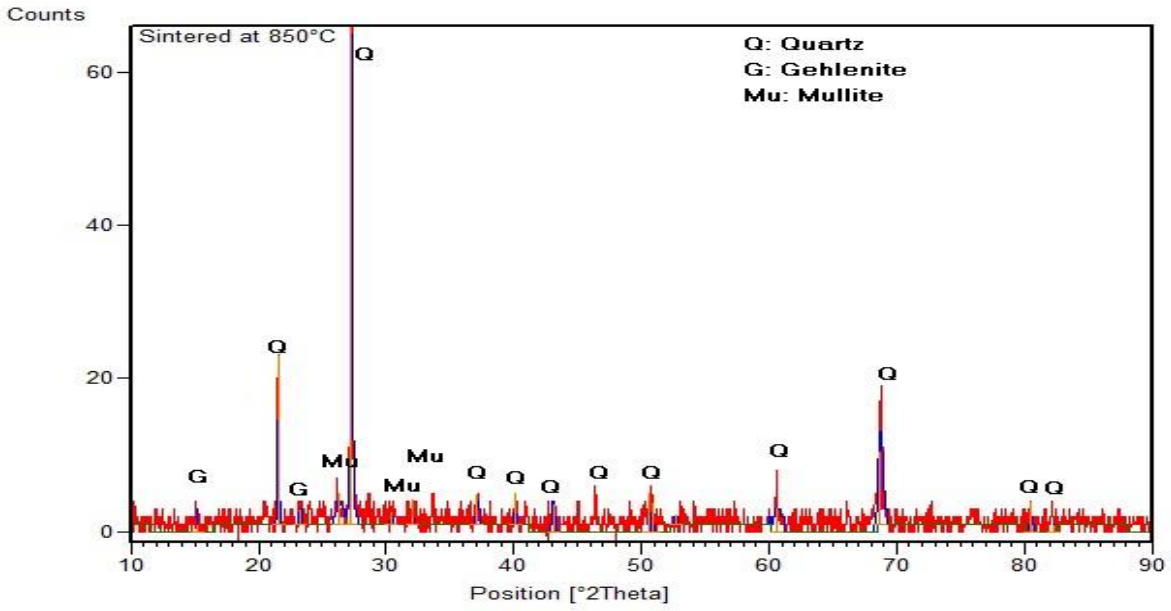

Fig.IV.12: XRD pattern of sample (from mixed of clay with Sahara sand) sintered at 850°C for 2 hours.

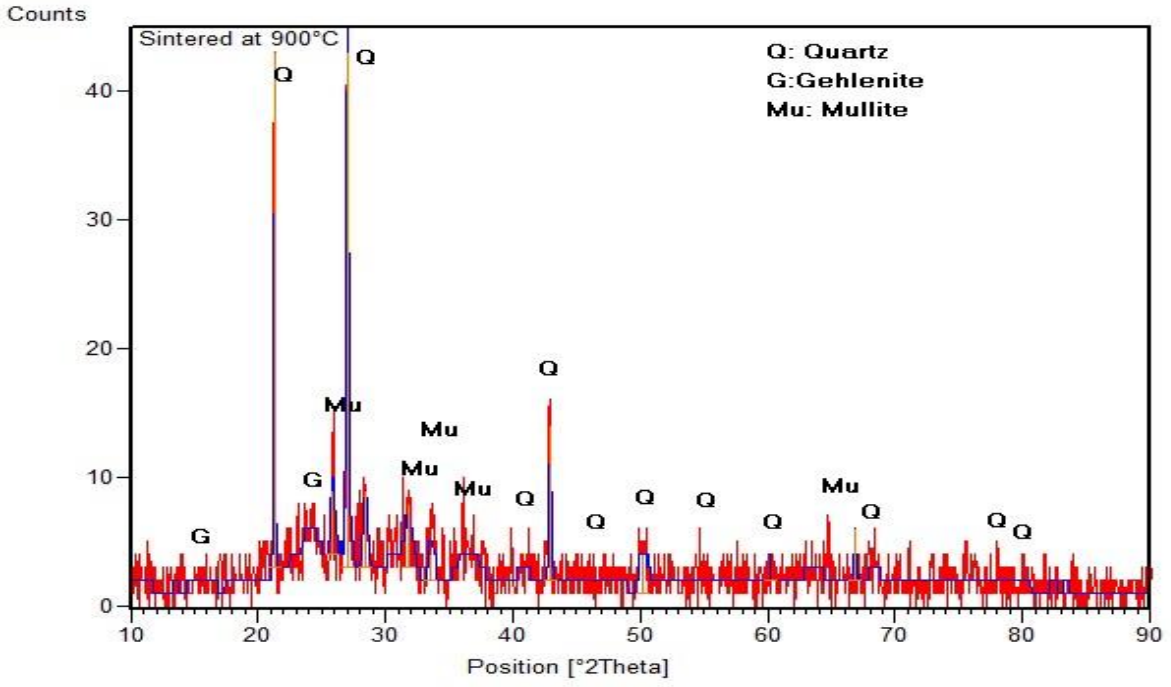

Fig.IV.13: XRD pattern of sample (from mixed of clay with Sahara sand) sintered at 900°C for 2 hours.

Fig.IV.14 shows the XRD patterns of samples (prepared from the mixed of clay and Sahara sand), sintered at different temperatures, in order to compare between them.

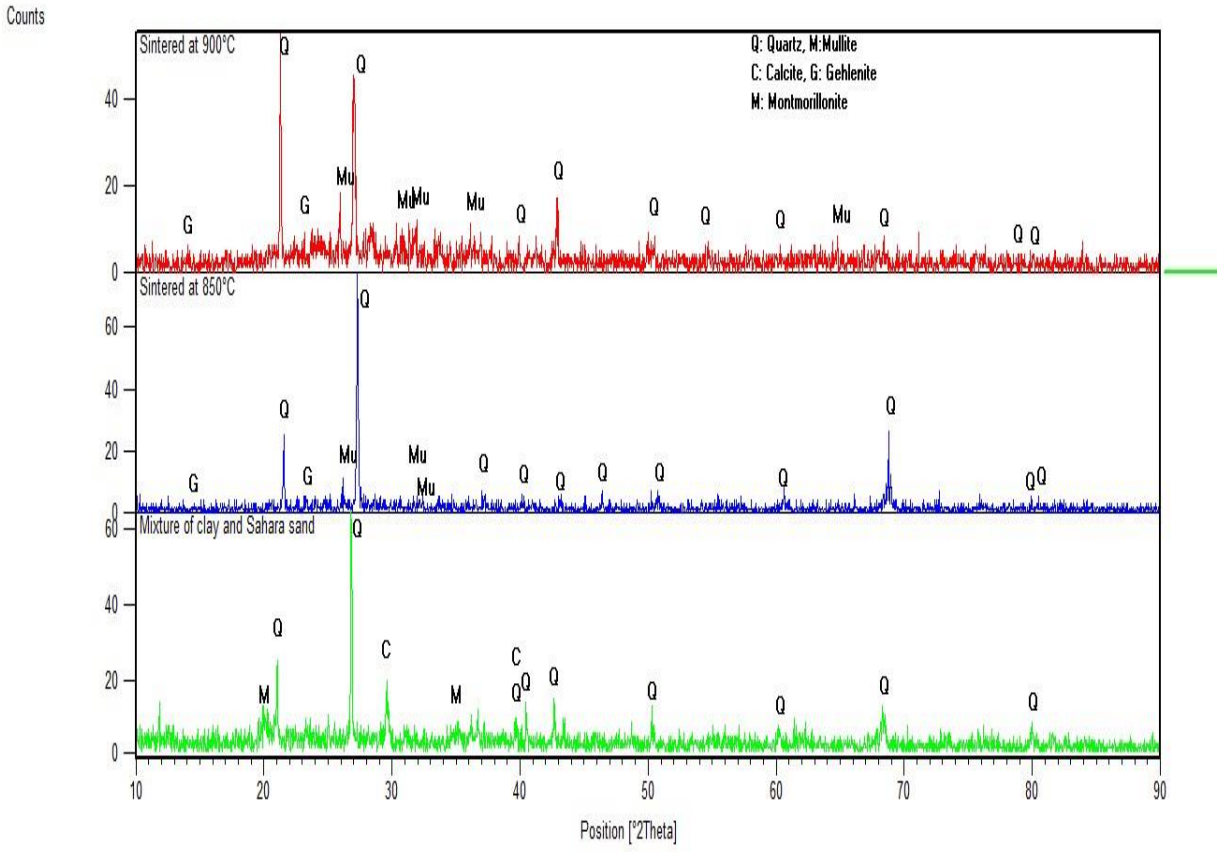

Fig.IV.14: XRD patterns of samples (from mixed of clay and Sahara sand) sintered at different temperatures for 2 hours.

XRD patterns of sintered samples at 850°C and 900°C for 2 hours are presented in **Fig. IV.14**. It can be seen that between the raw material and 900°C the peaks of calcite and montmorillonite disappear. At 850 ◦C the carbonate decomposition (calcite) is complete, and we also see the appearance of the mullite ($3Al_2O_3.2SiO_2$) and gehlenite **(**$Ca_2Al_2SiO_7$). All peaks of quartz remain visible during treatment.

We deduce that these transformations are the same observed and discussed in the XRD patterns of prepared samples from the mixed of clay and Biskra sand.

IV.4 Microstructures of different samples

Fig.IV.15 and **Fig.IV.16** show the microstructures of prepared samples from the two mixtures (clay with Biskra and Sahara sand) under two loads: 6 and 4 tonnes, the microstructures are of the dried samples (before sintering), and the samples sintered at 750 °C, 850 °C, 900 °C, 1000 °C for 2 hours .

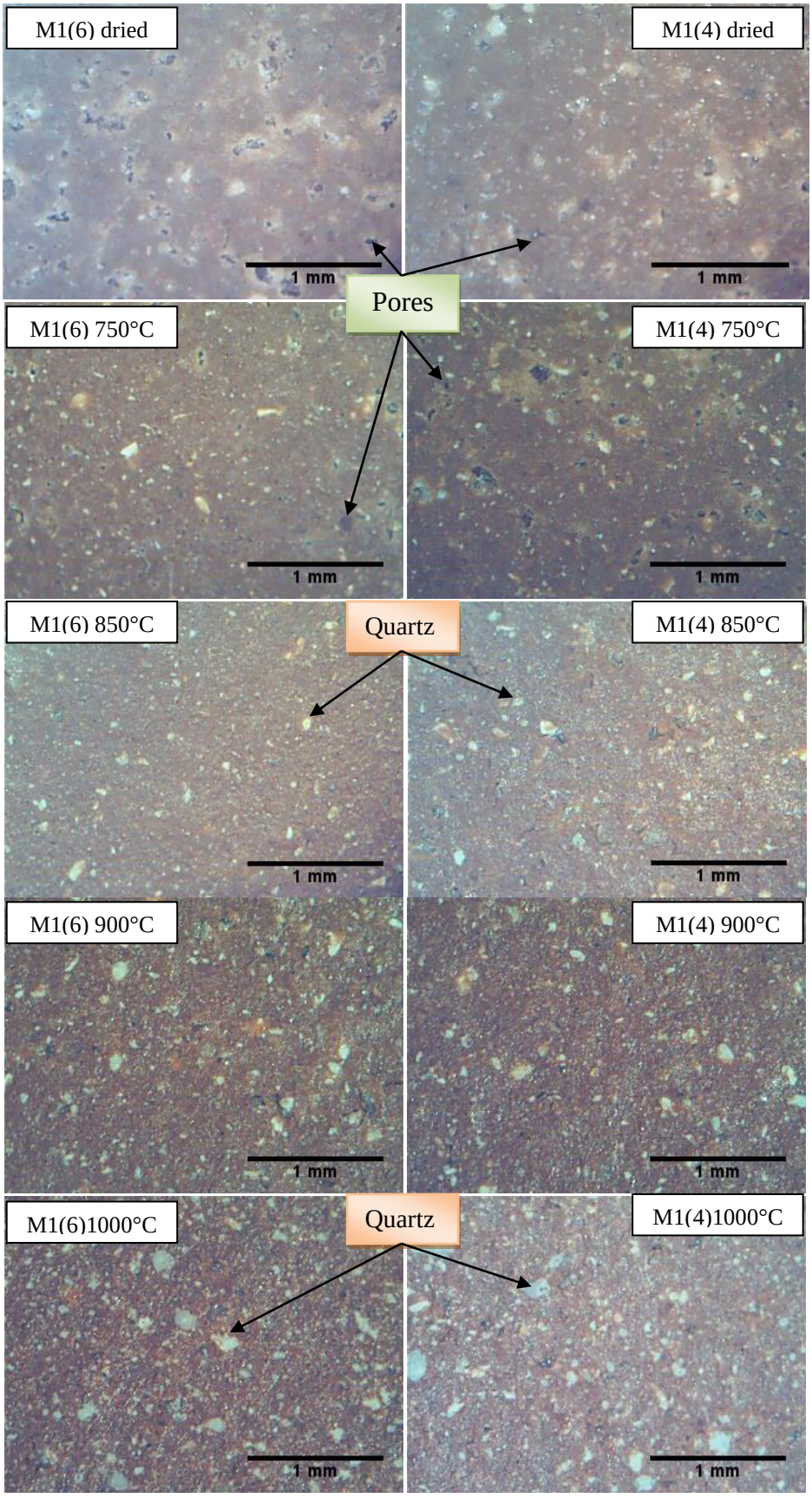

Fig.IV.15: Microstructures of prepared samples from the mixed clay and Biskra sand (M1), under two loads: 6,4 tonnes and sintered at different temperatures.

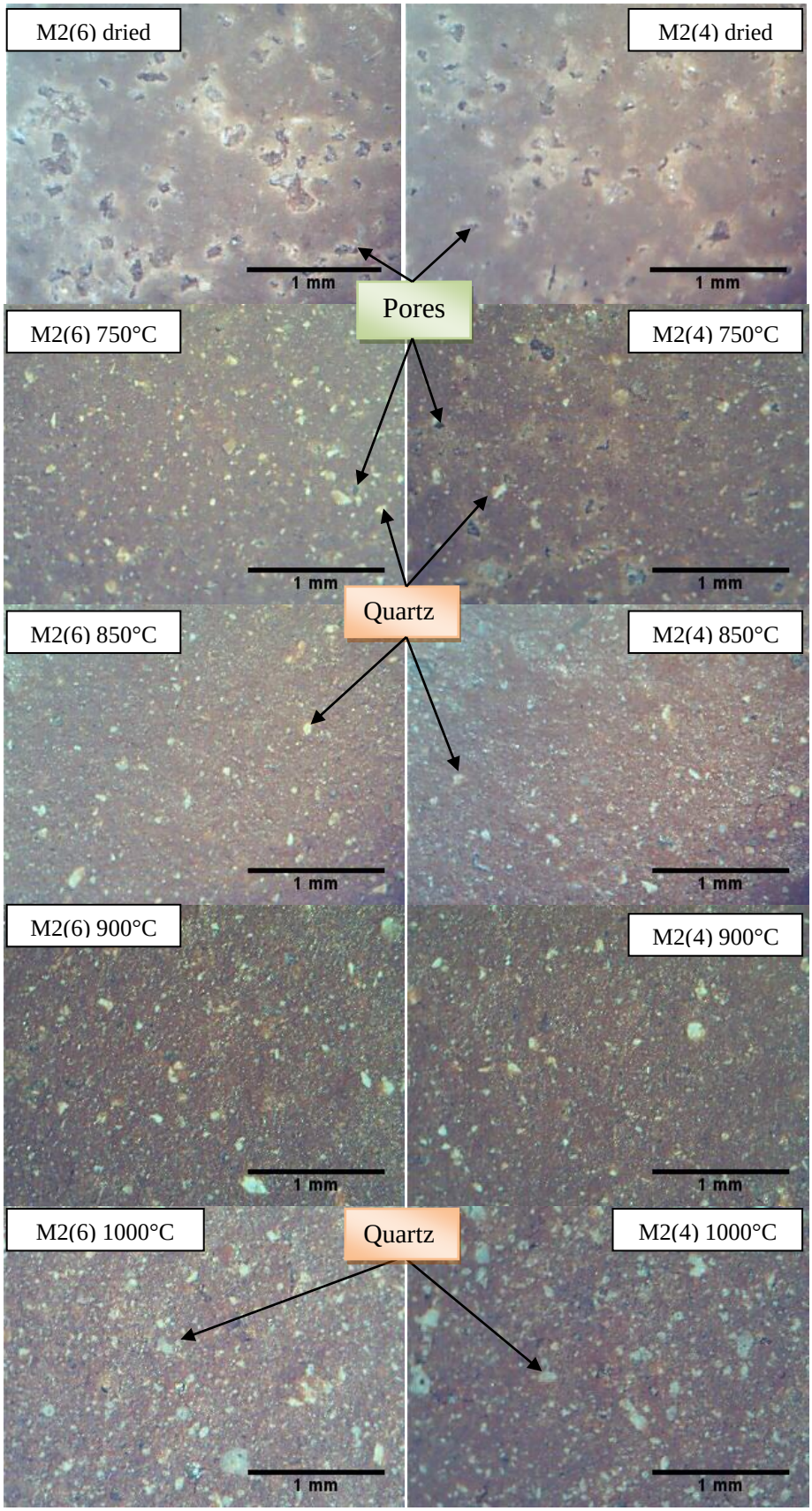

Fig.IV.16: Microstructures of prepared samples from the mixed clay and Sahara sand (M2), under two loads: 6,4 tonnes and sintered at different temperatures

From these microstructures, we deduce that:

- The main phase at different sintering temperatures is the quartz (white colour) in the two types (two types of bricks samples); this phase was in growth (particle size increase) with the increasing in the sintering temperature.
- The pores (black colour) decreased with the increasing in sintering temperatures.
- In these microstructures the effect of loads are not observed. The difference between them can be seen by SEM, where the pores sizes are depicted in the samples

The effect of sintering temperature to microstructure of brick samples was shown in **Fig.IV.15** and **Fig.IV.16.** When temperature was increased, the grain of samples showed growth but were non-homogenous because the high sintered temperature caused the evaporation of some compounds.

In general, quartz is the most common mineral phase in the raw materials; the other components are phyllosilicates . The < 2 mm fraction includes smectite (montmorillonite). Sintering causes significant changes in the phyllosilicates. During sintering three kinds of processes take place: decomposition, phase transformation, and sintering with partial melting, with both decomposition and phase transformations affect development and extent of the subsequent sintering [47]

Mullite may appear at different temperature, which could be related to the presence of enough content of illite/montomorillonite. At this range of temperature, phyllosilicates have already disappeared in all samples, being transformed into mullite plus a melt [48].

Oscar et al [45] the degree of vitrification increases gradually up to almost complete melting resulting in a glassy appearance. Among the crystalloclasts, quartz is predominant. Several studies reveal that quartz, plagioclase, rare biotite and occasionally minerals, such as zircon, rutile... Quartz displays molten rims with some invasion of iron oxides. Further determination in terms of mineral composition is not possible.. The matrix has different appearances due to the development of hematite where it can be recognized as few small crystals dispersed in a uniform red Fe-rich surface. And Johari et al [31], Confirmed that a solid state sintering is a process that promotes atomic bonding between particles by a diffusion mechanism. This diffusion followed by grain growth will create a dense structure with significant shrinkage, causing the reduction in volume for brick sintered within this

range of temperature. The optimum temperature of the sintering process is reached at 1000 °C and whereby its microstructure contains minimum pores.

IV. 5Tests

IV.5.1 Apparent porosity

The results of apparent porosity of samples at different sintering temperatures are presented in **Tab.IV.5**.

Tab. IV.5: The results of apparent porosity of samples at different sintering temperatures.

Temperatures(°C)		Apparent porosity (%)			
		M1		M2	
	Loads (tons)	6	4	6	4
750		10.16	11.47	11.11	11.66
850		5.89	7.43	6.77	8.20
900		4.81	6.08	5.86	6.89
1000		4.53	5.63	5.10	6.65

The different curves of sintering temperature effect on the apparent porosity of samples are illustrated in **Fig. IV.17 - Fig.IV.20**.

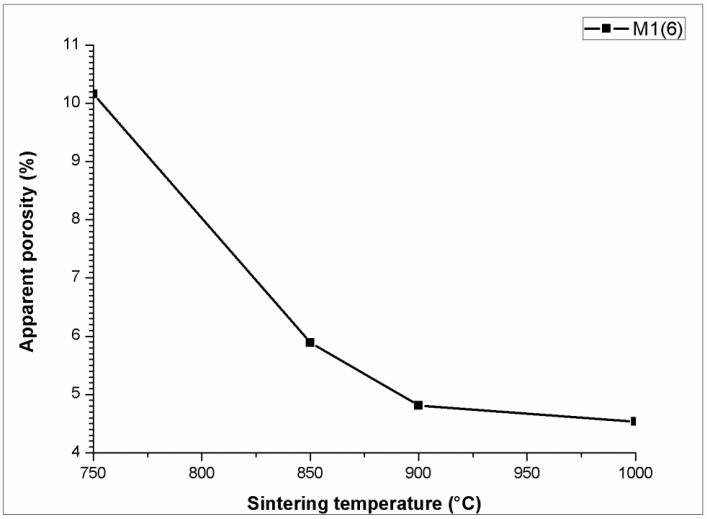

Fig.IV.17: Effect of sintering temperature on apparent porosity of the samples prepared from mixture of clay and Biskra sand at 6 tonnes.

From Tab**. IV.5** and **Fig. IV.17,** the apparent porosity is first decreased rapidly from 10.16 % to 5.89% at 750°C and 850°C respectively and then decreased slowly with increasing the sintering temperature. However the lower value of apparent porosity is 4.53 % at high temperature (1000°C).

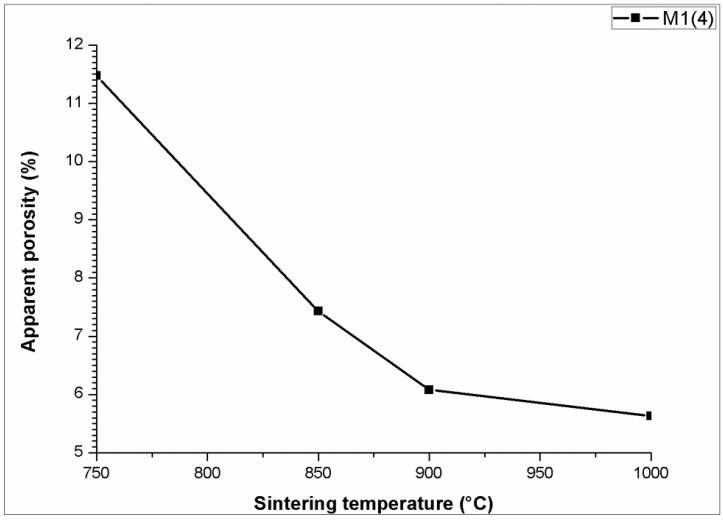

Fig.IV.18: Effect of sintering temperature on apparent porosity of the samples prepared from mixture of clay and Biskra sand at 4 tonnes.

Tab IV.5 and **Fig. IV.18** confirm that the apparent porosity is first decreased rapidly from 11.47 % to 7.43 % at 750°C and 850°C respectively and then decreased slowly with the increase of the sintering temperature. At high sintering temperature (1000°C), the apparent porosity was equal to 5.63 %.

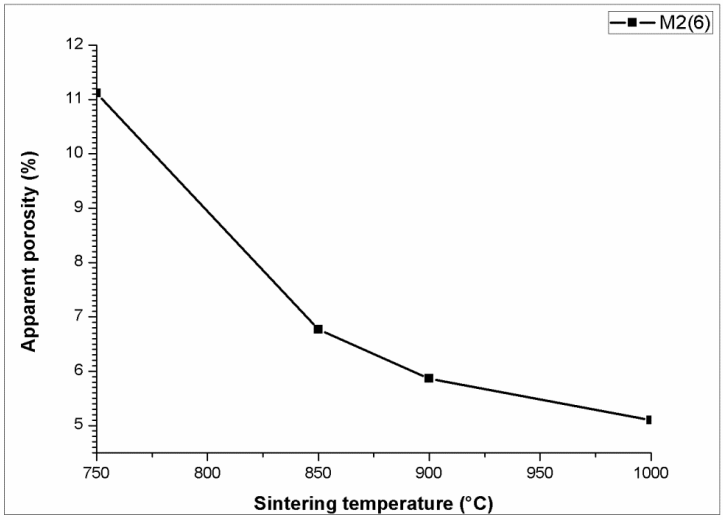

Fig.IV.19: Effect of sintering temperature on apparent porosity of the samples prepared from mixture of clay and Sahara sand at 6 tonnes.

From **Tab. IV.5** and **Fig. IV.19** the apparent porosity is first decreased rapidly from 11.11 % to 6.77 % at 750°C and 850°C respectively and then decreased slowly with increasing in the sintering temperature; the last value of decrease is 5.10 % at 1000°C.

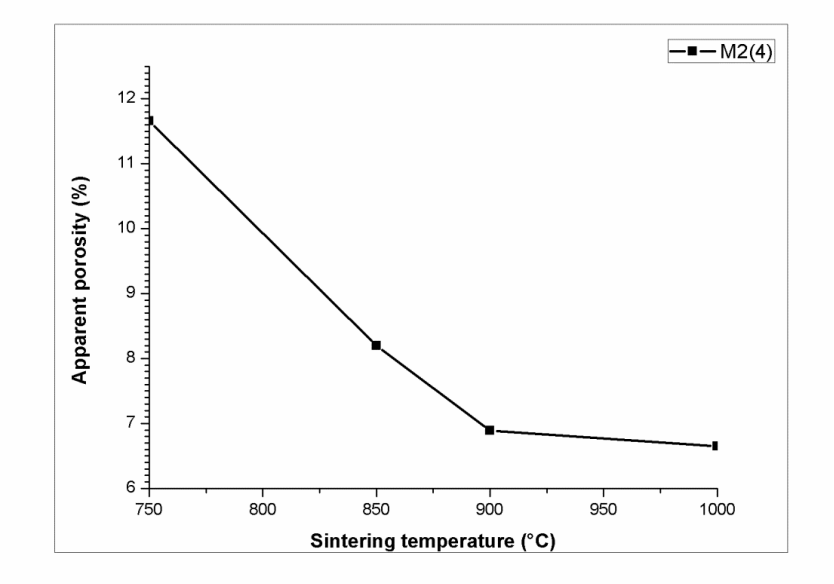

Fig.IV.20: Effect of sintering temperature on apparent porosity of the samples prepared from mixture of clay and Sahara sand at 4 tonnes.

The **Tab. IV.5** and **Fig. IV.20** ilustrate that the decrease of apparent porosity firstly was rapid from 11.66 % to 8.2% at 750°C and 850°C respectively and then decreased slowly with the increase of sintering temperature. The lowest value is 6.65 % at high temperature (1000°C).

In order to compare between the different curves of sintering temperature effect on apparent porosity of prepared samples, we put them in the same graph (**Fig.IV.21**).

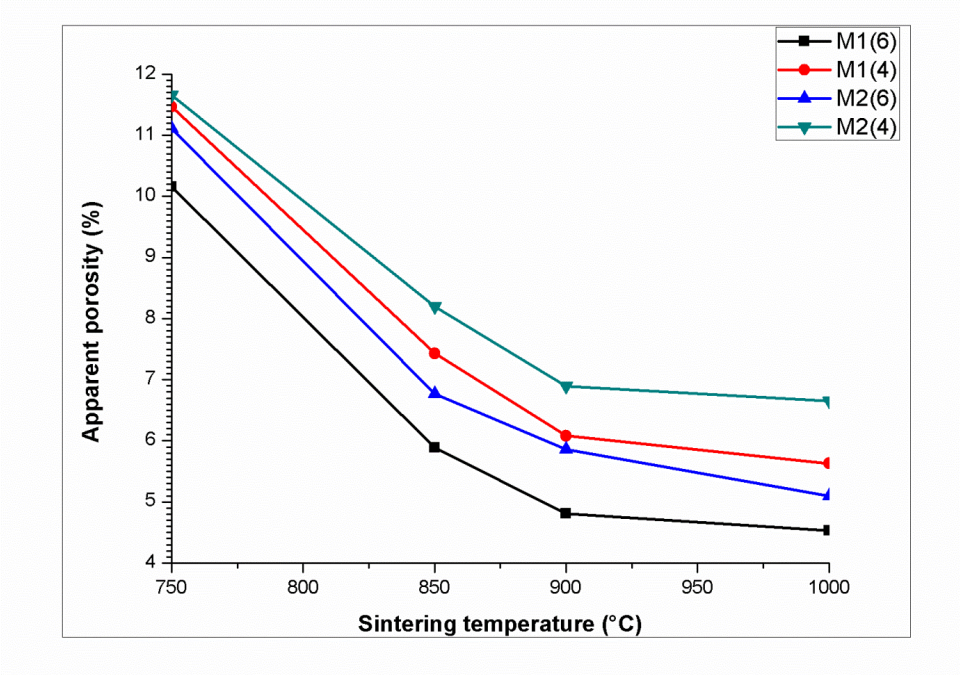

Fig.IV.21: Effect of sintering temperature on apparent porosity of prepared samples.

- The curves illustrate that the apparent porosity decreases with an increase in the sintering temperature.
- The samples prepared at 6 tonnes have a value of apparent porosity less than the value of samples prepared at 4 tonnes. But the apparent porosity of samples prepared from the mixture of clay and Biskra sand is less than the samples prepared from the mixture of clay Sahara sand at two loads 6 and 4 tonnes:

$$AP_{M1\,(6)} < AP_{M2\,(6)} < AP_{M1\,(4)} < AP_{M2\,(4)}$$

Where AP is the apparent porosity; M1, M2 are bricks samples prepared from mixed clay with Biskra sand ,Sahara sand respectively at loads equal to 6 and 4 tonnes.

- We can say also that the loads have an effect on apparent porosity, the apparent porosity decrease with the increase in the load.

The effect of sintering temperature on apparent porosity

From the different results of apparent porosity **(Tab. IV.5)** and their curves **(Fig.IV.21)**, the effects of sintering temperature on the apparent porosity of the sintered samples are vividly shown. It is observed that the apparent porosity of the sintered sample prepared from two mixtures at different load: M1(6), M2(6), M1(4) and M2(4) is observed to decrease with increase in sintering temperature. When samples were sintered at 750°C, they had an apparent porosity of 10.16%, 11.11%, 11.47% and 11.66% respectively when the sintering temperature was increased to 850°C their apparent porosity reduced to 5.89%, 6.77%, 7.43% and 8.2% respectively. Further increase in the sintering temperature to 900°C resulted in reduction in the apparent porosity of the samples to 4.81%, 5.86%, 6.08% respectively and 6.89%. And lastly at 1000°C the apparent porosity reduced to 4.53%, 5.1%, 5.63% and 6.65% respectively. This is due to the sintering process; according to Calister, [46] voids exist between particles of the newly formed green (unfired) ceramic, much of these inter-particles voids are eliminated during firing/sintering to produce sintered ceramic. However, it is often the case that this pore elimination process is incomplete and some residual porosity will remain.

According to Aramide [41], many factors determine the amount of these pores that will be eliminated during sintering these include:

- The temperature at which the ceramic is sintered.
- The higher amount of the pore that will be filled/eliminated during the sintering operation.
- The composition of the ceramic raw materials.

The effect of compacting load on apparent porosity:

When pouring powder, particles become arranged by acting of gravitational forces.poured powder include bridges and cavities which can be reduced by jolting and vibration. The density increases with the increase of pressure (applied load), which resulting a decrease in the apparent porosity, because it reduces the void between particles.

IV.5.2 Water absorption

The results of water absorption of prepared samples at different sintering temperatures and loads are presented in **Tab. IV.6**.

Tab. IV.6: Effect of sintering temperature on the water absorption of samples.

Temperatures(°C)		Water absorption (%)			
		M1		M2	
	Loads(tons)	6	4	6	4
750		9.09	11.36	10.46	11.49
850		4.76	5.81	5.20	6.11
900		4.70	5.80	4.92	5.90
1000		2.29	3.48	2.73	4.56

The different curves of the water absorption as function sintering temperature of prepared samples are illustrated in **Fig.IV.22** to **Fig.IV.25**.

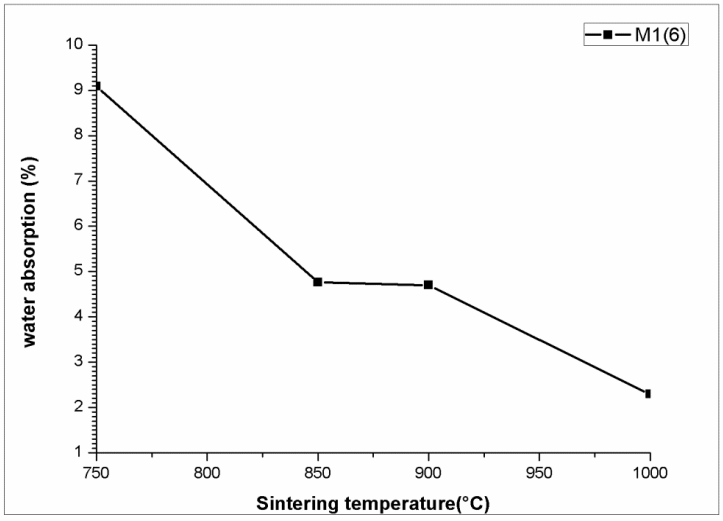

Fig.IV.22: Effect of sintering temperature on water absorption of samples prepared from mixture of clay and Biskra sand at 6 tonnes.

We show in **Fig.IV.22** and **Tab. IV.6** that the water absorption is first decreased rapidly from 9.09 % to 4.76% at 750°C and 850°C respectively and then decreased slowly with increasing the sintering temperature; until the water absorption reaches 2.29 % at 1000°C.

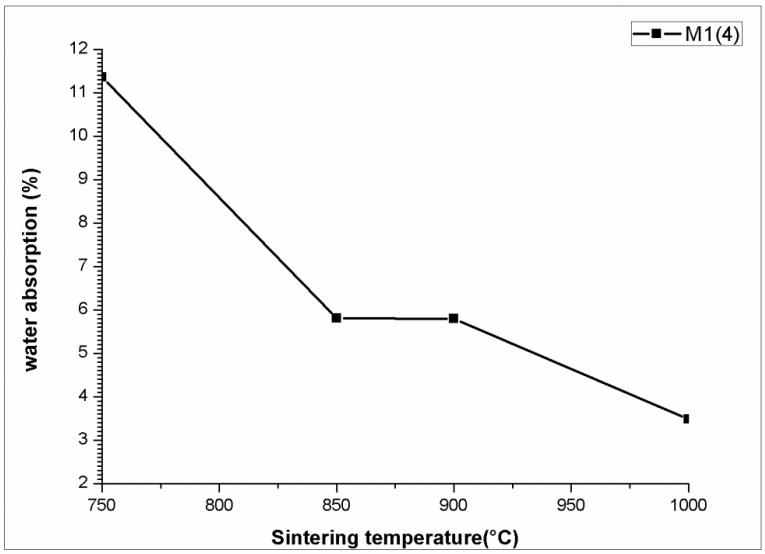

Fig.IV.23: Effect of sintering temperature on water absorption of samples prepared from mixture of clay and Biskra sand at 4 tonnes.

From **Fig IV.6** and **Tab. IV.6 ,** The water absorption decreases rapidly from 11.36 % to 5.81% at 750°C and 850°C respectively and then decreases slowly with the increase in sintering temperature, to reach the value is equal to 3.48 % at 1000°C.

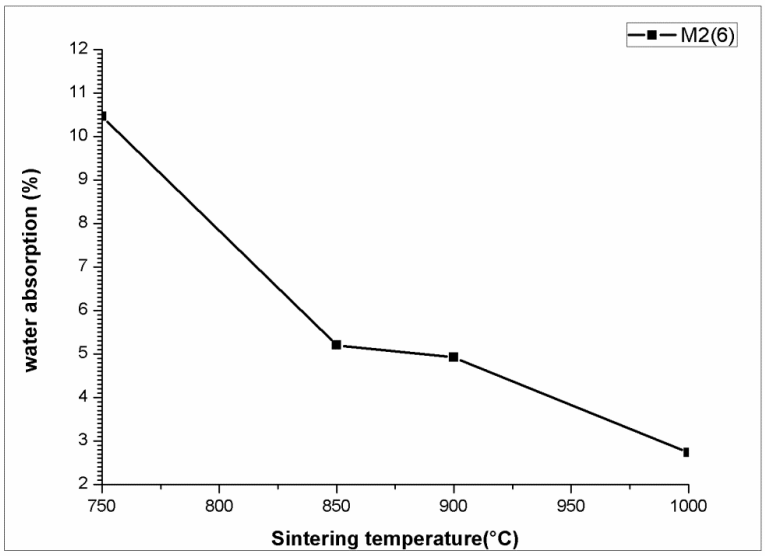

Fig.IV.24: Effect of sintering temperature on water absorption samples prepared from mixture of clay and Sahara sand at 6 tonnes.

Fig.IV.24 illustrate the decrease of water absorption; and **Tab.IV.6,** shows that the water absorption is also first decreased rapidly from 10.46 % to 5.20 % at 750°C and 850°C

respectively and then decreased slowly with an increase in sintering temperature; until this decrease stops at 2.73 % at 1000°C.

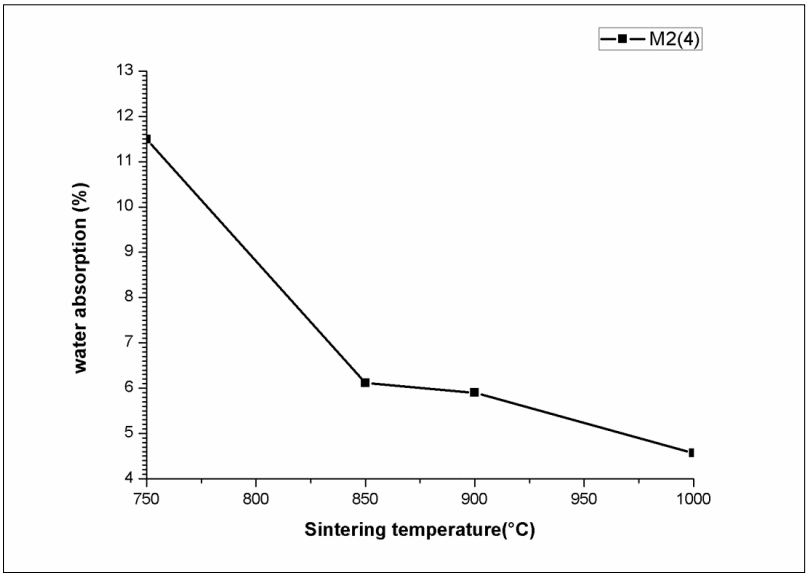

Fig.IV.25: Effect of sintering temperature on water absorption samples prepared from mixture of clay and Sahara sand at 4 tonnes.

From **Fig. IV.25** and **Tab. IV.6**, the water absorption is first decreased rapidly from 11.49 % to 6.11% at 750°C and 850°C respectively and then decreased slowly with increasing in sintering temperature, the last value is 4.56 % at 1000°C.

The different curves of the water absorption as function of sintering temperature of prepared samples are presented in the same graph to compare between them (**Fig. IV.26)**.

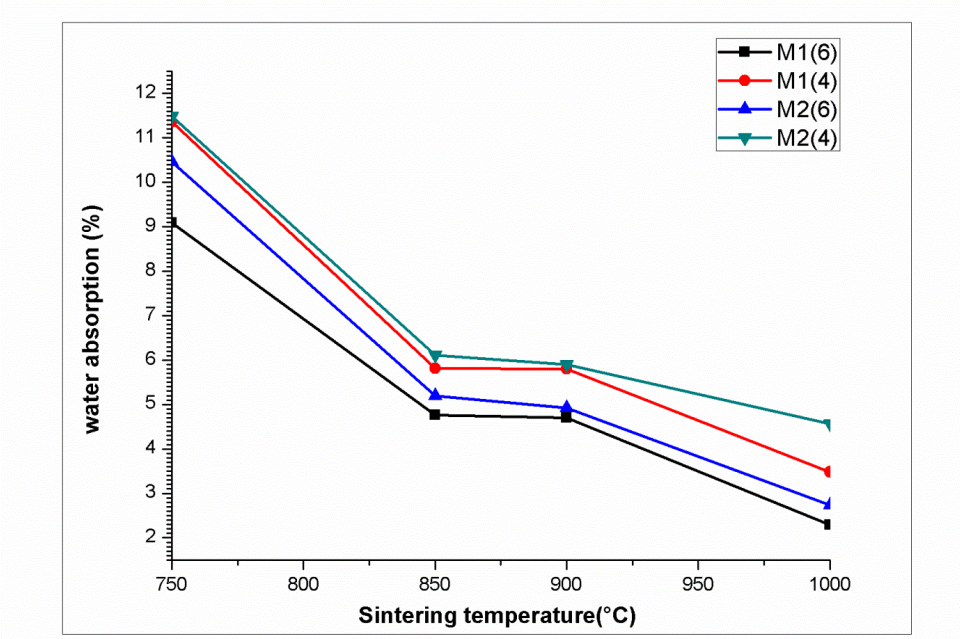

Fig.IV.26: Effects of sintering temperature on the water absorbtion of the samples prepared from different mixture at different loads

- The curves illustrate that the water absorption decreased with an increase in the sintering temperature.
- The samples prepared at 6 tonnes have a value of water absorption less than the value of samples prepared at 4 tonnes. But the water absorption of samples prepared from the mixture of Biskra sand is less than the samples prepared from the mixture of Sahara sand at two loads (6and 4 tonnes:

$$WA_{M1\,(6)} < WA_{M2\,(6)}) < WA_{M1\,(4)} < WA_{M2\,(4)}$$

Where WA is the water absorption; M1, M2 are the mixture with Biskra sand ,Sahara sand respectively and 6,4 are the loads in tonnes.

- From this, we can say also that the loads have an effect on water absorption, when water absorption decreases with the increase in the load.

The effects of sintering temperature on the water absorption of the sintered samples are clearly shown. It is observed that the water absorption of samples prepared from the two mixtures at different load and sintered at 750°C, 850°C°,900C° and 1000C°: M1(6), M2(6), M1(4) and M2(4) is observed to decrease with increase in sintering temperature. When samples were sintered at 750°C, they had water absorption of 9.09%, 10.46%, 11.36% and 11.49 % respectively but the sintering temperature was increased to 850°C their water absorption reduced to 4.76%, 5.2%, 5.81% and 6.11%. Further the increase in the sintering temperature to 900°C is resulted another reduction in the water absorption of the samples to 4.7%, 4.92%, 5.8% and 5.9% respectively, and then to 2.29%, 2.73%, 3.48% and 4.56% respectively at a high sintering temperature of 1000°C.

The test of water of absorption of samples determines the measure of the extent to which the samples is susceptible to seepage of water through its pores when immersed in water.

This water absorption test gives an idea on how the brick products produced will behave when it is used in environment. Tested samples having higher water of absorption means they are more porous in nature. It could also be observed that, as the clay content reduced, the water of absorption decreased. This could be attributed to the raw material quantity in the fired brick and of all the batches. Low water of absorption in the tested samples will have higher strength and durability. Since if the water of absorption is low, it restricts the amount of water may cause deterioration. Water existing in the pores of the products will be cyclically expanded and contracted and this will generate stresses within the material thereby resulting in the weakening of the product [40]. Even though the porosity value is lower, this only affects on the water absorption properties, when the apparent porosity decreases the water absorption decreases.

IV.5.3 Bulk density

The results of water absorption of prepared samples at different sintering temperatures are presented in **Tab.IV.7**.

Tab.IV.7: Effects of sintering temperature on the bulk density of the samples.

Temperatures(°C)		Bulk density(g/cm^3)			
		M1		M2	
	Loads(tons)	6	4	6	4
750		1.508	1.451	1.483	1.390
850		1.603	1.581	1.584	1.543
900		1.615	1.603	1.615	1.592
1000		1.641	1.629	1.634	1.625

The different curves sintering temperature effect on the apparent porosity of samples are illustated in figures (**Fig.IV.27 - Fig. IV.30)**.

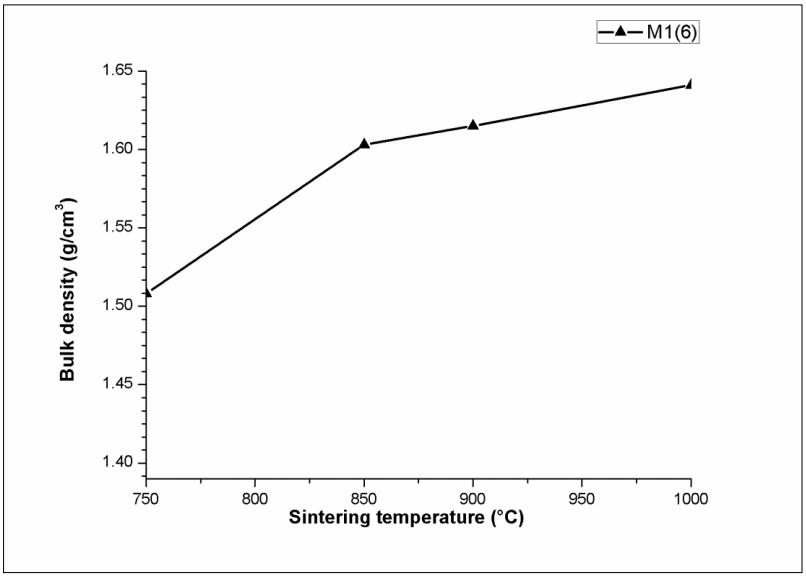

Fig.IV.27: Effects of sintering temperature on the bulk density of the samples prepared from mixture of clay and Biskra sand at 6 tonnes.

From **Fig IV.27** and **Tab.IV.7.** the bulk density of this samples is first increased rapidly from 1.508 g/cm^3 to 1.603g/cm^3 at 750°C and 850°C respectively and then increased slowly with increasing in the sintering temperature, the best value is 1.641g/cm^3 at high temperature (1000°C).

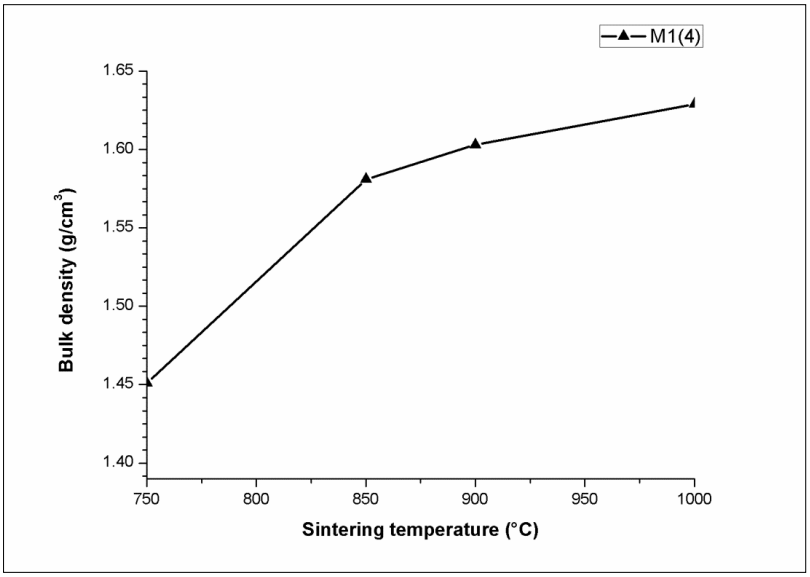

Fig.IV.28: Effects of sintering temperature on the bulk density of the samples prepared from mixture of clay and Biskra sand at 4 tonnes.

Fig. IV.28 shows the increase of bulk density with the increase of sintering temperatures and from **Tab. IV.7**, we observe that the bulk density of this samples is first increased rapidly from 1.451g/cm^3 to 1.581g/cm^3 at 750°C and 850°C respectively and then increased slowly with increasing in sintering temperature, until the BD reaches to 1.629/cm^3 at 1000°C.

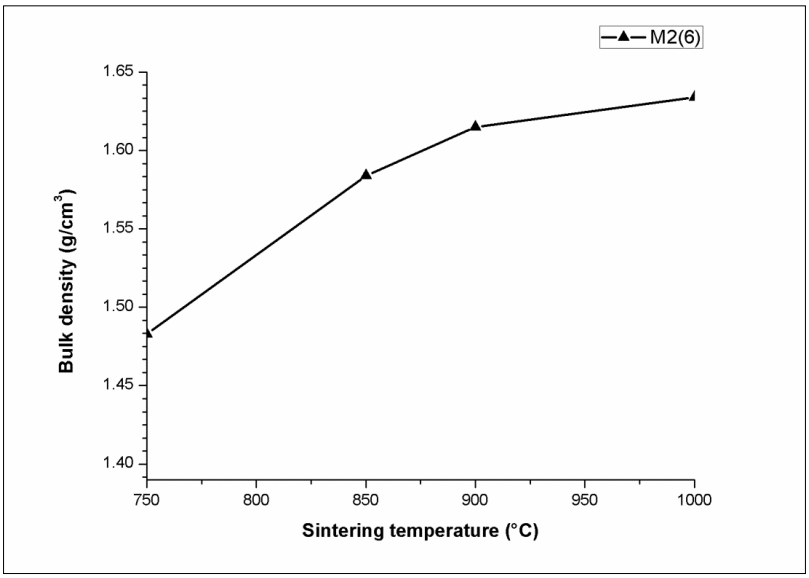

Fig.IV.29: Effects of sintering temperature on the bulk density of the samples prepared from mixture of clay and Sahara sand at 6 tonnes.

From **Fig.29** and **Tab.7**the bulk density of this samples is first increased rapidly from 1.483g/cm^3 to 1.584 g/cm^3 at 750°C and 850°C respectively and then increased slowly with increasing in sintering temperature, the last value is 1.634g/cm^3 at 1000°C.

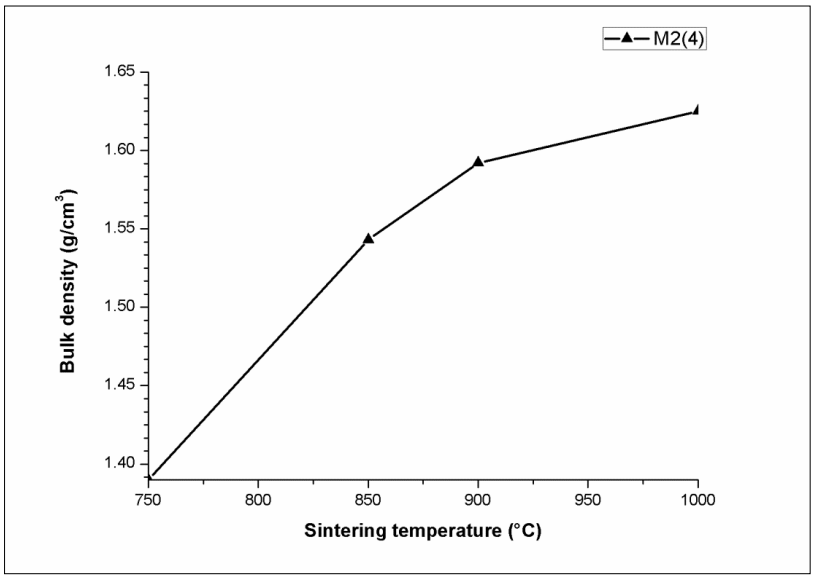

Fig.IV.30: Effects of sintering temperature on the bulk density of the samples prepared from mixture of clay and Sahara sand at 4 tonnes.

From **Fig.30** and **Tab7. ;** the bulk density of this samples is first increased rapidly from 1.390g/cm^3 to 1.543 g/cm^3 at 750°C and 850°C respectively and then increased slowly with increasing in sintering temperature, the last value is 1.625 g/cm^3 at 1000°C.

To compare between the bulk densities of samples prepared at different conditions (sintering temperature and loads), we put them in the same graph (**Fig.IV.31)**.

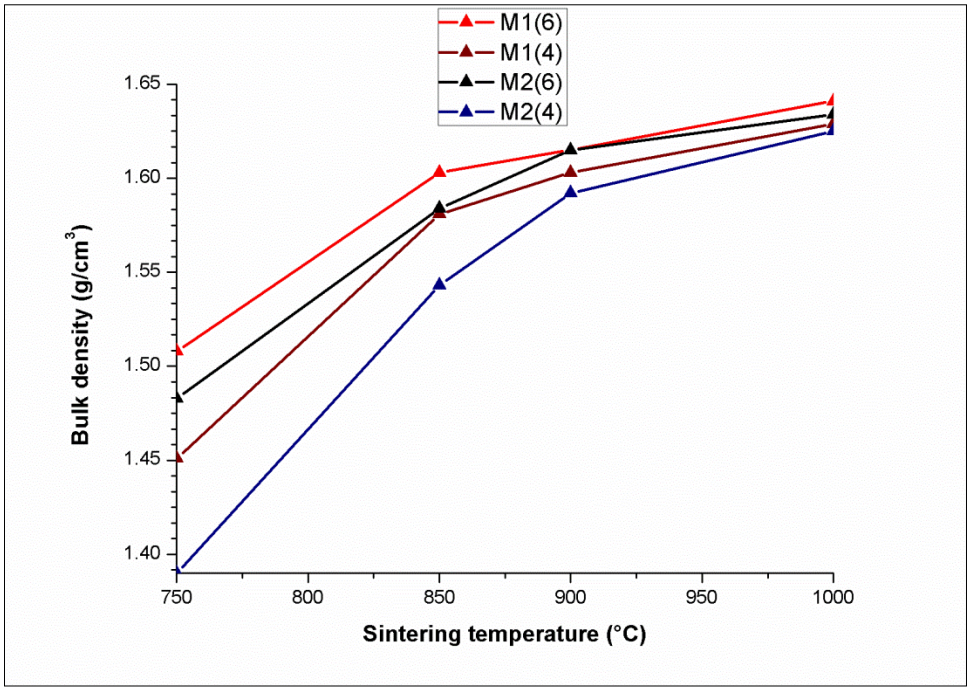

Fig.IV.31: Effects of sintering temperature on the bulk density of the samples prepared from different mixture at different loads.

Comments:

- The curves illustrate that the bulk density increased with increasing in sintering temperature.
- The samples prepared at 6 tonnes have a high value of bulk density than the samples prepared at 4 tonnes. But the bulk density of samples prepared from the mixture of Biskra sand is higher than the samples prepared from the mixture of Sahara sand at two loads (6and 4 tonnes):

$$BD_{M1\,(6)} > BD_{M2\,(6)} > BD_{M1\,(4)} > BD_{M2\,(4)}$$

Where BD is bulk density; M1, M2 are the samples prepared from the mixed of clay and Biskra sand ,Sahara sand respectively and 6,4 are the loads in tonnes.

- From this we can say that the loads have an effect on bulk density, when the load increases the bulk density increases

From **Tab.IV.7** and **Fig.IV.31,** the effect of increase in sintering temperature on the bulk density of the sintered samples is clearly depicted. Contrary to the relationship which existed between the sintering temperature and the apparent porosity as discussed above, it is observed that the bulk density of the samples increases with the increase of the sintering temperature. This is expected because as the inter-particle voids/pores are progressively filled up with increasing sintering temperature, the volume of the ceramic samples can be said to reduce with increased sintering temperature. This behavior is also due to the reduced porosity of the sample as explained above which lead to increase in the amount of matter in the sample per unit volume [49].

During the sintering process, polymorphic phase transformations occur as a result of chemical reactions leading into complex compounds at high temperatures. These transformations tend to aid in the quick sintering process and impacts on the stability of the material due to the decrease or increase in the volume of the system [31, 50]

At temperatures beyond 900ºC, D. Dodoo-Arhin et al [40], proved that the presence of fluxes (K_2O,Na_2O, Fe_2O_3, and CaO) in the composite bricks begins to yield glassy phases aligning themselves very well along the grain boundaries of the mixtures to achieve high densification which increase the bulk density and consequently the mechanical strength.

IV .6 Results of brick sample (SARL.Eloutaya.Poterie)

IV .6.1 Phases identification of factory samples

The X-ray diffraction (XRD) of SARL Eloutaya.Poterie samples are presented in **Fig.IV.32** and **Fig.IV.33**: the first is of the dried sample at 80°C after molding and the second of the sintered sample at 850°C for 8 hours.

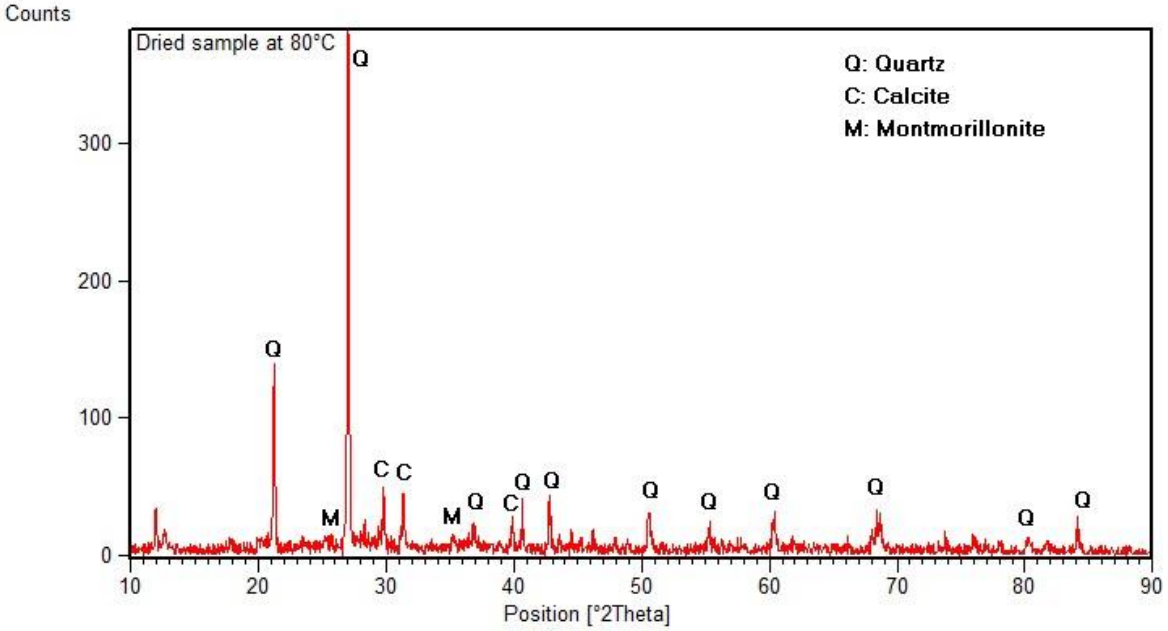

Fig.IV.32: XRD pattern of SARL Eloutaya dried sample at 80°C.

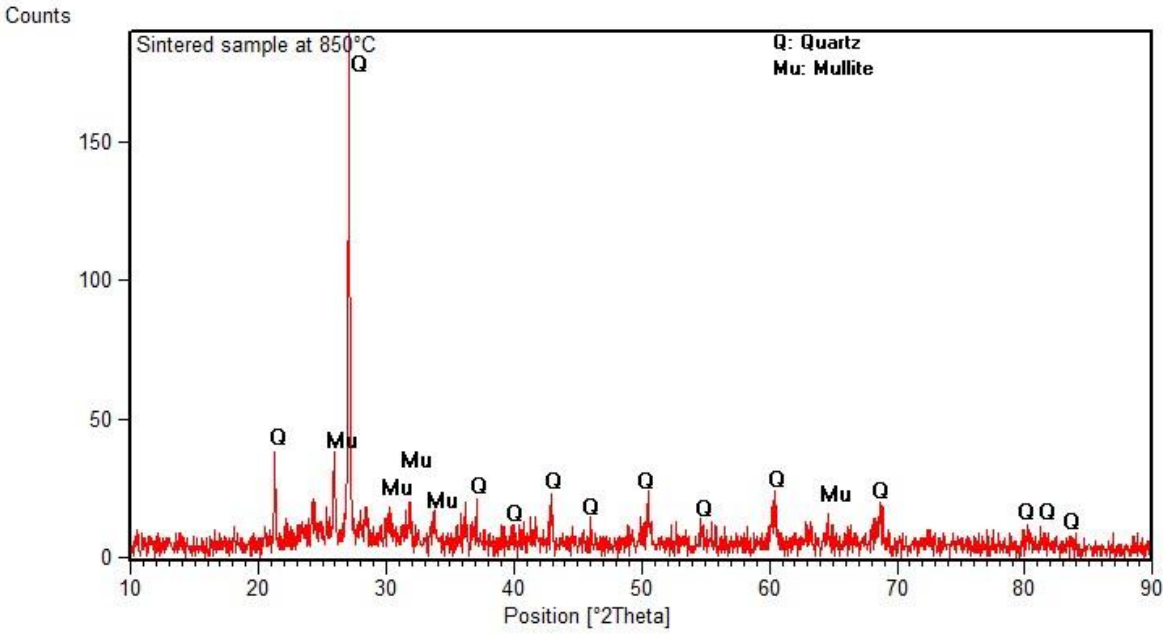

Fig.IV.33: XRD pattern of SARL Eloutaya of sintered sample at 850°C.

Fig.IV.34 shows the XRD patterns of samples prepared in SARL Eloutaya. Poterie, and sintered at different temperatures, in order to compare between them.

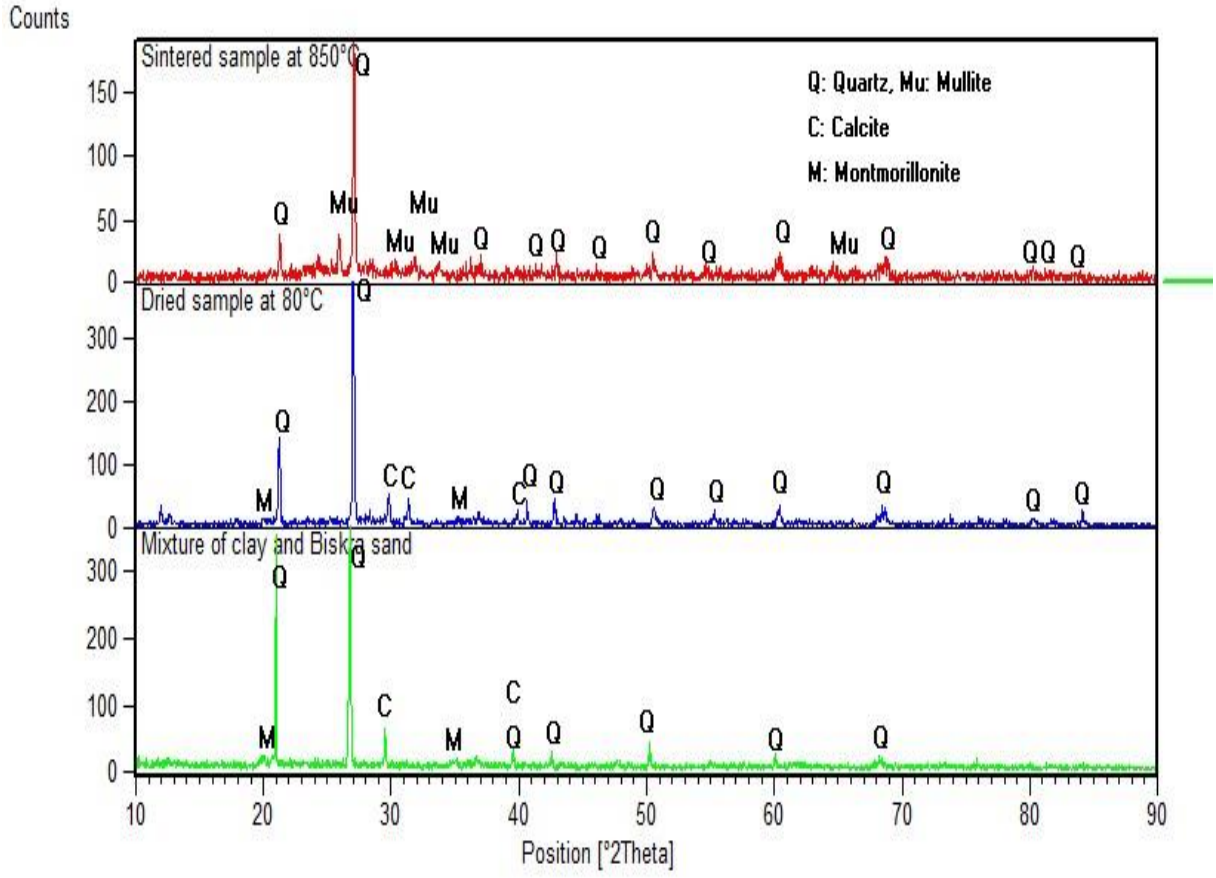

Fig.IV.34: XRD pattern of SARL Eloutaya samples at different temperature.

IV.6.2 Microstructure of brick sample

The microstructure of brick sample produced by factory (SARL.Eloutaya.Poterie) is presented in **Fig. IV.31**.

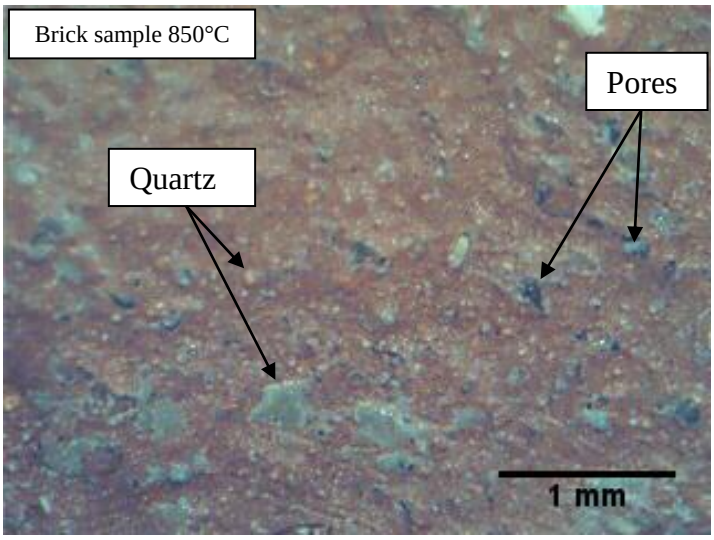

Fig.IV.35: The microstructure of brick sample of SARL.Eloutaya sintered at 850°C.

- The main phase in this microstructure is quartz (white colour).this similar with our result.
- The pores in this microstructure have a black colour.

IV.6.3 Physical properties

The different properties of brick sample of the factory are presented in **Tab. IV.8**.

Tab. IV.8: The properties of brick sample of SARL.Eloutaya, sintered at 850°C.

Properties	**Apparent porosity (%)**	**Water absorption (%)**	**Bulk density(g/cm^3)**
Value	11.48	6.57	1.45

If we compare these results with the results of our prepared samples and sintered at the same temperature (850°C), we found that the different properties of our prepared samples are better than the properties of factory sample. Where the apparent porosity of samples sintered at 850 °C is 8.5 %, the water absorption less than 6.11 %, and bulk density more than 1.543 g/cm^3.

The difference between the two kind of brick samples :

At the same temperature (850°C)

- The firs reason is the particle size of clay, because our prepared samples have 315um less than 2 mm which is used in the factory.
- The second is the shaping process; in our work we use powder metallurgy process not molding.

At high temperatures (900 and 1000°C)

This case was discussed above when we compared between our samples.

IV.7 Conclusion

The main results of this chapter are summarized:

- The effect of sintering temperature on the microstructure of brick samples was studied; we found that when the sintering temperature was increased, the grain of samples showed growth.
- When the load increases, the apparent porosity and water absorption of bricks samples decrease. But the bulk density increases.
- When the sintering temperature increases, the apparent porosity and water absorption of bricks decrease. While the bulk density increases.

General conclusion and perspectives

General conclusion

The objective of this dissertation was to investigate the effect of sintering temperature and load application on properties of bricks product.

To achieve our aim, we have taken as material to study the bricks product produced by SARL Eloutaya.Poterie in Biskra. We have also changed the sand of Biskra by the sand of Sahara (Ouargla).

The different techniques have been used:

1) Particle size analysis
2) Infrared spectroscopy
3) X.ray diffraction
4) Microstructure observation
5) Physical tests (Apparent porosity, water absorption and bulk density)

From this dissertation, we have found these following results:

- The fineness modulus (M_f) of Biskra and Sahara sands are 1.72 and 1.08 respectively, the two kinds of sands have a very fine particle size.
- The results of infrared spectroscopy were in agreement with those found from XRD. They confirm the presence of quartz, montmorillonite and calcite in our studied materials (raw materials).
- When the sintering temperature was increased, the grain of samples showed growth.
- When the load increases, the apparent porosity and water absorption of bricks samples decrease. But the bulk density increases.
- The apparent porosity and water absorption of bricks is decreased with an increase in the sintering temperature. While the bulk density increases.
- In this research we found that the optimum sintering temperature was at high temperature 1000 °C under load equal to 6 tonnes where the samples of brick had good physical properties.
- Our samples, which was prepared by powder metallurgy process has better properties than the samples of SARL.Eloutaya Poterie factory prepared by molding process.

General conclusion and perspectives

- Finally, we deduce that the Sahara sand can be used in the preparation of brick product.

Perspective

- Using some mechanical testing such as compressive strength
- Seen the pores size with SEM

References

[1] K.R. Suresh, S. Mahendran, M.S.Krupashankara, L. Avinash, Influence of powder composition & morphology on green density for powder metallurgy processes, International journal of innovative research in science, Engineering and technology, Vol. 4, issue 1, January 2015, 2347-6710.

[2] A.AL-Tounsi, Effect of sintering parameters on the mechanical and physical properties of sinter formed materials, Doctoral thesis, Scientific studies and research center, Damascus - Syria 1992.

[3] EETM: Emission Estimation Technique Manual, Non-metallic mineral product manufacture, National pollutant inventory, December 1999.

[4] Metso, Basics in minerals processing, Edition 10, 2015.

[5] K.Skotnicovà, M.kursa,I.Szurman, Powder metallurgy, University textbook, Ostava,2015

[6] F. A. J. Nichols, On the spheroidization of rod-shaped particles of finite length, Materials and science, Vol.11, 1976, 1077.

[7] M.N.Rahaman, Ceramic processing and sintering, Edition 2, MDI, New York.

[8] H. P.Stuwe, O.Kolednik, Shape instability of thin cylinders, Acta metall. 1988, Vol. 36, 1705.

[9] C.Suryanarayana, Mechanical alloying and milling progress, Materials Science, N° 46, 2001, 1–184.

[10] R.M.German, Powder metallurgy science, Edition 2, 1994.

[11] C. Alice, M.S.De Bellis, computer modeling of sintering in ceramics, Doctoral thesis, University of Pittsburgh, 2002.

[11]: K.Mohammed, Jasim Kadhim, Adil, A. Alwan, Iman, J. Abed, Simulation of cold die compaction alumina powder, Trends in mechanical engineering& technology, Vol.1, Issue 1, February, STM journals, (2011), 1-21.

[12] LPR GLOBAL, Powder compacting presses, Korea.

[13] R.Agarwal, and M.Shashikanth, Sintering behaviour of red mud compact, National institute of technology Rourkla, Orissa,2008.

[14] B.Verlinden,L.Froyen, Aluminum powder metallurgy, Training in aluminium application technologies , European aluminium association, 1995.

[15]: R. Riedel, I-W. Chen, Synthesis and processing, First edition, Ceramics science and technology: Vol.3, 2012.

[16] P. Boch, Matériaux et processus céramiques, Hermes science Europe LTD, 2001.

References

[17] S.Gasiorek, K.Maciejko, J.Szatkowska proceeding of 4th international conference on modern ceramic technologies, Italy, 1979, 223.

[18] K.R.Suresh, S.Mahendran, M.S.Krupashankara, L.Avinash, Influence of powder composition & morphology on green density for powder metallurgy processes, International journal of innovative research in science, Engineering and technology, Vol. 4, Issue 1, January 2015, 2347-6710.

[19] Franz X. Zimmerman Jerry Toops, Hot isostatic pressing, Avure Technologies, January, 2008.

[20] R.M. German, Sintering theory and practice. 1996, New York: John Wiley and Sons.

[21] European powder metallurgy association (EPMA), Powder metallurgy, 2008.

[22] A.Redjechta, Etude microstructurale et mécanique des alliages Cu-Zn frittés sous pression et par électrodéposition, Doctoral thesis, University of Ferhat Abbas, Setif 1, 2015.

[23] M. Eudier, Métallurgie des poudres, Fabrication des produits frittés, Technique de l'Ingénieur, M864, M866.

[24] J. Curé, Métallurgie appliquée, book, 1970.

[25] L.C. DeJongheand, M.N. Rahman, Sinterring of ceramics, Handbook of advanced ceramics, 2003.

[26] C. Chlique. Préparation et caractérisation de poudres et céramiques (oxy) sulfures pour applications en optique active et passive. Doctoral thesis, University of Rennes 1, 2011.

[27]: A.Aytimur ,S.Koçyigit , I.Uslu, Calcia Stabilized Ceria Doped Zirconia Nanocrystalline Ceramic, 2014, J Inorg Organomet Polym , 2014, 927–932

[28]: G.C. Kuczynski, N. Hooton, C.F. Gibbon, Sintering and related phenomena (Gordon & Breach), New York, 1967.

[29]: L.R.Olmos, Etude du frittage de poudres par microtomographie in situ et modélisation discrète, Doctoral thesis, L'Institut polytechnique, Grenoble, 2010.

[30] J. G.Song, F. Wang, X. B. Bai, D.M. Du, Y.Y. Ju, M.-H. Xu , G. C. Ji , Effect of the sintering technology on the properties of fired brick from quartz sands, Journal of Ceramic Processing Research, Vol.12, N° 4, 2011, 357-360.

[31] I. Johari, S. Said, B. Hisham, A. Bakar, Z. A. Ahmad ,Effect of the change of firing temperature on microstructure and physical properties of clay bricks from Beruas (Malaysia) science of sintering, N°42 ,2010, 245-254.

References

[32] J. A. Amkpa, N. A. Badarulzaman, A. B. Aramjat, Influence of sintering temperatures on physico-mechanical properties and microstructure of refractory fireclay bricks, international journal of engineering and technology (ijet), vol. 8, N° 6, (2016), 2319-8613.

[33] D. Mcglinchey, Characterisation of bulk solids, CRC Press, 2005.

[34] AFNOR Association Française de Normalisation, XP P18-540, October 1997.

[35] F. A.Settle,. Handbook of instrumental techniques for analytical chemistry; Prentice Hall PTR (Upper Saddle River), NJ, 1997.

[36] S. Wartewig, IR and Raman spectroscopy (Fundamental processing), Wiley-VCH, 2003.

[37] Moore, D. M. and R. C. Reynolds, Jr. 1997. X-Ray diffraction and the identification and analysis of clay minerals. 2nd Ed. Oxford University Press, New York.

[38] ASTM Standard Test Methods for apparent porosity, liquid absorption, apparent specific gravity, and bulk density of refractory shapes by vacuum pressure designation, C 830– 00. 1 ASTM Committee C-8 on physical tests.

[39] SU Adikary, M Ashokcline and K Nirojan, Characterization of montmorillonite clay from naturally occurring clay deposits in Murunkan area, Proceedings of 8th international research conference, KDU, November 2015.

[40] D. Dodoo-Arhin, D. S Konadu, E. Annan, F. P Buabeng, A. Yaya, B. Agyei-Tuffour, Fabrication and characterisation of Ghanaian bauxite red mud-clay composite bricks for construction applications, American journal of materials science N° 3,(2013), P. 110-119.

[41] F.O. Aramide, Effects of sintering temperature on the phase developments and mechanical properties ifon clay, Leonardo Journal of Sciences, Issue 26, January-July 2015, p. 67-82.

[42] F.Gridi-Bennadji, B. Beneu, J. P.Laval, P. Blanchart, Structural transformations of muscovite at high temperature by X-ray and neutron diffraction, Applied clay science, 2008, 38 (3-4),P 259-267.

[43] X.Liu, N.Zhang, H.Sun, J.Zhang, and L.Li, Structural investigation relating to the cementitious activity of bauxite residue-red mud, cement and concrete research, Vol.41, N°.8, P. 847-853, 2011.

[44] S. Ferrari, A.F.Gualtieri, The use of illitic clays in the production of stoneware tile ceramics, Applied Clay Science, (2006), N°32, 73-81.

[45] A.Oscar Mauricio Castellanos, R.Carlos Alberto Ríos, G. Miguel Angel Ramos , P.Eric Vinicio Plaza, A comparative study of mineralogical transformations in fired clays from the laboyos valley, upper magdalena basin (Colombia), Inicio,(2012),Vol.34, N°1..

References

[46] S.Ergul, M.Akyildiz,A. Karamanov, ceramic material from basaltic tuffs, industrial ceramics, 2007, 27(2), P. 89-94.

[47] Baccour, H., Medhioub, M., Jamoussi, F., Mhiri, T., and Daoud, A. 2008. Mineralogical evaluation and industrial applications of the Triassic clay deposits, Southern Tunisia. Materials Characterization, 59(11): 1613-1622.

[48] Cultrone, G., Rodriguez-Navarro, C., Sebastian, E., Cazalla, O., and de la Torre, M.J. 2001. Carbonate and silicate phase reactions during ceramic firing. European Journal of Mineralogy, 13(3): 621-634.

[49] F. O.Aramide, production and characterization of porous insulating fired bricks from ifon clay with varied sawdust admixture, journal of minerals and materials characterization and engineering, 2012, 11, P. 970-975.

[50] S. A. Bernal, R. M. Gutiérrez, A. L. Pedraza, J. L. Provis, E. D., Rodriguez, S. Delvasto, Effect of binder content on the performance of alkali-activated slag concretes, Cement and concrete research,N° 41, (2011), P 1-8.

Annexes

The different data of phases from the high score

1) Quartz

Name and formula

Reference code: 00-046-1045
Mineral name: Quartz, syn
PDF index name: Silicon Oxide
Chemical formula: SiO_2

Crystallographic parameters

Crystal system: Hexagonal
Space group: P3221
Space group number: 154

a (Å): 4.9134
b (Å): 4.9134
c (Å): 5.4052
Alpha (°): 90.0000
Beta (°): 90.0000
Gamma (°): 120.0000

Comments

Color: White

Peak list

No.	h	k	l	d [A]	2Theta[deg]	I [%]
1	1	0	0	4.25499	20.860	16.0
2	1	0	1	3.34347	26.640	100.0
3	1	1	0	2.45687	36.544	9.0
4	1	0	2	2.28149	39.465	8.0
5	1	1	1	2.23613	40.300	4.0
6	2	0	0	2.12771	42.450	6.0
7	2	0	1	1.97986	45.793	4.0
8	1	1	2	1.81796	50.139	13.0
9	0	0	3	1.80174	50.622	1.0
10	2	0	2	1.67173	54.875	4.0
11	1	0	3	1.65919	55.325	2.0
12	2	1	0	1.60827	57.235	1.0
13	2	1	1	1.54153	59.960	9.0
14	1	1	3	1.45289	64.036	2.0
15	3	0	0	1.41841	65.786	1.0
16	2	1	2	1.38210	67.744	6.0
17	2	0	3	1.37496	68.144	7.0

18	3	0	1	1.37188	68.318	5.0
19	1	0	4	1.28791	73.468	2.0
20	3	0	2	1.25595	75.660	3.0
21	2	2	0	1.22832	77.675	1.0
22	2	1	3	1.19982	79.884	2.0
23	2	2	1	1.19779	80.047	1.0
24	1	1	4	1.18399	81.173	2.0
25	3	1	0	1.18017	81.491	2.0
26	3	1	1	1.15298	83.840	1.0
27	2	0	4	1.14065	84.957	1.0
28	3	0	3	1.11455	87.439	1.0
29	3	1	2	1.08155	90.831	2.0

Stick Pattern

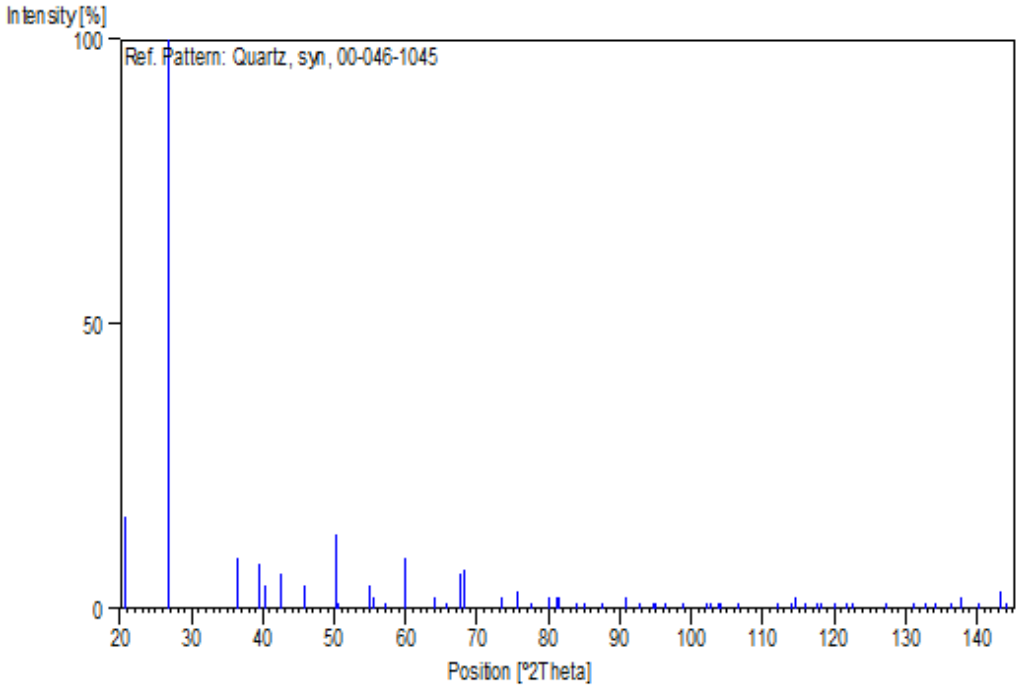

2) Montmorillonite

Name and formula

Reference code: 00-029-1499

Mineral name: Montmorillonite-21A
PDF index name: Sodium Magnesium Aluminum Silicate Hydroxide Hydrate

Empirical formula: $Al_2H_{18}Na_{0.30}O_{20}Si_4$

Annexes

Chemical formula: $Na_{0.3}$ (Al, Mg) 2Si4O10 (OH) 2 ·8H_2O

Crystallographic parameters

Crystal system:	Hexagonal
Space group:	P
a (Å):	5.2100
b (Å):	5.2100
c (Å):	22.0000
Alpha (°):	90.0000
Beta (°):	90.0000
Gamma (°):	120.0000

Peak list

No.	h	k	l	d [A]	2Theta[deg]	I [%]
1	0	0	1	21.50000	4.106	100.0
2	0	0	2	10.60000	8.335	18.0
3	1	0	1	4.45000	19.936	55.0
4	1	0	7	2.56000	35.023	35.0
5	0	0	13	1.69000	54.233	8.0
6	2	0	11	1.49500	62.028	25.0
7	3	0	8	1.32500	71.092	8.0

Stick Pattern

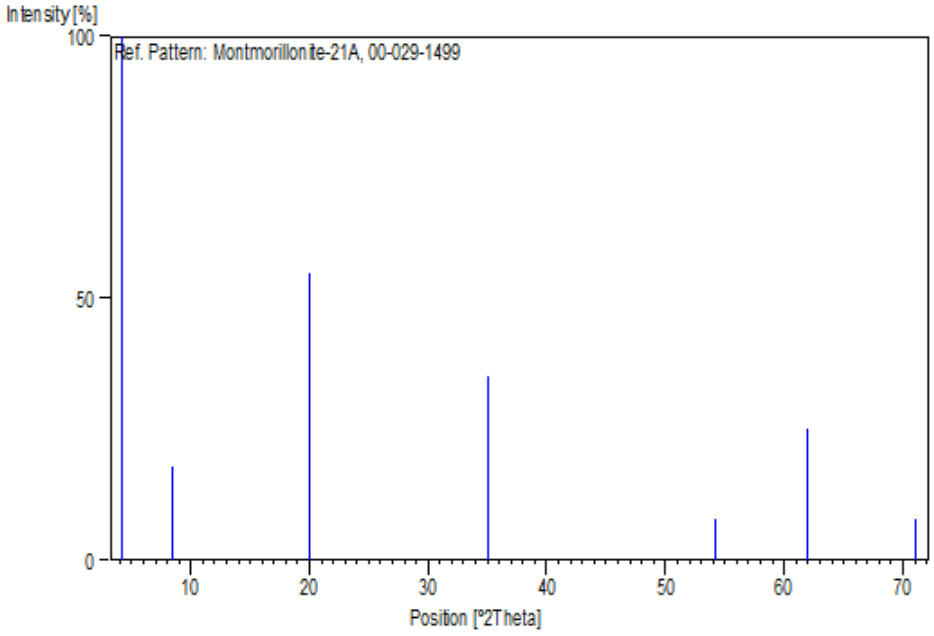

Annexes

3) Calcite

Name and formula

Reference code: 00-005-0586

Mineral name: Calcite, syn
PDF index name: Calcium Carbonate
Chemical formula: $CaCO_3$

Crystallographic parameters

Crystal system: Rhombohedral
Space group: R-3c
Space group number: 167

a (Å): 4.9890
b (Å): 4.9890
c (Å): 17.0620
Alpha (°): 90.0000
Beta (°): 90.0000
Gamma (°): 120.0000

Comments

Color: Colorless

Peak list

No.	h	k	l	d [A]	2Theta[deg]	I [%]
1	0	1	2	3.86000	23.022	12.0
2	1	0	4	3.03500	29.406	100.0
3	0	0	6	2.84500	31.418	3.0
4	1	1	0	2.49500	35.966	14.0
5	1	1	3	2.28500	39.402	18.0
6	2	0	2	2.09500	43.146	18.0
7	0	2	4	1.92700	47.124	5.0
8	0	1	8	1.91300	47.490	17.0
9	1	1	6	1.87500	48.514	17.0
10	2	1	1	1.62600	56.555	4.0

Stick Pattern

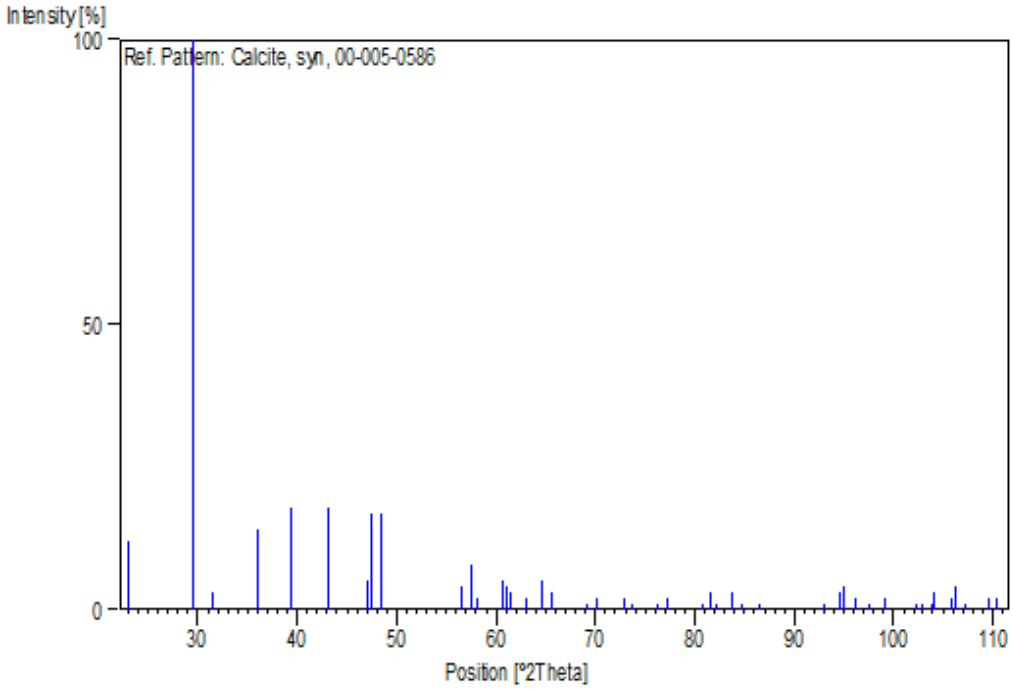

4) Gehlenite

Name and formula

Reference code:	00-020-0199
Mineral name:	Gehlenite, syn
PDF index name:	Calcium Aluminum Silicate
Empirical formula:	$Al_2Ca_2O_7Si$
Chemical formula:	$Ca_2Al_2SiO_7$

Crystallographic parameters

Crystal system:	Tetragonal
Space group:	P-421m
Space group number:	113
a (Å):	7.6940
b (Å):	7.6940
c (Å):	5.0770

Annexes

Alpha (°):	90.0000
Beta (°):	90.0000
Gamma (°):	90.0000

Peak list

No.	h	k	l	d [A]	2Theta[deg]	I [%]
1	1	1	0	5.46000	16.221	6.0
2	0	0	1	5.08000	17.443	6.0
3	1	0	1	4.22000	21.035	4.0
4	1	1	1	3.71000	23.967	20.0
5	2	1	0	3.43000	25.956	2.0
6	2	0	1	3.07000	29.063	25.0
7	2	1	1	2.85000	31.362	100.0
8	2	2	0	2.72000	32.902	6.0
9	0	0	2	2.53500	35.380	8.0
10	3	1	0	2.43500	36.884	20.0
11	2	2	1	2.40400	37.377	25.0
12	3	0	1	2.29200	39.277	14.0
13	3	1	1	2.19500	41.089	2.0
14	2	0	2	2.12600	42.486	2.0
15	2	1	2	2.04300	44.301	16.0
16	3	2	1	1.96700	46.110	2.0
17	4	0	0	1.92400	47.202	8.0
18	4	1	0	1.86400	48.818	6.0

Stick Pattern

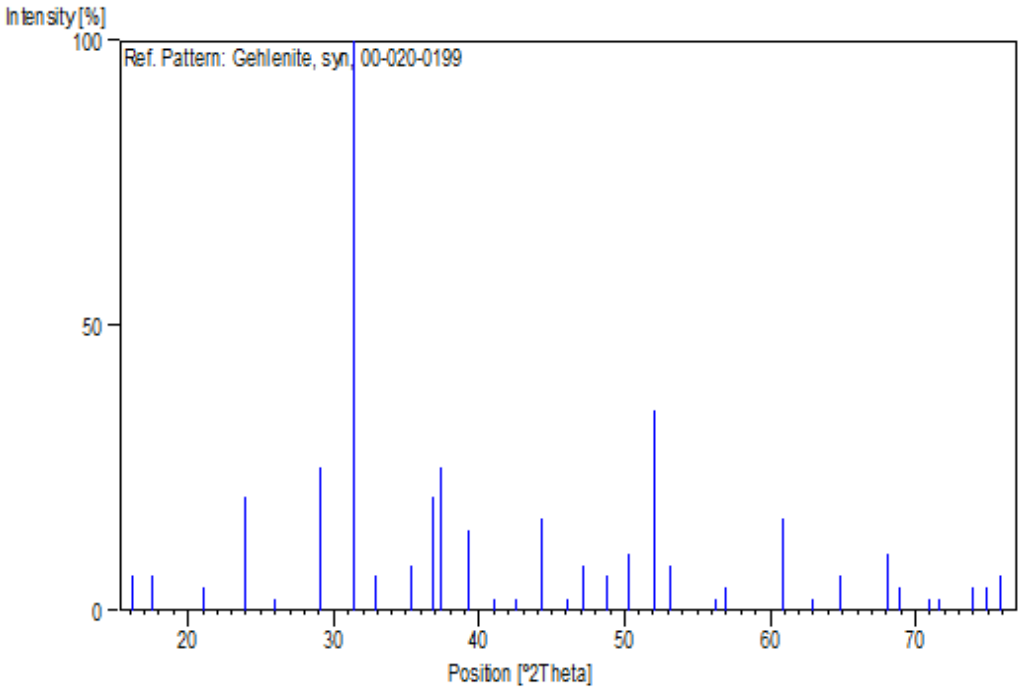

5) Mullite

Name and formula

Reference code: 00-002-0415

Mineral name: Mullite
PDF index name: Aluminum Silicon Oxide
Chemical formula: $3Al_2O_3 \cdot 2SiO_2$

Crystallographic parameters

Crystal system: Unknown

Peak list

No.	h	k	l	d [A]	2Theta[deg]	I [%]
1				3.44000	25.879	100.0
2				2.90000	30.808	40.0
3				2.70000	33.153	50.0
4				2.56000	35.023	60.0
5				2.43000	36.963	30.0
6				2.30000	39.135	40.0
7				2.21000	40.798	70.0
8				2.13000	42.402	50.0
9				1.89000	48.104	20.0
10				1.84000	49.498	30.0
11				1.70000	53.888	60.0
12				1.60000	57.559	40.0
13				1.53000	60.459	70.0
14				1.48000	62.728	20.0
15				1.45000	64.179	40.0
16				1.40000	66.763	20.0
17				1.33000	70.785	60.0
18				1.27000	74.679	60.0
19				1.24000	76.809	30.0
20				1.19000	80.678	40.0
21				1.10000	88.898	40.0
22				1.01000	99.401	40.0

Stick Pattern

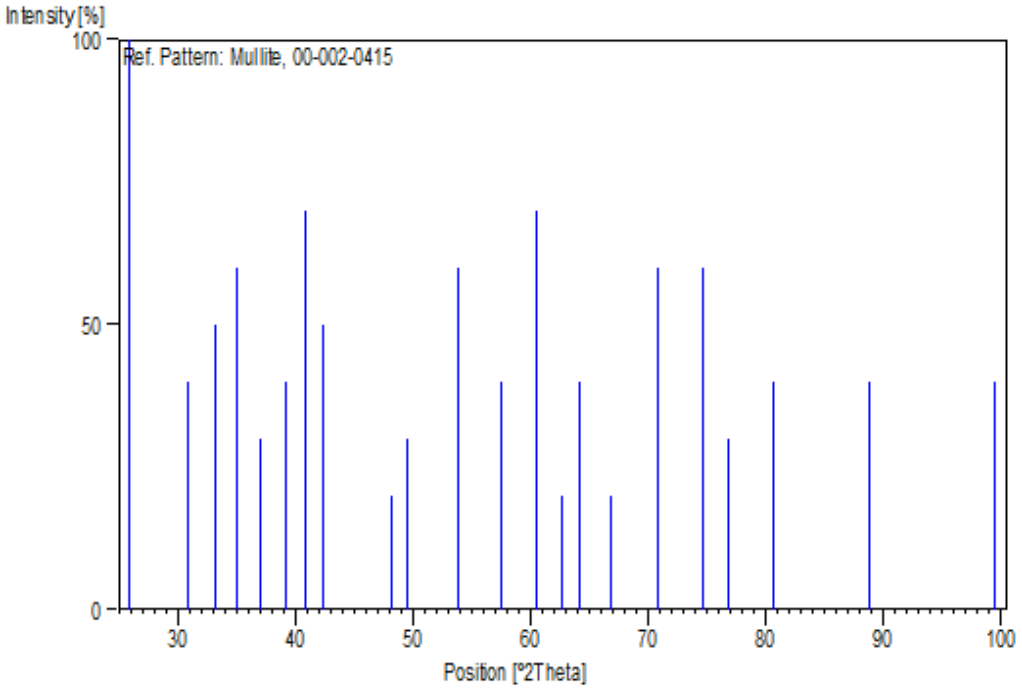

Abstract

The objective of this dissertation is to study the effect of the applied load of compaction and sintering temperature on the final properties of bricks product, such as bulk density, water absorption, and apparent porosity. The samples were compacted under two different loads (6 and 4 tonnes) and sintered at different temperatures: 750°C, 850°C, 900°C, 1000°C and 1200°C after that tested in laboratory.

Key-words: Load, compaction, sintering, final properties, bricks.

الملخص

الهدف من هذه المذكرة هو دراسة تأثير الحمولة المطبقة اثناء عملية الضغط و درجة حرارة التلبد على الخصائص النهائية لمنتج الأجر كالكثافة الحجمية، امتصاص الماء و المسامية الظاهرة. العينات تم تحضيرها في المخبر تحت حمولتين مختلفتين (6 و 4 طن)، و من ثم لبدت تحت درجات حرارة : 750 °C ، 850 °C ، 900 °C ، 1000 °C و 1200 °C، من ثم اختبرت.

الكلمات المفتاحية: الحمولة، الضغط، التلبيد، الخصائص النهائية، الاجر.

Résumé

L’objectif de ce mémoire est l’étude de l’effet de la charge applique et la température du frittage sur les propriétés finales du produit des briques, comme la densité volumique, l’absorption d’eau et la porosité apparente. Les échantillons sont compactés dans le laboratoire sous deux charges différentes (6 et 4 tonne) et fritté à 750°C, 850°C, 900°C, 1000°C et 1200°C.

Mots-clés : Charge, compactage, frittage, les propriétés finales, briques.